A SCANNING ELECTRON MICROSCOPIC STUDY OF THE MARMOSET PALATE AND PERIODONTIUM MICROVASCULATURE USING CORROSION CASTS

A report submitted in partial fulfillment of
the requirements for the degree of
Master of Dental Surgery

by

DAVID LEE, B.D.S.

Department of Dentistry,
The University of Adelaide,
South Australia

November, 1988

TABLE OF CONTENTS

LIST OF ILLUSTRATIONS

LIST OF TABLES

SUMMARY

Previous plastic perfusion studies in mice, rats and dogs have indicated that important species differences exist in the oral microvasculature.

Earlier microvascular studies were hampered by technical limitations of the light microscope. The SEM, with its superior resolution, magnification and depth of focus, has enabled detailed examination of the microvasculature to be undertaken.

The aim of this study was to investigate the microvasculature of the marmoset palate and periodontium using SEM stereopair micrographs of microcorrosion casts for three-dimensional evaluation of species differences.

Eight adult female marmosets (*Callithrix jacchus*) were used. The animals were anaesthetized and perfused with Mercox resin. The tissues were corroded with 10% HCl and 10% KOH solutions and the cleaned casts were coated and examined in the SEM.

Vascular casts were classified according to their endothelial imprint pattern (Hodde, 1981), branching pattern, and vessel diameter (Rhodin, 1967, 1968).

Throughout the entire hard palate, a series of papillary loops extended perpendicularly from a subpapillary plexus to the connective tissue papillae. These loops showed a general sagittal orientation, and were aligned on the crests of the rugae to form a well-delineated spine. The subpapillary plexus formed a canopy over an underlying venous network which lacked a definite orientation.

In the gingivae of upper and lower premolar and molar teeth, a gap was observed between the vasculature on the

sulcular side and on the vestibular and palatal side. Despite the gap, anastomoses occurred between the two sides at a deeper level.

Under the crevicular epithelium, a circular plexus of vessels encircled each tooth. Crevicular loops arose from this circular plexus, also encircling the tooth.

The periodontal ligament vasculature consisted of a network of occluso-apically orientated vessels, comprising mainly postcapillary-sized venules. Capillaries and arterioles were less abundant. Perforating branches from the alveolar bone contributed to the periodontal ligament network.

Vessels of the gingival plexus anastomosed with those of the periodontal ligament and the palate.

Species differences with the mouse, rat and dog were reflected in all sites studied at the microvascular level. These differences may be important in understanding oral microvascular bed function and the vascular response in periodontal disease.

STATEMENT

This report contains no material which has been accepted for the award of any other degree or diploma in any university.

To the best of my knowledge and belief, this report contains no material previously published or written by another person, except where due reference is made in the text of the report.

The author consents to the thesis being made available for photocopying and loan if accepted for the award of the degree.

D. LEE

ACKNOWLEDGEMENTS

I would like to express my sincere appreciation to:

Dr. M.R. Sims, Reader in Orthodontics at the University of Adelaide for providing invaluable guidance throughout the study and editorial assistance in preparing this report;

Dr. K. Bartusek of the Electron Optical Centre for access and instruction in the use of the scanning electron microscope;

Dr. P.R. Crowe for assistance in surgical procedures;

Ms. J. Fuss for her advice on technical matters; and

The A.S.O. Foundation for Research and Education for financial support.

INTRODUCTION

The vasculature acts as a transport system to bring nutrients to and remove waste products from the oral tissues, and is intimately involved in inflammation and wound healing. Spatial appreciation of the oral microvasculature is important for an understanding of its physiologic function.

The architecture of the oral vasculature has been studied in various animals, including mice (Wong, 1983; Wong and Sims, 1987), rats (Kindlova and Matena, 1959, 1962; Weekes, 1983; Weekes and Sims, 1986a, 1986b), dogs (Egelberg, 1966; Nuki and Hock, 1974; Kishi and Takahashi, 1977; Takahashi *et al.*, 1985), and monkeys (Kindlova, 1965; Castelli and Dempster, 1965; Rohen, Arnold and Wachter, 1984).

The oral microvasculature has been shown to be peculiar to each species, varying from tooth to tooth and changing with different locations around the tooth (Kindlova, 1965; Kishi and Takahashi, 1977; Weekes, 1983; Wong, 1983).

Various methods have been used to study the arrangement of the blood vessels. The corrosion cast technique produces a three-dimensional replica of the blood vessel lumen. The vascular architecture can then be studied with the scanning electron microscope (SEM), using its superior magnification, resolution and depth of focus. A list of SEM investigations using corrosion casts is provided by Lametschwandtner, Lametschwandtner and Weiger, (1984).

Stereopair viewing of SEM micrographs provides a clearer three-dimensional picture of the vascular bed (Howell, 1975). It allows the connection, orientation and distribution of vascular elements to be visualized.

The rodent and dog periodontium are subjected to different patterns of masticatory forces because of differences in their diet and masticatory apparatus. On the other hand, the nonhuman primate dentition is similar to that of man. The marmoset periodontium shows pathologic and age changes similar to those seen in man (Levy, 1971; Levy *et al.*, 1970, 1972a). The marmoset temporomandibular joint shows similar movements to that of man (Wilson and Gardner, 1982). The study of the monkey microvasculature could provide information for extrapolation to man in understanding oral microvascular bed function in health and disease.

None of the studies on monkey oral microvasculature provide sufficiently detailed information of the microvasculature. Vessel classification and true three-dimensional presentation using stereopairs is seldom employed. An SEM study of microcorrosion casts of the oral microvasculature of the primate will help to fill the void in our current knowledge.

AIMS OF THE INVESTIGATION

The aim of this investigation is to study the normal microvascular architecture of the marmoset palate and periodontium to enable species comparison for understanding vascular physiology. Methacrylate corrosion casts will be studied using SEM stereopair imaging.

Vascular casts will be classified using the imprint patterns on the casts described by Hodde *et al.* (1977), the branching pattern, and the vessel diameters described by Rhodin (1967, 1968).

The results will enable comparisons to be made with similar studies on the periodontal and palatal vasculature of mice (Wong, 1983), rats (Weekes, 1983), and dogs (Takahashi *et al.*, 1985). From the limited number of animals, an attempt will be made to compare the vasculature of young and old adult marmosets to evaluate ageing changes in the microvascular bed.

LITERATURE REVIEW

Many investigations have been carried out on the vasculature of the oral cavity. A variety of techniques have been used, mostly involving perfusion of the vascular tree. Animals that have been studied include mice, rats, hamsters, dogs, cats, guinea pigs, opossums, rabbits, monkeys and man (Kindlova & Matena, 1959, 1962; Boyer and Neptune, 1962; Huelke and Castelli, 1965; Carranza *et al.*, 1966; Cohen, 1960; Weekes, 1983; Castelli, 1963).

TECHNIQUES FOR STUDYING THE VASCULAR ARCHITECTURE

I. Histological techniques

The vasculature can be studied in stained sections or cleared sections by perfusing the vessels with a dye or contrast medium (Castelli, 1963; Egelberg, 1966). The three-dimensional architecture is then reconstructed from serial sections. The limited depth of focus with the light microscope poses a severe limitation for the study of the vascular architecture.

II. Micro-angiographic Techniques

The specimen is injected with a radio-opaque solution, sectioned, exposed to X-rays and the image recorded on a photographic plate. The image can be enlarged or examined under the light microscope. Unfortunately, the image is two-dimensional, with super-impositioning of images from different tissue planes.

III. **Microsphere Technique**

Folke and Stallard (1967) infused blood vessels with microspheres of about 15um (±5) diameter to study the vascular network. Tissue sections were examined to study the size and distribution of the periodontal vessels. However, the limitations of light microscopy restrict the usefulness of this technique.

IV. **Vital Microscopy**

Superficial blood vessels can be observed *in vivo* under the light microscope. Deeper vessels cannot be observed, so this technique is unsuitable for detailed study of the vascular architecture and its connections in three dimensions.

V. **Corrosion Cast Techniques**

Most investigators refer to the casting by the gross anatomical term "*corrosion cast*" (Murakami 1971, 1972). Gannon (1978) calls them *vascular casts*. The terms *injection method, microcorrosion cast, injection replica* and *vascular corrosion cast* have all been used. To standardize terminology, Lametschwandtner *et al.*, (1984) recommended that the term *vascular corrosion cast* be used for casts of the blood vessels and lymphatics.

The vascular casting technique has been in use for hundreds of years for anatomic study. The earliest reported study was by Leonardo da Vinci (1452-1519), who cast the heart chambers and cerebral ventricles with wax (Hodde and Nowell, 1980).

With this technique, the vascular tree is perfused with a liquid from the venous or arterial end. When the liquid

solidifies, the tissues are corroded away to leave the luminal contents as a three-dimensional cast of the lumen.

The resulting cast is examined under the stereo light microscope (Kindlova & Matena 1959, 1962; Lenz 1968) or scanning electron microscope (Lenz 1968, 1974; Ichikawa *et al.*, 1977; Nakamura *et al.*, 1983).

The SEM allows the examination of surface detail of a structure in three dimensions. It provides much better magnification, resolution and depth of field than the optical microscope. The SEM can resolve topographical details of less than 50 Angstroms with a depth of focus 500 times that of an optical microscope at equivalent magnifications (Black, 1974). The specimen need not be sectioned to thin slices and it can be rotated, tilted, and moved along three axes in the SEM. Images can be recorded for future reference and for scientific communication.

The advantages of the SEM corrosion cast technique have been summarized by Lametschwandtner *et al.* (1984):

1. The SEM provides a quasi three-dimensional image of the vascular bed with greater depth of focus.
2. Large specimens can be examined.
3. Excellent manipulation of the specimen in the SEM specimen stage is possible by tilting, rotating and shifting in three planes of space.
4. Vessels can be identified by luminal diameter and endothelial imprints on the casts (Hodde 1981).
5. Vascular structures like circular constrictions, sphincters, anastomoses *etc.* can be visualized.

6. Vascular routes can be traced and photographed, and presented in stereopair images for three-dimensional visualization.
7. Individual vessels can be studied with respect to their origin, course, number of branches, branching angles and direction of orientation. Three dimensional connections in the vascular network can be visualized.
8. SEM images provide much more information than reconstructions from serial sections and enable us to study large areas in one view.

The disadvantage of corrosion casting is that all tissues are corroded away, leaving only a replica of the vascular channels. Spatial orientation to other structures such as cementum and bone, is lost.

Gannon (1985), therefore, suggested using corrosion casting in conjunction with other techniques such as histology, TEM, tissue SEM and intravital microscopy to study the vasculature.

Sobin and Tremer (1980) emphasized that vascular perfusion demonstrates the total vascular bed rather than the functional vascular bed, unless the dynamic state of the vascular bed at the time of perfusion is captured by quick-freezing. Furthermore, significant dimensional changes in the blood vessels occur with such techniques, due to agonal constriction of vessels which alters the microvascular bed.

The criteria for selecting corrosion casting compounds have been discussed by Nowell and Lohse (1974) and Gannon (1978). There are two main types of casting material

currently used that satisfy most of the criteria: rubber compounds and polymeric resins (Hodde and Nowell, 1980).

Rubber Compounds

Latex has been used by various investigators including Kindlova and Matena (1959, 1962), Kindlova (1963, 1965, 1970) and Nowell and Lohse (1974). The use of the SEM to study latex microcorrosion casts was first reported in 1970 by Nowell, Pangborn and Tyler. Dried latex casts readily droop, shrink and adhere, and are therefore not suitable for scanning electron microscopy (Murakami, 1971).

Silicone rubber compounds do not survive the digestion process due to the fragility of the silicone polymer (Gannon, 1978) and are generally unsuitable for SEM observation.

Polymer Resins

In 1971, Murakami introduced SEM examination of acrylic resin corrosion casts of blood vessels. Methyl methacrylate casts can withstand strong acid and alkali corrosion; they are dimensionally stable and strong enough to maintain the vascular architecture and not collapse under their own weight. The casts can be rendered conductive and examined in the SEM.

CLASSIFICATION OF BLOOD VESSELS

In spite of the fact that there have been many investigations into periodontal ligament vasculature, few investigators have attempted to provide a classification of blood vessels. Those who did gave only very brief criteria for their classification, or none at all.

The identification of vessels by diameter alone has been criticized because in the living animal, the vessel diameter is not constant due to autoregulatory mechanisms. Also, the diameter of a small arteriole in one specific vascular bed may be quite different from that in the same tissue of a different animal (Wiedeman, 1984). Differences exist in different tissues as well.

Rhodin (1968) advised that vascular diameter, perivascular elements and the relationship of the vessel to the vascular system as a whole be considered for accurate classification of microcirculatory segments. Ideally, a combination of criteria should be used in identifying each segment of the microcirculation.

Rhodin (1967, 1968) classified vessels of the fascial (subdermal) circulation of the rabbit thigh muscles, according to internal diameter, endothelial cell morphology, presence of pericytes, veil cells and muscle cells.

Since the ultrastructural detail of the vessels will be lost after tissue corrosion, Rhodin's classification cannot be fully applied. However, part of his criteria relating to internal diameter is useful for corrosion casts and will be applied in this study (Table 1).

VESSEL	INNER DIAM. (um)
Arteriole	50 - 100
Terminal arteriole	<50
Precapillary sphincter	7 - 15 (these taper off to an arterial capillary within 50um) Average diameter 10um
Venous capillary	Up to 8
Postcapillary venule	8 - 30
Collecting venule	30 - 50
Muscular venule	50 - 100
Collecting vein	100 - 300

Table 1: Inner diameter of blood vessels.

(From Rhodin, 1967, 1968)

Rhodin (1967) cautioned that the arteriolar diameter that he reported may vary by ±2um since the diameter measured in his specimen may not be the maximum diameter. Also, the state of dilation or constriction of the vessels at the time of examination was unknown.

Endothelial Imprint Pattern

Since all the tissues are corroded away in this corrosion cast study, all that remains to help in identification of the vessels is the vascular replica. Fortunately, the vessel endothelium leaves a characteristic imprint on the vascular cast which could be used to distinguish between arteries and veins (Hodde *et al.*, 1977; Hodde and Nowell, 1980). Also, vessel diameter, vessel shape,

the pattern of branching and interconnection with other vessels aid in vessel identification.

Hodde (1981) described the arterial endothelial cell outline as being oblong, and having ovoidal nuclei with microvillous protrusions. The long axes of the nuclei were parallel to that of the vessel. Venous endothelial cells had irregular outline. Their nuclei were circular, and without microvillous protrusions. The venous nuclear imprints did not have as flat a base as the arterial imprints. Precapillary sphincters were recognized as regions of increased density of the endothelial cell nuclei imprints and reduced vessel diameter.

According to Miodonski, Kus and Tyrankiewicz (1981), both types of imprint patterns may be observed on vessels of diameter greater than 8-10μm in completely filled and cleaned casts. The surfaces of the casts of the capillaries was usually smooth.

In summary, it is possible to provide a reasonably accurate classification of the internal replica of the periodontal vasculature using the following criteria :

1. vessel diameter
2. vessel shape
3. patterns of branching and anastomosis
4. cellular impressions on the cast surface

   These impressions arise from :

   a) endothelial cell nuclei

   b) endothelial cell borders

Oral Vasculature in various animals

The vasculature of the periodontal ligament has been reviewed by Saunders and Rockert (1967), Edwall (1982) and Schroeder (1986). Although there are basic similarities in the vasculature amongst the animals, there exist distinct differences between the different species in the blood supply to the periodontal ligament.

Within each species, there are differences in the vasculature in different teeth and in different locations in the periodontium of the same tooth (Kindlova, 1970; Weekes, 1983; Wong, 1983).

The blood supply to the periodontal ligament can be said to arise from three sources:

1. Branches of the dental artery arising apically,
2. Branches from the alveolar bone, and
3. Branches from the gingiva at the neck of the tooth.

Vessels in the periodontal ligament form a longitudinal network. These vessels are located closer to the bone than to the root. The vascular pattern in the periodontium and palate of various species will be reviewed.

Oral Vasculature in Monkeys

Cutright and Hunsuck (1970) studied cleared sections of macaque tissue injected with silicone latex. They described vessels of the hard palate anastomosing, via the gingiva, with the periodontal ligament plexus and with vessels of the buccal alveolar mucosa.

In the oral mucosa, each connective tissue papilla was supplied by one or more simple or helical capillary loops. Capillary loops were longest on the palatal mucosa and

gingiva, and shortest between the rugae and on the flat surfaces of the palate, the loops at the tips of the rugae and on the alveolar mucosa being intermediate in height. The loops of the hard palate were shorter than those of the soft palate in all areas. Cutright and Hunsuck (1970) did not find any generalized relationship between the height of the loops and the physiology or function of an area. However, Stablein and Meyer (1984) suggest that a relationship exists between the height of the loops and the thickness of the overlying epithelium.

In the alveolar mucosa, Cutright and Hunsuck (1970) noted an antero-posterior orientation of blood vessels. The gingiva received its blood supply from three sources:

1. from mucosal blood vessels (the largest supply),
2. from gingival vessels anastomosing with the periodontal ligament, and
3. from the alveolar bone (minor contributions).

Gingival loops originated at the junction of the attached and free gingiva and ran to the gingival crest. These loops in the cervical third of the free gingiva had many interconnecting anastomoses. However, Cutright and Hunsuck (1970) did not describe the periodontal ligament and crevicular gingival vasculature in any detail.

More detailed information about the periodontal ligament and crevicular vasculature was reported by Kindlova (1965), who studied the macaque using latex corrosion casts and histological sections. She described the main vessels of the periodontal ligament as running longitudinally and located adjacent to the bony wall, partly grooving it. These vessels gave off branches towards the tooth that formed a flat

irregular network of capillaries. This pattern was present in all teeth on all aspects except adjacent to the interradicular septum of multi-rooted teeth. The flat capillary network was located closer to the tooth than the main periodontal vessels. Unfortunately, connections between the capillary network and periodontal veins were not established as the venous vessels failed to fill with latex.

Although the periodontal ligament received its blood supply from both gingival and alveolar bone vessels, this difference in source did not influence the structure of the capillary network, whose architecture apparently depended on the character of the tissues supplied. No criteria of vessel classification or dimensions were mentioned by Kindlova (1965), although she used the terms "arteries" and "veins" to describe vessels in the periodontium.

Kindlova (1965) also described anastomoses between the periodontal ligament vessels and the gingival vessels at the marginal part of the periodontium. Saunders (1967) and Lenz (1968)[cited by Schroeder, 1986] confirmed this gingival-periodontal anastomosis. In the region of the anastomoses arose two or three rows of straight slender loops with arterial and venous limbs of equal length. These extended into the crest of the free gingiva where there was another anastomosis with the capillary loops supplying the oral epithelium. However, Kindlova (1965) did not mention the orientation and height of the capillary loops on the oral aspect of the gingiva.

In the coronal extremity of the periodontal ligament, the flat capillary network was condensed into a narrow band (figure 1). Coiled capillaries resembling glomeruli arose

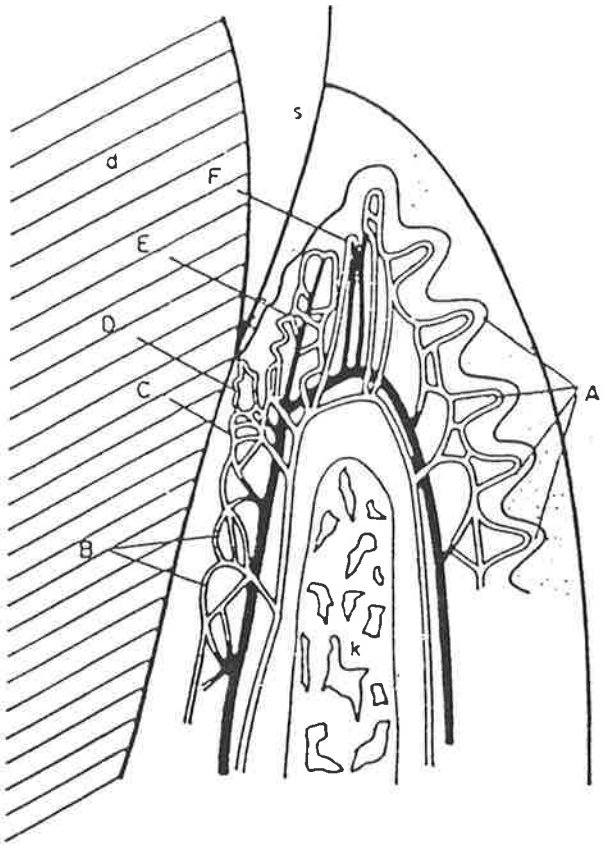

Figure 1. The blood supply of the marginal periodontium in the monkey. (From Kindlova, 1965).

A - Subepithelial capillary network of the gingiva

B - Flat capillary network of the periodontal ligament

C - Narrow band of denser capillary network

D - Coiled capillaries resembling glomeruli

E - Capillary loops with amply coiled arterial part

F - Simple capillary loops

s - enamel

d - dentine

k - bone

from this band. These capillaries appeared to be present to a greater extent in the posterior teeth than in anterior teeth and were most numerous interdentally. Coronal to these glomeruli were "tenuously looped capillaries with clearly coiled arterial parts" found near the epithelial attachment. These glomeruli were considered by Kindlova (1965) to be part of the periodontal ligament, although other workers (Wong, 1983; Weekes, 1983) disagreed.

Kennedy (1969) studied the periodontal vasculature of squirrel monkeys using India ink perfusion. Direct communication was occasionally found connecting supra-periosteal vessels to those of the periodontal ligament. This communication was also found in rats (Garfunkel and Sciaky, 1971). Although the gingiva received blood from the periodontal ligament and the supraperiosteal vessels, Folke and Stallard (1967) and Kennedy (1969) stated that the primary blood supply came from supraperiosteal vessels. This was later confirmed by Cutright and Hunsuck (1970). However, Kennedy (1969) did not clarify whether this arrangement was found in all sites in the mouth.

Kennedy (1974) noted that the supply to the gingival col was derived from supraperiosteal vessels and vessels perforating the crest of the interdental septum. He did not establish blood supply to the col from the periodontal ligament, as reported by Garfunkel and Sciaky (1971) in rats.

From the examination of two macaque monkeys in each study, Cutright and Bhaskar (1967) and Rohen, Arnold and Wachter (1984) could not find the coiled capillaries described by Wedl (1881) and Schweitzer (1909) in the periodontal ligament.

Castelli and Dempster (1965) described the blood vessels entering the periodontal ligament space mainly through perforations in the cribriform alveolar plate. These were most numerous in the middle and apical thirds of the socket. They found no arterial vessels from the gingiva supplying the mandibular periodontal ligament, but these were present in the maxilla, especially in the incisor region. Upon entering the periodontal ligament space, interalveolar arterioles immediately broke into capillaries with a polyhedric plexiform pattern orientated axially. These capillaries formed a layer close to the cementum. Venules, seen as thick irregular vessels, were present in the ligament and anastomosed with one another to form a mesh closer to the alveolar wall than the capillary layer.

Castelli and Dempster (1965) noted two directions of venous drainage from the periodontal ligament,

a) apically towards the apex and,
b) through the cribriform plate into the bone marrow network in the interradicular and interalveolar septa.

Periodontal veins increased in diameter as they coursed towards the apex. These veins joined with those from the pulp at the apex to form a dense venous plexus in the bone marrow. The periodontal ligament veins also anastomosed with those of the gingiva, forming a drainage outlet primarily for the gingival crevice region.

According to Folke and Stallard (1967), the vessels supplying the epithelial attachment in the squirrel monkey were derived mainly from the alveolar crest. These vessels were arranged parallel to the epithelium. The col region was supplied by vessels from the crestal bone as well as from the

periodontal ligament. However, there was no mention of supply from supraperiosteal vessels of the lingual and buccal interdental papillae, reported by Garfunkel and Sciaky (1971) and Kennedy (1974). Furthermore, there was no mention of any circular vessel related to the epithelial attachment (Wong, 1983; Weekes, 1983).

Cutright and Bhaskar (1967) described the source of the periodontal ligament vasculature in the apical region as the interalveolar and apical arteries, whereas the cervical portion obtained its supply not only from the interalveolar arteries, but also from the vascular plexus of the gingiva. However, they did not describe the gingival vasculature in any detail.

Levy, Dreizen and Bernick (1972a) provided little information about the marmoset periodontal vasculature with their histological study. They described interalveolar branches perforating the cribriform plate into the periodontal ligament. Vessels in the periodontal ligament ran closer to the bone than to the root; arterioles and capillaries were given off and passed towards the cementum. This arrangement of capillaries closer to cementum was noted by Castelli and Dempster (1965). Above the alveolar crest, Levy *et al.* (1972a) described vascular branches arising from the periodontal ligament, palate and alveolar mucosa supplying the gingival area. No detailed description of the vascular architecture was given, and there was no mention of which teeth they studied.

In the interproximal region, vessels passing gingivally from the mesial surface of one tooth and the distal surface of an adjacent tooth formed a plexus which sent capillaries

into the connective tissue papillae. However, there was no mention of any contribution from the interdental papillae or from alveolar crest vessels. The orientation of the col network could not be established with their histological technique.

Levy *et al.* (1972a) noted that on the buccal and lingual surfaces of the teeth, a plexus of terminal capillary loops was formed by vessels from the periodontal ligament and from the buccal and lingual mucous membranes. However, they did not mention the height and orientation of these loops.

Oral Vasculature in man

Detailed information on the oral microvascular architecture in the human is lacking.

Hayashi (1932) obtained serial sections of the jaws of cadavers injected with carmine gelatin. He described the dental artery running through the bone, giving off first the interalveolar branches near the bottom of the alveolus. These branches ran coronally on both the labial and lingual aspects to surround the alveolus, and perforated the cribriform plate to supply the periodontal ligament. On entering the periodontal ligament, each dental artery gave off side branches, termed periodontal rami, which surrounded the root. The periodontal ligament vessels had a longitudinal orientation, and received blood from the gingival vessels.

Steinhardt (1935) found the blood supply to the periodontal ligament to be better in the gingival and apical parts than in the middle part.

Castelli (1963), studying mandibular material cleared by the Spalteholz method, found that veins emerging from the

periodontal ligament and alveolar bone united with one another and also with the veins of the interalveolar or interdental septa. The illustration in his paper showed a longitudinal arrangement of periodontal ligament vessels, but he did not state which of the teeth he studied. The gingival circulation was not described.

Provenza, Biddix and Cheng (1960) noted the presence of convoluted vessels in the periodontal ligament of two patients with periodontal disease. These structures, which they called glomera, were found throughout the periodontal ligament (Provenza, 1964), but were more abundant apically. They were most abundant in the interradicular periodontal ligament (Provenza *et al.*, 1960). These glomera were observed histologically, and their three-dimensional pattern was not described. No section of any glomus was observed to possess the characteristics of capillaries.

Provenza (1964) suggested that the glomera in the human periodontal ligament may act as shunts for blood to pass from arteries to veins.

Oral vasculature in mice

Freeman and Ten Cate (1971) observed that in the developing mouse periodontium, blood vessels occurred closer to the alveolar bone than to the root surface. This finding was supported by Carranza *et al.*, (1966).

Carranza *et al.* (1966) also described the presence of a circumferential plexus close to the epithelial cuff, composed of vascular loops. However, they did not relate these loops to any circular band (Kindlova and Matena, 1962; Kindlova, 1965). The morphology and orientation of the vascular loops were not described.

Carranza *et al.* (1966) reported that connections between gingival and periodontal blood vessels were scarce. Blood vessels in the alveolar bone supplied branches to the periodontal ligament, particularly in the middle and apical thirds of the root. Perforating vessels emerging in the periodontal ligament immediately pursued a course parallel to the long axis of the tooth.

Sims (1983) stated that in the cervical and apical regions of the mandibular molar, the ligament vascular network was a predominantly venous pool of postcapillary-sized venules. These vessels were larger and more numerous apically, and they did not exhibit the features of postcapillary venules found in other microvascular beds.

Wong (1983) conducted a methacrylate corrosion cast study of the blood supply of mouse molar periodontium which he assessed with stereopair imaging using the SEM. Maxillary and mandibular molar periodontal ligaments were reported to have similar microvascular patterns.

The gingival vasculature consisted of an outer circular vessel system located occlusally and connected to the mucosal vessels, and an inner circular vessel group situated adjacent to the epithelial attachment (figure 2). The outer (capillary) and inner (venous) systems were linked by radially orientated anastomoses; the latter anastomosed with the periodontal ligament vessels.

The outer circular system enclosed the three molars in a continuous path just beneath the crestal epithelium, and curved interdentally without traversing the col. The principal vessel in this outer circular system was a single, 7*um* capillary, with two groups of capillary-sized vessels branching off inferiorly down the inner (crevicular) and outer (vestibular) slopes of the alveolar bone.

The outer slope consisted of a capillary network of flattened fish-net pattern which communicated with mucosal capillaries. However, there was no mention of loops in this outer slope, described by Cutright and Hunsuck (1970) in monkeys.

The inner circular system venous vessels (10-15*um* in diameter) encircled each molar just below the epithelial attachment (Wong and Sims, 1987). In the col region, the inner circular systems of adjacent teeth joined to form a single vessel 7*um* in diameter.

Wong (1983) also described the presence of glomerular-like vascular formations radiating towards the crevicular epithelium from the inner circular vessel system (figure 2). These glomerular-like structures were found on all aspects of the tooth socket, but they appeared to be fewer in number

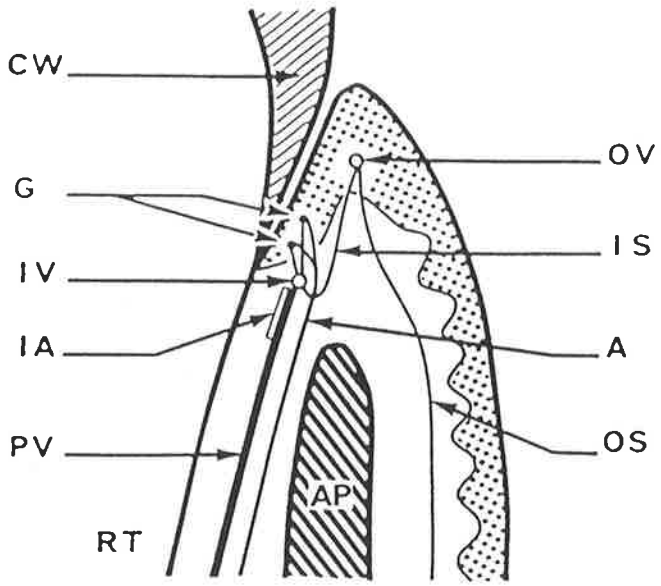

Figure 2. Diagram showing the bucco-lingual gingival vessels through a mid-coronal section of a molar. (From Wong, 1983).

A - arterial vessel.

AP - alveolar process.

CW - crown enamel.

G - glomerular vascular structures.

IA - axially aligned inner vessel.

IS - inner slope vessel.

IV - inner single circular vessel.

OS - outer slope vessel.

OV - outer single circular vessel.

PV - periodontal ligament venous vessel.

RT - root.

along the mesial and distal slopes of the marginal gingivae. He suggested that these glomerular-like structures may give rise to interstitial crevicular fluid and thus flush the gingival crevice. In contrast to the findings of Kindlova (1965), these glomeruli were located in the crevicular gingiva (*vide supra*: 3.13).

Large venous-like periodontal ligament vessels found in the coronal third of the ligament were connected to the inner circular vessel system by short axial connecting vessels of the same size.

The major periodontal ligament vessels were arranged in a palisade manner, extending towards the apex to form a hammock-like cushion arrangement. The periodontal ligament vessels were axially orientated, occurring as single vessels or in tracts. Wong (1983) found a dense plexus of veins in the apical third of the periodontal ligament, with a mean diameter of 26um, forming a hammock arrangement. The apical network vessels were larger than those of the cervical third, and more closely packed. The interradicular ligament area had huge reservoir-like venous cushions.

Medullary vessels anastomosed with gingival and periodontal ligament vessels at various levels. Vertically orientated capillary-like loops were found in the mid-third of the periodontal ligament, connecting arterial vessels to venous vessels.

Wong (1983), and Wong and Sims (1987), stated that the palatal mucosa vasculature consisted of repeating consecutive units of crests and troughs. Each rugal crest consisted of a compact group of transversely-orientated vessels, 8-10um in diameter, surmounted by a single 10um capillary.

Numerous capillary vessels (8um in diameter) branched off at regular intervals perpendicular to this single crestal capillary. These branches were parallel to each other, orientated sagittally, and thrown into loops (Wong and Sims, 1987). They could be found on the anterior and posterior slopes of the ruga.

The branches sloped down from the crest in a wavy manner and linked up with a few large underlying venous-like vessels. The looped capillaries changed to a flattened plexus in the inter-rugal troughs. These underlying venous vessels, 50-150um in diameter, were only found in some of the inter-rugal areas. When present near the epithelial surface, they were often not covered by the fine vessels of the trough. However, there was no mention of the orientation of the venous vessels.

Oral vasculature of rats

In the palate of the rat, Weekes (1983) found a random capillary network in the inter-rugal troughs, comprising capillaries 8-10um in diameter. The capillary plexus was flat and parallel to the surface epithelium. There was neither mention of capillary loops in the inter-rugal troughs, nor were loops illustrated. This capillary plexus was supplied by arterioles coming up from the deeper connective tissue perpendicular to the epithelial surface. Capillary branches radiated from the top of each arteriole resembling the spokes of a wheel.

The capillary plexus drained into postcapillary venules 25-30um in diameter, which coalesced to form collecting venules and drained into the deeper connective tissue.

However, the orientation of the arterial and venous network was not mentioned.

On the slopes of the ruga, the capillary plexus was organized into parallel rows running in a sagittal direction, breaking up into a disorganized random capillary plexus 200-250um away from the rugal crest. Unlike the inter-rugal capillary plexus, the vessels on the slopes of the rugae "followed a sinuous path with the plane of the curves perpendicular to the epithelial surface". Weekes (1983) did not actually describe any loop arrangement. These sinuous vessels were drained by postcapillary venules which branched off at right angles into the deeper connective tissues.

On the rugal crest, there were capillary loops arranged transversely along the ruga to form a vascular spine. These capillary loops were hairpin shaped and clustered together on the rugal crest. The height and density of the capillary loops was not described nor illustrated. These crestal capillary loops drained into postcapillary venules that drained back into the rugal connective tissue, or into sinuous capillary vessels on the slopes of the rugae.

Boyer and Neptune (1962) noted that branches of the inferior alveolar artery and the incisal periodontal ligament network supplied the interradicular and interdental bone, the periodontal ligament, and pulp of the rat molar teeth. A similar vascular arrangement was found for the hamster mandibular molar.

Kindlova and Matena (1962), in a latex corrosion cast study of the rat lower molar, described arteries of the periodontal ligament with a palisade formation, running axially to the neck of the tooth and partly embedded in bone.

These arteries were connected by capillaries that supplied the periodontal tissue. Interproximally, capillary loops from adjacent teeth anastomosed. The sizes of the arteries were not mentioned.

Veins drained the ligament in an axial direction towards the apex where they formed a plexus. At the peak of the interradicular septum, they formed a rich network (figure 3).

Gingival capillaries connected with the capillary loops of the periodontal ligament at the alveolar margin by venous anastomoses. These gingival vessels did not extend below the contact point of adjacent teeth. The interdental papilla was claimed to be supplied solely by vessels of the periodontal ligament.

Although anastomoses do occur between the periodontal ligament and gingival network, each forms a separate system (Kindlova and Matena, 1962). The network in the coronal part of the periodontal ligament is characterized by the presence of "coiled periodontal loops" arising from a "horizontal circulus" formed by arcades of periodontal ligament vessels (figure 3).

Weekes (1983), and Weekes and Sims (1986a, 1986b) investigated the rat molar periodontal blood supply with an SEM study of methyl methacrylate corrosion casts. The periodontal ligament was found to contain capillaries and postcapillary-sized venules arranged occluso-apically in tracts of four to six vessels. These vessels could be traced uninterrupted, from the apex to the gingival plexus. Except at the interradicular septum, the ligament vasculature arose mainly from the deeper gingival vessels.

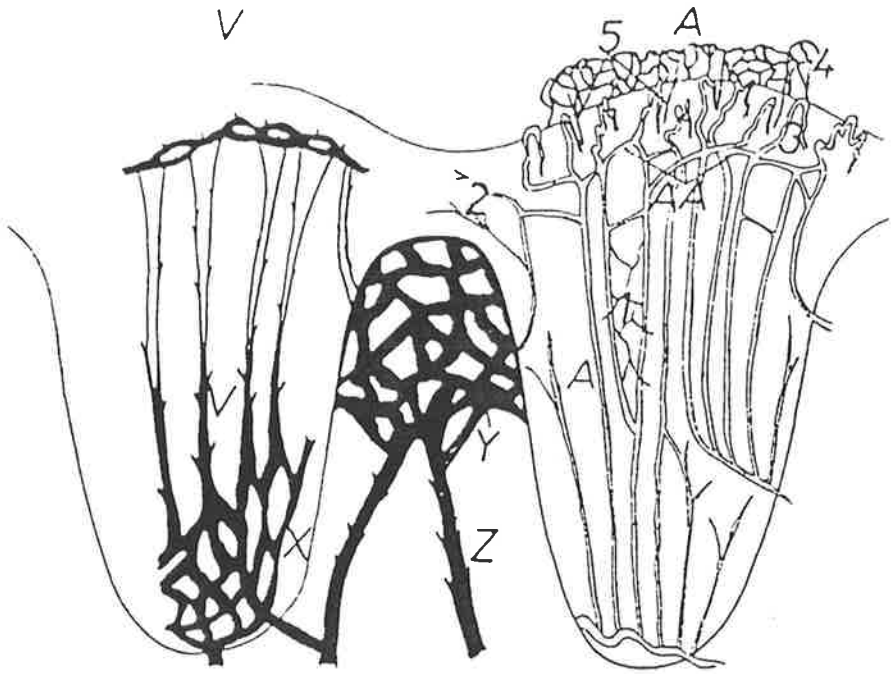

Figure 3. Diagram of the periodontal vasculature of the rat molar. Arterial system (A) on the right with the venous system (V) on the left and the bifurcation pattern in between. (From Kindlova and Matena, 1962).

A - Arteries.

AA - Arcade-shaped communication of periodontal arteries, forming a horizontal circulus.

1 - Capillary network supplying periodontal ligament.

2 - Capillaries supplying periodontal tissue above the interradicular septum.

3 - Coiled periodontal loops supplying marginal part of periodontium.

4 - Capillary network supplying marginal gingiva.

5 - Communications of gingival with periodontal capillaries.

V - Veins.

X - Venous rete below apex.

Y - Venous rete on peak of interradicular septum.

Z - Veins draining blood from the interradicular septum.

These ligament vessels were situated closer to bone than to the tooth, a finding similarly reported by Nakamura *et al.*, (1983). The proximal periodontal ligament (over the interdental septum) was more dense than the network on the buccal and lingual walls.

Loops were demonstrated in the cervical third of the periodontal ligament, and in the apical region (Weekes and Sims, 1986a). In the apical region, these loops were postcapillary-sized venules 100*um* in height and 15*um* in diameter, and located over the interdental septa. No explanation was given for the distribution of these loops.

According to Weekes and Sims (1986a), arterioles were not found to course in the periodontal ligament on the buccal, lingual or proximal aspects. Medullary arterioles drained into the occluso-apically orientated postcapillary-sized venules of the periodontal ligament directly, without passing through a capillary bed. However, in the inter-radicular ligament, communications between the ligament plexus and the medullary network were predominantly venular (Weekes, 1983).

The interradicular periodontal ligament was supplied by terminal arterioles from the bone that emerged into or joined with occluso-apically orientated postcapillary-sized venules, forming a complex vascular plexus of postcapillary-sized venules.

These postcapillary-sized venules did not run uninterruptedly all the way from the apex to the crest of the septum. Instead, they coursed occluso-apically in a series of repeating segments of 100-400*um* within the ligament. Venular loops were also described in the inter-radicular ligament,

but their significance was not explained (Weekes and Sims, 1986a).

Weekes (1983) reported vessels from adjacent molar sockets anastomosing over the crest of the interdental septa, thus confirming the findings of Garfunkel and Sciaky (1971). The periodontal ligament vessels anastomosed freely with vessels in the gingiva and alveolar bone.

Weekes (1983) suggested that the occluso-apical orientation of ligament vessels helped to maintain the patency of the blood vessels during functional loading of the tooth.

In the gingival connective tissue beneath the crevicular epithelium, Weekes and Sims (1986b) described a flat capillary plexus extending from the cemento-enamel junction up to the crest of the free gingival margin. On the buccal and lingual aspects of the tooth, twisted vascular loops comprising mainly postcapillary-sized venules arose from the middle third of this plexus. These loops had a capillary ascending limb which wound around itself and the postcapillary venule descending limb.

In the interproximal col, these vascular loops exhibited a more complex vascular arrangement, resembling kidney glomeruli or intestinal villi, and occupied most of the volume of the col tissue. In contrast, glomeruli were found within the periodontal ligament in monkeys (Kindlova, 1965), *vide supra*: 3.13. Garfunkel and Sciaky (1971), on the other hand, could not demonstrate glomeruli with their India ink perfusions.

Weekes and Sims (1986b) found the apical and coronal extents of the flat plexus demarcated by a circularly

orientated vessel at each end, with the flat plexus extending between them. The apical circular vessel was continuous, but the coronal circular vessel exhibited some discontinuity.

Arterial supply to the flat plexus came from the gingiva proper, but venous drainage from the plexus was directed into the periodontal ligament plexus as well as the deeper gingival vessels. Connection with the vestibular vasculature was not described in detail.

In the interproximal col region, the flat network narrowed to a thin band, occupying the lower half of the crevice, adjacent to the epithelial attachment. Arterial supply to the col region was from the tissues of the buccal or lingual interdental papillae. However, the orientation of the col vasculature was not described.

Weekes (1983) did not find the horizontal inter-communicating plexus between periodontal ligament vessels and capillary loops in the cervical region described by Kindlova and Matena in 1962. The vestibular aspect of the gingiva was not described in his study.

Nakamura *et al.* (1983) studied the rat molar vasculature using light microscopy with colloidal carbon perfusion, and using SEM examination of corrosion casts. In the light microscope, vessels were seen running parallel to the long-axis of the tooth. At the root apex, the blood vessels were relatively thick and "basket-shaped", and arranged radially. They suggested that the apical vessels may act as a cushion between the tooth and alveolar bone. Hairpin loops were found, but their height, orientation and distribution were not mentioned.

Sims, Sampson and Fuss (1988) have demonstrated the presence of glomeruli in the germ free rat gingival crevice, on the buccal, lingual and proximal aspects of upper and lower molars. These glomeruli were thought to be the result of gingival inflammation (Egelberg, 1966; Hock and Nuki, 1970 and 1975), but their presence in the gingiva of germ free rats leads to the conclusion that they are a normal feature of clinically healthy gingivae.

Oral vasculature of dogs

Takahashi *et al.* (1985) divided the palatal vasculature into three layers: the lamina propria, the submucosa, and the subperiosteum. They described the presence of a venous plexus "running longitudinally" in the submucosa of the hard and soft palate. This plexus received blood from venules of the overlying lamina propria at regular intervals, but mainly under the rugae.

From the rear of the molar teeth region to the soft palate, they noted large numbers of bicuspid venous valves in the submucous venous vessels of inner diameter of 100-800um. The existence of many valves in minute veins in the palate indicated that they may participate in regulating blood flow in this area.

Takahashi *et al.* (1985) suggested that the venous plexus acted as a cushion for a mass of food taken into the mouth and impacted on the palate wall, since dog mastication primarily involved hinge motion. It was postulated that the venous plexus, together with the dense vascular capillary network of the tunica propria, might play some role in the

control of oral surface temperature, very similar to that of the tongue in the regulation of peripheral body temperature.

Takahashi *et al.* (1985) did not describe the capillary architecture and vascular connections between the palate, gingiva and periodontal ligament.

Kishi *et al.* (1986a) studied the gingival and mucosal vasculature of the dog using SEM examination of corrosion casts. Unfortunately, they did not demonstrate their micrographs in stereopairs.

Supraperiosteal arteries crossed the alveolar crest and divided into two groups. One group ran towards the crevicular epithelium, the other curved along the vestibular epithelium of the gingiva, giving off numerous branches to the surface.

Capillary loops were found on the vestibular surface of the gingiva, essentially consisting of hairpin loops. The actual height of the loops and their orientation was not described. No particular orientation was evident in their illustrations. Furthermore, the sites from which their illustrations were taken were not revealed.

Loops were found extending from the gingival margin to the muco-gingival junction. The loops became shorter and the space between the two limbs of a loop became narrower towards the muco-gingival junction (Kishi *et al.*, 1986a). Venules 45-55um in diameter and arterioles 15-20um in diameter were found running parallel to each other beneath the capillary network. However, their orientation was not described.

The capillary network in the alveolar mucosa was denser in arrangement and different from that of the gingiva. Capillary loops were also present in the alveolar mucosa, but they were extremely low in height and few in number. The

capillary network formed a pattern of continuous wave-like juxtaposed layers, running mesio-distally. However, they did not mention which region of the mouth they examined, or whether it was from the upper or lower jaw.

Nobuto *et al.* (1987) studied the microvasculature of dog gingiva, using histological sections and SEM examination of corrosion casts. The blood vessels in normal mucosa were arranged in two layers - a supraperiosteal plexus and an overlying subpapillary plexus.

Anastomoses were found between the supraperiosteal plexus and the medullary vessels via Volkmann canals. At the alveolar crest, the supraperiosteal plexus communicated with the periodontal ligament plexus. Hairpin capillary loops arose from the subpapillary plexus to extend into the connective tissue papillae.

Loops in the attached and free gingiva were about the same height, but at the muco-gingival junction, loops in the alveolar mucosa suddenly became shorter, displaying a flat net-like arrangement. However, they did not describe the orientation of the capillary loops or the capillary network in the alveolar mucosa.

At the gingival margin of clinically healthy gingivae, Egelberg (1966) found a crevicular plexus of blood vessels 7-40*um* in diameter lying close to the crevicular epithelium on the buccal, lingual and proximal aspects. Capillary loops, found elsewhere in the oral epithelium, were not found under the crevicular epithelium in the crevicular plexus, except at the very marginal part. The vessels of the crevicular plexus were not classified by Egelberg, but were found to be mainly of the venular type.

However, the specimens injected with carbon-gelatin mixture were examined in thin sections (less than 300um) and did not provide the depth with which to evaluate the three-dimensional branching of the vasculature, with instruments available at that time.

Using the SEM corrosion cast technique in a study of dog periodontal ligament, Kishi and Takahashi (1977) reported the presence of a bilaminar arrangement of blood vessels from the apical to the cervical region. There were numerous arterio-venous, arterio-arterio and venous-venous anastomoses in the apical third. There was a fence-like network running longitudinally close to the tooth and another layer closer to the bone consisting of arterioles and venules passing to and from the periodontal ligament. This vascular bilayer has also been described by Castelli and Dempster (1965) in macaques and Garfunkel and Sciaky (1971) in rats.

Oral vasculature of other animals

The periodontal vasculature of other animals such as rabbits, opossums, hamsters, guinea pigs and cats has also been studied (Boyer and Neptune, 1962; Carranza *et al.*, 1966; Cohen, 1960).

The gingivae of rats, mice, hamsters, guinea pigs, cats and dogs derived their blood supply mainly from mucosal blood vessels. Gingival vascular loops were arranged circumferentially around the tooth, closely applied to the epithelial cuff (Carranza *et al.*, 1966). The periodontal ligament plexus had a general occluso-apical orientation and was located closer to bone than to cementum.

MATERIALS AND METHODS

Eight healthy adult female cotton ear marmosets (*Callithrix jacchus*, also called *Hapale jacchus*) were used in this study. Marmosets are New World primates or platyrrhine (broad-nosed) monkeys belonging to the suborder *Anthropoidea*, infraorder *Platyrrhini*, superfamily *Ceboidea* and family *Callithricidae* (*Hapalidae*)(Hill, 1957; James 1960).

The gross anatomy of the common marmoset has been extensively described by Beattie (1927). In the permanent dentition, all the incisors, canines and premolars are single-rooted, the mandibular molars two-rooted and the maxillary molars three-rooted (Shaw and Auskaps, 1954).

The marmosets were divided into 2 groups :

Young adults aged about 16 months

Old adults aged from 4 to 7 years

The animals were perfused with Mercox resin and the vascular casts examined with the SEM to study the vasculature. The SEM images were recorded in stereopair.

The vascular architecture in the palate, gingiva and periodontal ligament were examined and the results in young and old animals were compared.

Choice of animal model

The impracticality of making in-depth studies of fresh periodontal tissue in man stimulated the search for a suitable experimental analogue that reacts to environmental factors in a way similar to man (Levy *et al.*, 1972a).

Levy *et al.* (1972a) state that the marmoset has a dental apparatus similar to that of man. It is omnivorous and

subsists largely on a diet of fruit, tender vegetation, seeds, seed pods, insects, bird eggs and nestlings.

Postmortem studies on the marmoset temporomandibular joint (Wilson and Gardner, 1982) indicate that mandibular movements occur in both synovial cavities of the joint. As in man, hinge movements occur in the lower joint cavity and sliding movements occur in the upper joint cavity.

According to Levy *et al.* (1972a), the marmoset gingiva is similar in structure to the human and consists of free and attached gingiva, with a free gingival groove in-between. The gingival epithelium contains prominent rete pegs. Mice, rats and hamsters have dentitions quite different from that of man and do not develop spontaneous periodontal disease. Marmosets, however, show a high prevalence of spontaneous periodontal disease.

Levy *et al.* (1972a) state that the natural history of periodontal disease in marmosets is similar to that postulated for man. Bacterial plaque and calculus form on the teeth just as they do in man. The gingivae of marmosets exhibit comparable reactions to injury as in man. Chronic destructive periodontitis in the marmoset is similar to that in man. Furthermore, the age changes in marmoset periodontal tissues are similar to those in man (Levy *et al.*, 1970).

The marmosets attain physical maturity at 12-18 months and weigh between 250g to 500g at maturity. They have an estimated lifespan in captivity of 15 years (Levy *et al.*, 1972a).

The small size, availability, ease of breeding and handling are a distinct advantage. The disadvantage is the high cost of each animal.

Care of animals

The teeth of the animals were initially scaled and brushed under surgical anaesthesia (Saffan). They were cleaned with a toothbrush and 0.2% chlorhexidine digluconate was applied thrice weekly for a period of three months to maintain gingival health. However, the gingival conditions in the older animals did not improve. The cleaning regime was then abandoned about a month before sacrifice.

All the animals were fed specially prepared marmoset diet and housed in similar conditions.

Anaesthesia

After weighing, the animal was injected with Saffan intramuscularly (alphaxalone alphadolone acetate, 19.5 mg/kg body weight) into the thigh quadriceps muscle (Phillips and Grist, 1975). Some animals took longer than others to become anaesthetized. Anaesthesia was tested by touching the cornea of the eye.

Dissection

The technique for vascular casting has been described by Tompsett (1970), Gannon (1978), Hodde and Nowell (1980), and Lametschwandtner *et al.*, (1984).

After the animal was anaesthetized, the femoral vein was exposed by dissection and 40 i.u. of heparin were given through a femoral vein to prevent blood clotting.

The neck was dissected and the left and right common carotid arteries identified. A 2cm section of each vessel

was cleared of fascia and fat. Black silk suture was loosely looped at the caudal and rostral ends.

An incomplete oblique cut was made in the vessel and the vessel was cannulated in a rostral direction. The cannula from the aspirating bottle had about 60 mm/Hg above atmospheric pressure to prevent backflow of blood into the cannula. The cannula was then secured tightly rostrally and caudally to the vessel.

The tubing was then clamped with haemostats. This was repeated for the other common carotid artery.

A horizontal incision was made in the abdomen just below the xiphoid cartilage. The diaphragm was dissected from the rib cage and the rib cage was cut with coarse scissors in the midaxial line up to the axilla on both sides. The rib cage was then reflected upwards and held there by haemostats.

The inferior vena cava was identified. Fascia was dissected away along a 2cm section and black silk suture loosely looped under at the rostral and caudal ends. An incomplete oblique cut was made and the vessel was cannulated. The cannula was secured by black silk suture tied rostrally and caudally. This cannula allowed egress of blood to be carefully observed.

The fascia and fat around the heart were cleared away and a black silk suture was tied around the aorta and pulmonary arteries at the base of the heart. This prevented flow of any perfusate to the pulmonary and general circulation.

PERFUSION APPARATUS

The equipment used for blood washout and subsequent resin casting was a modification of that used by Gannon (1978). It was essentially a controlled pressure unit comprising a one-litre aspiration bottle with a spout at the bottom (figure 4).

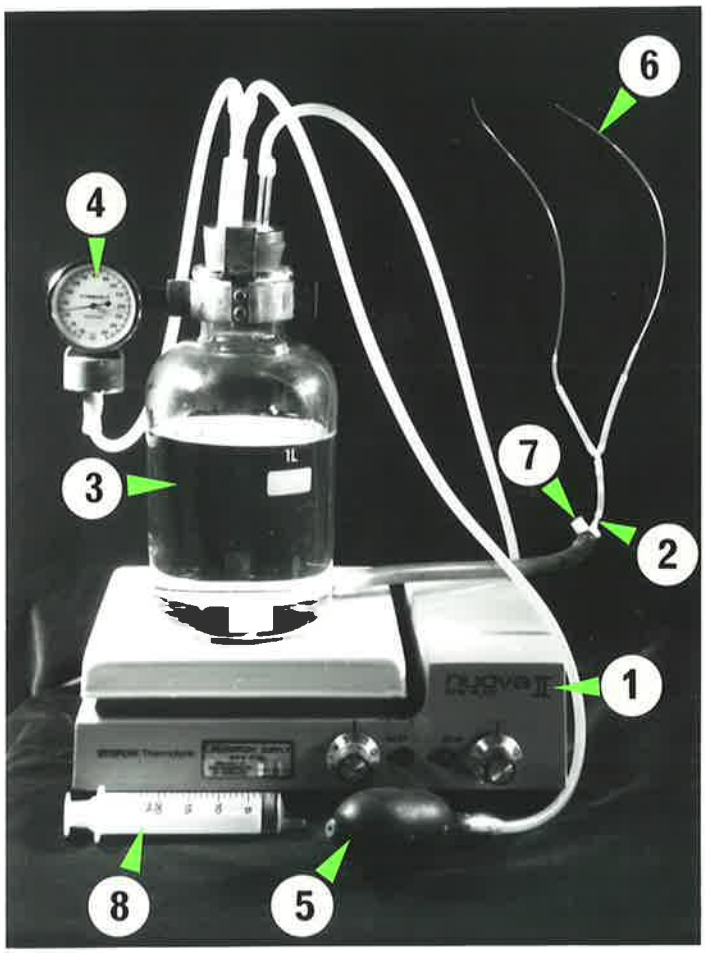

Figure 4. The perfusion apparatus.

1 - magnetic stirrer and heater

2 - spout with 18G needle attached

3 - aspirating bottle

4 - mercury manometer

5 - air pressure regulator

6 - tubing

7 - three-way stopcock

8 - 20ml syringe

The aspirating bottle could be pressurized at any level from 0 to 300 mm/Hg, using the air pressure regulator. The mercury manometer measured the pressure in the bottle.

The three-way stopcock could be closed when it was not required to perfuse from the aspirating bottle. The spout was connected to an 18G needle hub. The needle shaft was inserted into the beginning of a series of tubing of reducing diameter, which bifurcated to give two cannulae at the ends for the left and right common carotid arteries. The 18G needle hub could be removed from the spout and a 20ml syringe of resin or fixative could be attached to the 18G needle and the rest of the tubing.

Washout solution

300ml of blood washout solution was freshly prepared for each animal. The composition of one litre of washout solution was as follows :

Double-distilled water	1.00 litre
Sodium chloride	9.00 g.
PVP-40	58.74 g.
Sodium nitrite	0.07 g.
Papaverine HCl (120 mg/10ml)	0.10 ml.
Heparin (1000 i.u./1 ml)	5.00 ml.

Polyvinylpyrrolidone (PVP-40) provided a blood colloidal osmotic pressure of 25 mm/Hg. Sodium nitrite and papaverine served as vasodilators (Gannon, 1978). Heparin was used as an anticoagulant. It prevents clot and thrombus formation, which will result in incomplete casting.

The prepared solution was filtered through a 0.22*um* Membra-Fil filter, to remove minute particles which may clog up the fine vessels. The solution was then heated in a magnetic stirrer to a temperature of 37-40°C.

Replicating medium

Mercox resin (Hodde *et al.*, 1977) was prepared by mixing 20.0ml of polymethyl methacrylate Mercox resin with 0.5g of catalyst paste.

The resin has a viscosity of about 36 centistokes, measured with a modified Ostwald's viscometer. It sets quickly under pressure and in the absence of oxygen. There is shrinkage upon polymerization and the surface remains sticky.

Perfusion Procedure

After the animal had been cannulated, the pressure in the aspirating bottle was brought up to 240 mm/Hg. The clamps on the tubing were released and the washout solution was perfused through the animal. The site of cannulation was then checked for leakage.

Pressure was maintained at 360 mm/Hg while blood drained out of the inferior vena cava. After a few minutes of perfusion, the egress became clear. Washout was continued for about 10 minutes ensuring that the cephalic vascular system and oral tissues were cleared of blood. Clotted and uncleared blood remaining in the vasculature will give rise to incomplete filling and result in incomplete casts. The tongue and gingivae turned pale when the blood was washed out.

A 20ml syringe, containing 1% glutaraldehyde fixative prepared in 0.1M phosphate buffer, was inserted into the three-way stopcock. Care was taken to avoid the introduction of air bubbles into the tubing as this would block the microvessels and result in incomplete filling. The tap was turned off to the aspirating bottle but open for the syringe. Using hand pressure, fixative was perfused through the animal. The animal went into spasm and the eyes turned yellow when fixative was perfused. The animal was then perfused another 10 minutes with the washout solution.

Meanwhile, the replicating resin was mixed and sucked into a 20ml syringe. The spout of the aspirating bottle was removed from the 18G needle hub, and the 20ml syringe was connected to the 18G needle hub, taking care that no air bubbles were introduced in the transfer. The resin was perfused through the animal with hand pressure. Before the syringe was emptied, the inferior vena cava outlet and the common carotid inlets were clamped to keep the casting medium in the head and maintain the pressure in the system.

After perfusion, the animal was removed and placed in a warm bath at 50°C for one day to ensure complete polymerization of the resin and prevent dessication and shrinkage of the specimen (Lametschwandtner *et al.*, 1984). Also, immersion softens the tissues and makes tissue maceration easier.

Tissue corrosion

When the cast had completely polymerized, the animal was beheaded. The mandible and maxillae were dissected out and placed in 10% hydrochloric acid (HCl). The acid solution was

changed daily for 3-4 days to decalcify the hard tissues. The specimens were then rinsed in distilled water for 15 minutes, then placed in the freezer for at least 4 hours.

Excess tissue was trimmed away from the frozen specimen and the jaws sectioned sagittally across the midline and coronally across a premolar socket with sharp safety razor blades. The specimens were then placed in fresh 10% potassium hydroxide (KOH) solution in a 37°C oven for 24 hours to macerate the soft tissues.

The specimens were rinsed daily with warm distilled water and replaced in fresh 10% KOH for another day. Alternate soaking in KOH and rinsing in tap water was found useful for maceration (Hodde *et al.*, 1977). The process was repeated and could take 2 weeks to 3 months to be completed.

Cleaned casts were then rinsed in double-distilled water. After rinsing, a few drops of detergent were added to the water and the specimens were air dried on filter paper in a closed container to prevent dust contamination. The detergent served to reduce the surface tension of water so that the casts did not become distorted by surface tension during the drying process.

Cleaned and dried specimens were observed under the stereo dissecting microscope for their morphology, cleanliness and completeness. The gross anatomy of the vascular interconnections was noted. Knowledge of the anatomy at light microscope level facilitated the interpretation of the microcorrosion casts in the SEM (Gannon, 1978). It also allowed a quick orientation of the specimen in the SEM to locate the area of interest.

Sectioning

Some of the sockets were sectioned sagittally, others coronally, to get the different aspects of the periodontal ligament. The cleaned casts were embedded in blocks of ice and sectioned again with razor blades by carefully sawing through the ice. The ice helped to hold the delicate casts together during sectioning.

Mounting of sectioned casts

Clean, dry casts were mounted on 1cm diameter aluminium SEM stubs using double-sided tape and secured with Silver Dag conductive paint. Care must be taken with the Silver Dag as it tends to spread over the cast and may cover the area of interest. The orientation of the casts on the SEM stubs was important for subsequent coating and SEM viewing.

The purpose of mounting was to form a stable base for SEM examination and also to ground the casting to discharge electrons when it was bombarded in the SEM. This prevented charging of the specimen during examination (Lametschwandtner *et al.*, 1984).

Rendering the casts conductive

The Mercox casts are non-conductive for electrons. For SEM examination, they must be coated with a conductive layer which

a) facilitates the primary electrons grounding and thus prevents charge build-up on the specimen, and
b) gives off secondary electrons to produce a good image.

Osmification of specimens

The dry vascular casts were treated with vapourized osmium as suggested by Murakami *et al.* (1973), to ensure complete conductivity of the casts and to obtain well-contrasted images in the SEM.

Specimen stubs were placed on a glass rack and their positions noted. An ampoule of osmium tetroxide was broken in a sealed glass jar in the fume cupboard. The rack with specimens was placed in the jar for 48-72 hours. The rack was then transferred to another open jar to allow the osmium tetroxide to sublimate for an hour.

Specimen coating

The casts were coated with vapourized carbon and gold/palladium alloy intermittently for a total of 6 minutes to avoid overheating and distortion of the casts (Hodde and Nowell, 1980). The specimen mount was tilted at different angles to ensure even coating of the surfaces. This coating increased the electrical and thermal conductivity of the cast and prevented charge build-up during examination in the SEM.

SEM examination and recording

The specimens were examined with a Philips SEM 505 or an ETEC Autoscan SEM at 2.5-10kV accelerating voltages and working distances of 12-30mm. Accelerating voltages were kept low to minimize charging and thermal damage, so that deformation of the casts was minimized (Lametschwandtner *et al.*, 1984). The final condenser aperture was 20*um*.

Stereopair micrographs were taken at a 6° angle of tilt to provide stereopair three-dimensional images of the

microvascular replica. The technique for taking stereopair micrographs has been described by Boyde (1973), Howell (1975), Low *et al.* (1981), and Wergin and Pawley (1980). The micrographs were taken on the photographic equipment attached to the SEM, using Ilford FP4 120mm black and white film. Magnifications of the specimen were recorded on the film. Photomontages were taken to demonstrate vascular routes and to give a total view of any area of interest.

Developing and Printing

The films were developed using Ilford Microphen Developer and Ilford Hypam Rapid Fixer, following the manufacturer's instructions, in a Patterson developing tank. The negatives were printed on 10cm X 12cm Ilfospeed grade 3 glossy paper using a Durst Laborator 54 enlarger.

The prints were developed in Ilfospeed paper developer and fixed in Ilford Hypam Rapid Fixer according to the manufacturer's instructions. The prints were dried in an air dryer (Model RCD-33, FC Manufacturing Co. Ltd., Osaka, Japan) and stored in paper envelopes.

Examination of photomicrographs

All photomicrographs were examined in pairs using a Stereo Aids viewer (Rd. No. 70.485). This enabled all images to be visualized in three dimensions. More information can be obtained from these stereopair images than from similar material viewed singly at higher magnification. In examining the photomicrographs, the magnification factor should be ignored as the prints have been enlarged. The scale bar, however, can give a fair approximation of the magnification

as the scale bar is also enlarged as the photomicrograph is printed.

FINDINGS

Findings relating to the gingival and periodontal ligament (PDL) vasculature were derived from the maxillary and mandibular premolar and molar casts of all the animals. However, descriptions of the palatal vasculature were derived from the four young animals as the palatal subepithelial plexus in the older animals were incompletely cast.

The vascular architecture differed from region to region in the oral cavity. Generally, there was bilateral symmetry, with the left side being a mirror-image of the right. The periodontal vasculature of the three premolars in each quadrant was basically similar. There was also a basic pattern of gingival-periodontal anastomosis in the gingiva of all the premolar and molar teeth. Examination of the casts from the experimental animals, as well as teeth from one dry macerated skull, revealed that the upper third premolar was two-rooted.

The relationship of a vessel to other structures such as the root surface, alveolus or epithelium, were deduced from gross anatomic features and existing knowledge of the anatomy of the region.

The vasculature in each region will be described separately. The micrographs are illustrated in the latter part of this section, from pages 5.18 to 5.51.

RECOGNITION OF VESSELS

Endothelial imprint patterns were visible in the SEM on the surfaces of vascular casts of diameters larger than 8-10μm. Arterioles and venules could be distinguished on the basis of this imprint pattern (Hodde, 1981), in conjunction

with other criteria. Arterioles tended to be round in cross-section, had fewer branches, oblong endothelial cell outline and ovoidal nuclei orientated longitudinally. Venules were more oval in cross-section, received many tributaries at acute angles, had circular nuclei imprints and irregular endothelial outline (5.47/fig. 37).

Capillaries had small internal diameters and did not have any endothelial imprints. The surfaces of the capillary casts were usually smooth (5.47/fig. 37).

PALATAL VASCULATURE

The rugae extended laterally in the hard palate from the midline to each lateral incisor, canine, premolar and molar (5.18/fig. 8, 5.19/fig. 9). They formed a gradual curve which was convex anteriorly, each ruga forming a curve of a smaller arc from the incisor to the molar region. The bilaterally symmetrical rugae divided the palatal surface into a series of crests and troughs, ending at the last molar (5.19/fig. 9).

The entire hard palate was covered by a *subepithelial capillary network* of vessels 6-10 um in diameter, orientated in a general sagittal direction (5.20/fig. 10). This sub-epithelial network consisted of a flat *subpapillary plexus*, from which *papillary loops* projected perpendicularly into the connective tissue papillae (5.21/fig. 11). Short obliquely running vessels connected adjacent sagittally directed vessels of the subpapillary plexus in the inter-rugal troughs and on the rugae. No lateral connection could be found between adjacent papillary loops, except at the subpapillary level (5.22/fig. 12).

The papillary loops were capillaries 8-10 *um* in diameter and 70-250 *um* in height (5.22/fig. 12), each loop making a hairpin bend at its peak (5.23/fig. 13). These loops also displayed a sagittal orientation on the rugae, which became less definite on the lateral part of the palate near the tooth sockets (5.20/fig. 10). The tips of the loops were sometimes bent (5.22/fig. 12).

On the rugal crests, the papillary loops were also aligned transversely along the rugae to form a well-delineated spine (5.20/fig. 10). Each crestal loop was discrete and not interconnected to adjacent loops at their peaks (5.23/fig. 13). The loops on the rugae had a diameter of about 8-10 *um* and ranged from 150 to 250 *um* in height (5.23/fig. 13). Loops in these rugal crests were longer than those in the inter-rugal troughs, as well as raised topographically (5.20/fig. 10). Some of the rugal papillary loops showed localized constrictions, giving a linked-sausage appearance (5.23/fig. 13). The loops on the rugae were seen to twist upon themselves as they ascended and descended, and ran a slight wavy course.

The lateral extent of the palatal vasculature was demarcated by semi-circular rings of palatal gingival loops conforming to the contour of the palatal gingiva (Figure 5).

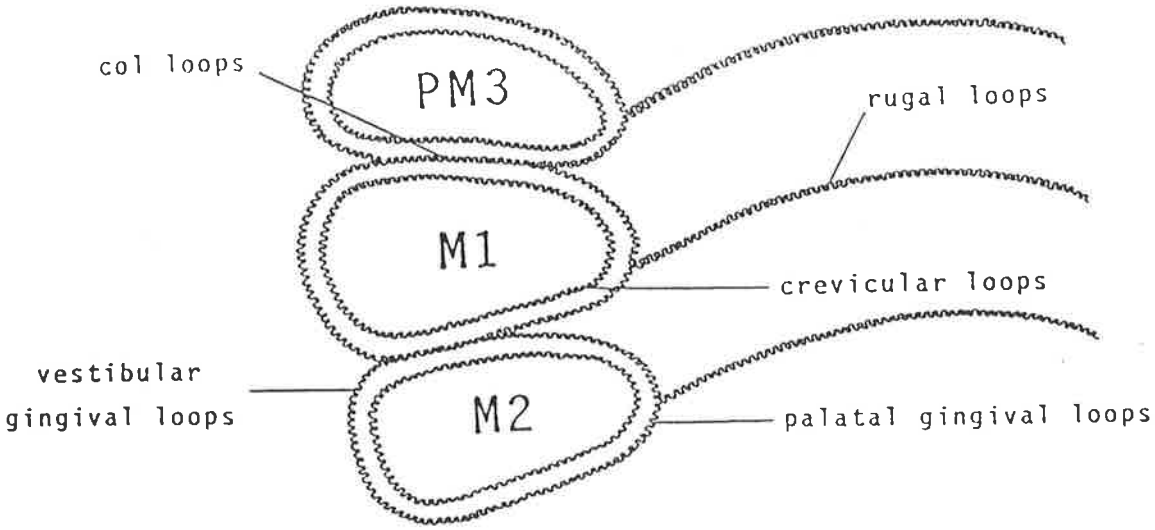

Figure 5: Diagram of gingival loop arrangement. The palatal and vestibular loops of the marginal gingivae, as well as loops in the col area, were separated from the crevicular loops by a gap. The palatal and vestibular loops connected across the interdental col.

The semi-circular rings of palatal gingival loops were separated from the *crevicular loops* located on the crevicular aspect of the gingiva (5.19/fig. 9), by a gap (5.27/fig. 17), *vide infra*: 5.10. However, there were anastomoses between the crevicular loops and the palatal gingival loops at a deeper level (*vide infra*: 5.10).

At the lateral extensions of the palate, the palatal gingival loops may drain into the crevicular gingival vessels on the gingiva. Both palatal and crevicular gingival loops

may be supplied by arterioles from the supracrestal deep gingival network (5.34/fig. 24). See figure 6: 5.9.

The rugal crest showed the highest density of loops, with about 200-270 hairpin loops per mm^2 (5.20/fig. 10). The anterior and posterior slopes of the rugae were equally dense with fewer loops (75-160 per mm^2). The trough area was also less dense than the crestal area (70-140 loops per mm^2), and the loops were shorter, ranging from 70-100um in height (5.22/fig. 12).

In both the rugal and inter-rugal areas, the subpapillary plexus formed a canopy which spread over and drained into another network of larger venous vessels (5.21/fig. 11). Superficially placed subpapillary capillaries 6-8um in diameter drained into what appeared to be an intermediate layer of postcapillary-sized venules, 10-15um in diameter, which drained into larger collecting-sized venules, 30-40um in diameter, at a deeper level (5.21/fig. 11). Neither the intermediate, the deep venous network, or the arterioles showed any definite sagittal orientation.

In the trough area, collecting-sized venules may coalesce with one another, forming a confluence of two to four venules. Fig. 11 illustrates an extreme example of a confluence of many vessels.

Arterioles were relatively scarce in the palatal network. Arterioles tended to lie at a deeper level than venules of corresponding size, and they branched less often.

The nasopalatine foramina (5.18/fig. 8) opened bilaterally behind the central incisor sockets, medial to the lateral incisor sockets. They were triangular in outline and lined by a capillary network, with short hairpin loops in

some parts, projecting into the lumen of the nasopalatine canal (5.24/fig. 14). It was inferred that epithelial tissue projected from the palatal surface into the lumen of the nasopalatine canal.

Distal to the last molar and in the soft palate, the subepithelial capillary network was less dense and lost its sagittal orientation (5.25/fig. 15). In this area, it was easier to look through the loose capillary network at the underlying venous network. The venous and arterial network also did not show any definite orientation. No rugae were found in the soft palate and perpendicularly projecting papillary loops were uncommon (5.25/fig. 15).

Numerous ring formations consisting of capillaries 8-10*um* in diameter could be seen in the soft palate, surrounding what appeared to be secretory ducts of the minor salivary glands (5.25/fig. 15, 5.26/fig. 16). These ring formations had a diameter of 80-200*um*. The capillaries drained into deeper postcapillary-sized venules 23-27*um* in diameter, and also anastomosed with vessels of the subepithelial capillary plexus. Arterial supply was derived from terminal arterioles of about 10*um* in diameter. The capillaries did not show imprint patterns on their surface and it was difficult to ascertain the direction of blood flow in these ring formations.

At a level corresponding to the distal surface of the second molars, the density of these rings was 10-20 rings per mm^2, with higher density medially than laterally (5.25/fig. 15). These rings were not found further anteriorly in the hard palate, nor were they found in the gingiva.

GINGIVAL VASCULATURE

There were significant differences between the vascular architecture of the buccal/lingual gingiva and that of the col tissue. Furthermore, the vasculature beneath the crevicular epithelium was different from that under the oral gingival epithelium. The vasculature related to the crevicular epithelium, oral gingival epithelium and interdental col will be discussed separately.

Crevicular vasculature

Adjacent to the junctional epithelium in both upper and lower premolar and molar teeth, was a *circular plexus* of vessels forming a ring that completely surrounded the tooth (5.27/fig. 17). *Crevicular loops* arose coronal to the circular plexus, and extended into the connective tissue papillae. The crevicular loops and the circular plexus together comprised the *crevicular plexus*.

The circular plexus was located at a level corresponding to the epithelial attachment. This plexus consisted of a circular band of one to four vessels, 10-25um in diameter, running roughly parallel to each other and encircling the tooth (5.27/fig. 17, 5.28/fig. 18).

Each *circular vessel* showed localized dilations along its path, separated by periodic annular constrictions, giving rise to a knotted appearance (5.28/fig. 18). Each circular vessel communicated with the adjacent circular vessel through short communicating links. The circular vessel had no distinct imprint patterns and had a diameter of 6-30um (fig. 18). It was difficult to estimate the direction of blood flow in most parts of the circular plexus, except where crevicular

loops arose and drained into it, and where periodontal ligament vessels anastomosed with it.

The circular plexus received blood mainly from the crevicular loops, but also from gingival loops on the oral/proximal aspect, and from the periodontal ligament (5.29/fig. 19, 5.30/fig. 20). Blood from the circular plexus drained into the periodontal ligament (5.30/fig. 20)

Arterioles from the periodontal ligament often by-passed the circular plexus to supply the crevicular loops (5.29/fig. 19). Capillaries, 8-10*um* in diameter, also arose from the circular plexus at the base of the gingival crevice, forming *crevicular loops* which ran back into the circular plexus as thickened and dilated postcapillary-sized venules, 10-30*um* in diameter (5.28/fig. 18, 5.29/fig. 19). The loops varied from 50-250*um* in height. Some crevicular loops arose from deeper gingival or palatal vessels instead (5.34/fig. 24). These deeper gingival vessels may have arisen from the alveolar crest (figure 6: 5.9).

There was considerable variation in the crevicular loop pattern, ranging from hairpin loops to complex convoluted loops with multiple branching (5.31/fig. 21). In the upper and lower canines and incisors, these complex loops formed bulb-shaped structures resembling renal glomeruli (5.32/fig. 22). These teeth were not studied in detail and will not be reported in this thesis.

Crevicular loops arranged themselves in a ring around the tooth in single (5.27/fig. 17) or multiple rows (5.33/fig. 23). These loops could be found on the mesial, distal, lingual and buccal aspects of the teeth. Each crevicular loop consisted of one or two thin capillary

ascending limbs and one or two thicker postcapillary-sized venule descending limbs (5.28/fig. 18). One ascending limb may branch to supply two loops, and two descending limbs from adjacent loops may coalesce into a common trunk as they descended. The descending limbs had a knotted appearance and a more variable diameter.

The arrangement suggested that blood from the descending limb could drain into the circular plexus, into the periodontal ligament (5.29/fig. 19), or into the deep gingival vessels. The deep gingival vessels, located above the alveolar crest, also received blood from the palatal vessels on the palatal aspects of upper teeth. These deep gingival vessels drained into the periodontal ligament, the alveolar bone, or into the palatal network (figure 6).

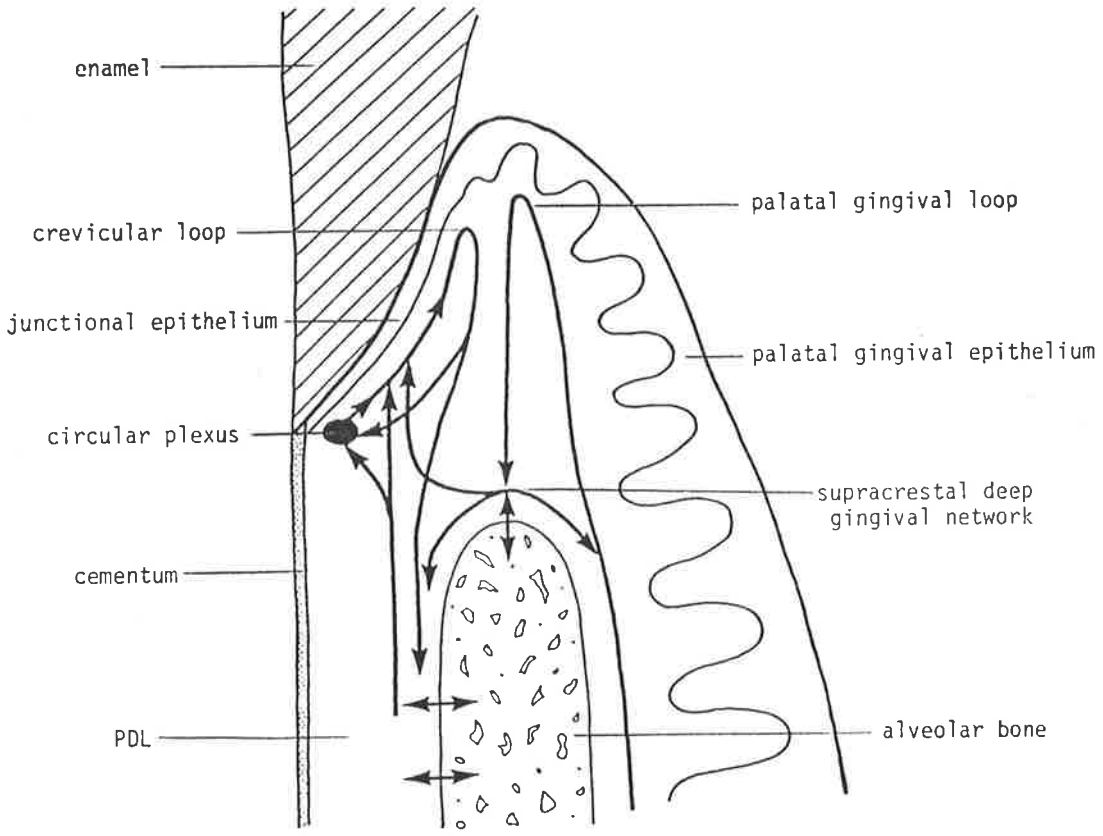

Figure 6: Diagram showing presumptive blood flow in the vasculature of the palatal gingiva.

Sometimes, a mass of extravasated material could be seen associated with the crevicular loops (5.35/fig. 25). The extravasated resin showed a delicate honeycomb pattern with small spaces between streaks of material 1-2*um* in diameter. These streaks did not have any imprint patterns on their surfaces.

Oral gingival vasculature

A distinct gap was observed between the vasculature on the crevicular aspect and on the oral aspect (5.19/fig. 9, 5.27/fig. 17, 5.34/fig. 24).

Below the gingival margin in upper premolar and molar teeth, the loops on the palatal aspect of the palatal gingiva were aligned and followed the palatal contour of the teeth, forming semi-circular rings (5.19/fig. 9, 5.4/fig. 5), *vide supra*: 5.3. Crevicular loops below the crevicular epithelium of the palatal gingiva formed a separate network.

The oral gingival loops, often longer than the crevicular loops, ringed the tooth sockets to form a crest, corresponding to the gingival margin. More often, these crestal vessels were composed of capillary loops. However, in the lower premolar and molar sockets, these loops were often replaced by a continuous capillary network, surmounted by a horizontal capillary (5.36/fig. 26, 5.37/fig. 27). This horizontal capillary ran a wavy course, joining the most occlusal arcades of adjacent capillary loops.

Despite the existence of a gap between the crevicular and oral/proximal vasculature, there were anastomoses between them at a deeper level (5.34/fig. 24, 5.38/fig. 28). Blood from the gingival margin could drain outwards into the oral

gingival network, or inwards into the crevicular plexus and into the periodontal ligament plexus (figure 6: 5.9).

It was difficult to ascertain the relative location of the free gingival groove and the muco-gingival junction from the casts. However, the location of the muco-gingival junction was inferred from the change in orientation and architecture of the capillary network, and measurement of the distance from the gingival margin.

The vasculature below the gingival margin had a horizontal orientation, conforming to the contour of the gingival margin (5.40/fig. 30). Further apically, the vasculature was composed of occluso-apically orientated capillaries, thrown into a series of occluso-apically orientated hairpin loops as they drained towards the vestibular sulcus (5.39/fig. 29, 5.40/fig. 30). Further from the gingival margin, there were only a few transverse branches linking up adjacent occluso-apically running capillaries.

The papillary loops were longer (60-120*um* in height) near the gingival margin (5.41/fig. 31), compared to those near the muco-gingival junction (40-60 *um* in height). These loops were mainly hairpin capillary loops with limbs further apart. They did not exhibit constrictions, in contrast to some rugal crest loops. The density of the loops was highest near the gingival margin, and reduced towards the muco-gingival junction (5.39/fig. 29).

At the muco-gingival junction, the orientation suddenly changed into an antero-posterior orientation (5.39/fig. 29). The most occlusally placed of the antero-posteriorly orientated vessels received tributaries on its occlusal

aspect from the occluso-apically directed capillaries. Loops were not found in the alveolar mucosa. Instead, capillaries appeared to be arranged in wide arcades.

The capillary network over the gingiva and alveolar mucosa lay over a deeper venous network comprising postcapillary-sized venules (5.39/fig. 29). These venules ranged from 10-30um in diameter and were also orientated occluso-apically. As they drained towards the vestibular sulcus, they enlarged or coalesced into larger collecting-sized venules and muscular venules 30-50um and 50-100um in diameter, respectively, also orientated occluso-apically (5.40/fig. 30).

Arterioles were also found in the deeper underlying network but were less numerous. Arterioles 50-100um in diameter arose from the sulcus and tapered off into terminal arterioles less than 50um in diameter as they ascended occlusally towards the gingival margin.

The buccal interdental papillae also exhibited the same occluso-apical orientation of capillaries, venules and arterioles. It could not be determined whether the interdental papilla was more vascular than the gingiva along the tooth axis.

The interdental col

The col connective tissue vasculature could be described as being characterized by capillary loops with a general bucco-lingual orientation (5.42/fig. 32). These loops arose from bucco-lingually orientated arterioles arising from the palatal vasculature, the interdental septa, the buccal gingiva, and from the adjacent periodontal ligament. Blood

from the loops drained into a bucco-lingually orientated network.

The circular plexus and the associated crevicular loops continued into the interdental papilla and into the interdental col. Vestibular and palatal gingival loops from the buccal and lingual interdental papillae extended into the col and anastomosed with each other at a subpapillary level (figure 5: 5.4).

Complex branching loops were abundant in some areas (5.43/fig. 33), but simple hairpin loops were more commonly found in other areas (5.42/fig. 32). It could not be determined which of these two patterns was more common in the upper or lower, premolar or molar gingivae.

PERIODONTAL LIGAMENT VASCULATURE

The periodontal ligament network in the cervical and middle third was composed mainly of postcapillary-sized venules 20-35*um* in diameter, running occluso-apically. As the vessels coursed apically, they frequently anastomosed with each other (5.44/fig. 34).

Arterioles were less commonly found in the periodontal ligament. They tended to have a constant diameter, ran a straighter course, and branched less often (5.45/fig. 35, 5.46/fig. 36), compared to venules which had a varying diameter, ran a more sinuous course, branched more often, and tended to be closer to the root surface.

Cervical Third

At the coronal extremity, apically directed postcapillary-sized venules, 10-25um in diameter, drained the circular plexus (5.30/fig. 20), as well as the crevicular loops coronal to the circular plexus (5.29/fig. 19). Terminal arterioles running occlusally supplied blood to capillaries which fed into the ascending limbs of the crevicular loops (5.29/fig. 19, 5.30/fig. 20). Capillaries from the periodontal ligament could also be found supplying blood directly to the circular plexus, but these connections were seldom found on the innermost of the circular vessels.

In some areas, the main periodontal ligament vessels were arranged occluso-apically in a palisade (5.45/fig. 35). In other areas, the vessels ran apically in an oblique direction (5.46/fig. 36). The lingual ligament vasculature tended to have a more oblique orientation and the mesial and distal vasculature tended to be more axial in orientation, compared to the buccal ligament.

Perforating capillaries from the alveolar bone contributed to the periodontal ligament plexus (5.46/fig. 36) and periodontal ligament venules perforated the alveolar bone to drain into medullary vessels. It could not be established whether the ligament plexus was closer to cementum or to alveolar bone, within the periodontal ligament space.

Capillaries were not so numerous as to form an extensive capillary network, but they were present linking adjacent postcapillary-sized venules, or linking the periodontal ligament vessels to the medullary network (5.47/fig. 37). In some sites, the blood flow in the capillaries appeared to be in an apico-occlusal direction over short distances, going

against the general occluso-apical drainage of postcapillary-sized venules (5.47/fig. 37). Arterioles could be found on either side of the venous network, but were more commonly found closer to the bone (5.47/fig. 37).

Hairpin capillary loops were sometimes found in the cervical third of the periodontal ligament, just apical to the circular plexus (5.35/fig. 25, 5.48/fig. 38), but were not found in the middle and apical thirds of the ligament. They ranged in height from 50-100um and were pointed in the direction of the root, and sometimes in an occlusal direction. They arose individually from axially orientated periodontal ligament capillaries or from medullary capillaries, and drained into occluso-apically orientated postcapillary-sized venules of the ligament.

These capillary loops did not coalesce to form a capillary network. Sometimes the descending limb expanded abruptly to join thick postcapillary-sized venules 30-40um in diameter (5.49/fig. 39). Annular constrictions may be found at the base of the descending limb, indicating the possibility of a sphincter-like function.

Vascular connections with the periodontal ligament plexus of the adjacent tooth over the interdental septum could not be established. This region requires further study.

Middle Third

No capillary loops were found in the middle third of the periodontal ligament. Ligament vessels continued occluso-apically and anastomosed with each other, and with medullary vessels through the cribriform plate.

Apical Third

The ligament vessels converged at the apex to form a basket-like network (5.50/fig. 40). There appeared to be a higher proportion of larger-sized venules in the apical third, compared to the cervical and middle thirds of the periodontal ligament. The vessels seemed more closely packed, with reduced distances between vessels.

Postcapillary-sized venules and collecting-sized venules tended to form a network closer to the root surface, while capillaries formed another network closer to the alveolar bone (5.51/fig. 41). No capillary loops have been found in the apical third.

Anastomoses occurred between periodontal ligament and pulp vessels at the apex (5.50/fig. 40), forming alveolar arterioles and venules as they perforated the cribriform plate. The pulpal and periodontal ligament vessels did not all coalesce into a common trunk. Rather, small branches radiated from the apex to perforate the cribriform plate separately.

Interradicular network

A loose vascular network could be observed in the interradicular region in the molar. This network continued with the periodontal ligament network down the root, and extended laterally to join the cervical network of the periodontal ligament.

At present, the upper and lower canine and incisor sockets have not been sectioned, so a detailed description of

the periodontal ligament network in these teeth cannot be given.

The micrographs in the following pages are accompanied by a data imprint showing the magnification of the specimen (figure 7). The magnification factor is not accurate as the prints have been further enlarged. However, a close approximation is provided by the scale bars, which were correspondingly enlarged during printing.

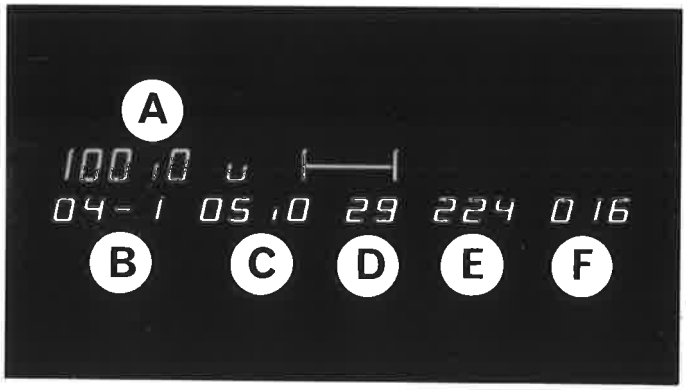

Figure 7. Data imprint on micrographs.

A = Length of scale bar in um (to one decimal place).

B = Magnification (Not accurate, as prints have been further magnified)

C = Accelerating voltage in kV (to one decimal place).

D = Working distance in mm.

E = Specimen code

F = Serial number

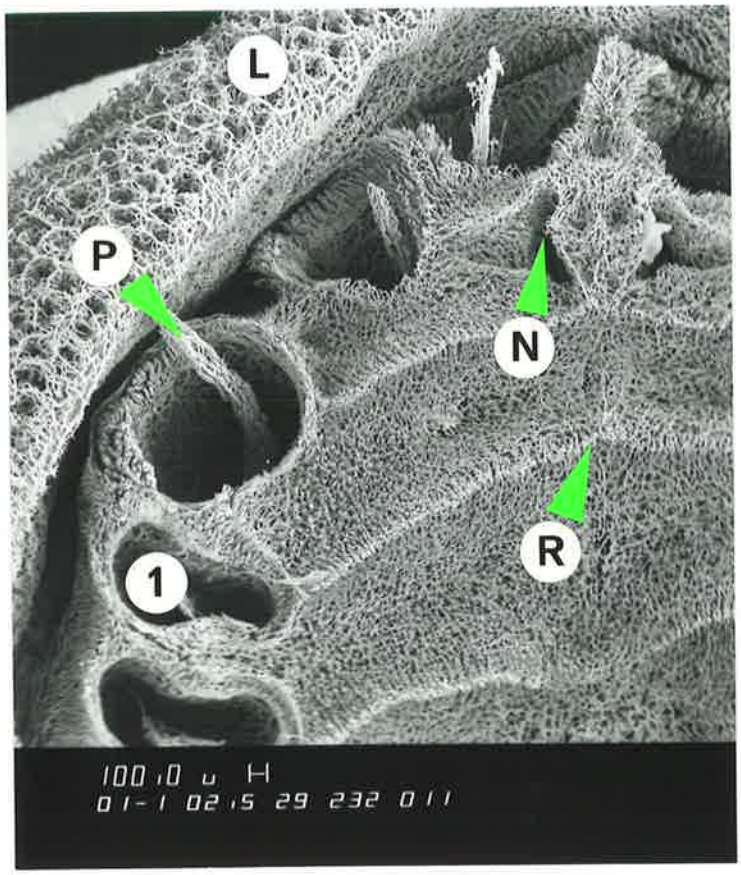

Figure 8. The right maxilla, showing the incisor, canine and premolar sockets.

Rugae extend to the palatal margin of the canine, first and second premolars. Vessels of the upper lip (L), can be seen labial to the sockets, surrounding the vibrissae.

1 = First premolar socket R = Ruga

N = Nasopalatine foramen P = Pulp vessels

100.0 µ H n 0.001
21 242 52 0.50 1-10 1/2

Anterior

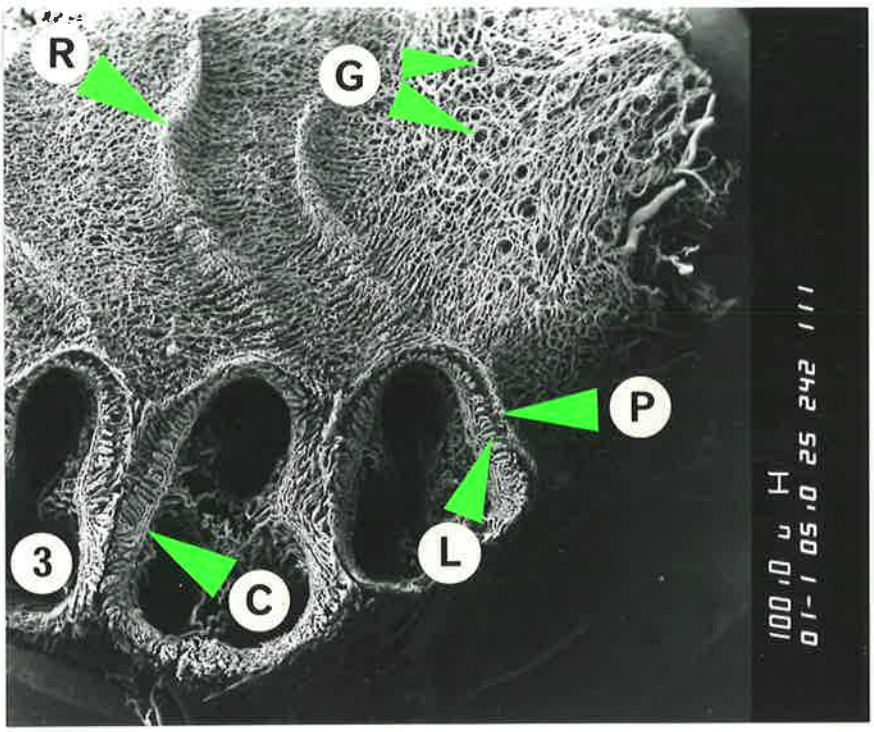

Figure 9. The right maxilla, showing the third premolar, and first and second molar sockets.

The last ruga terminates at the second molar. The circular plexus (C) of the marginal gingiva completely surrounds each tooth. The lateral extent of the palatal vasculature is demarcated by semi-circular rings of palatal gingival loops (P), separated from the crevicular loops (L) by a gap.

3 = Third premolar socket R = Ruga

G = Ring formations around minor salivary gland ducts

100 0.00 µ
20.0 1.50
242 42
901

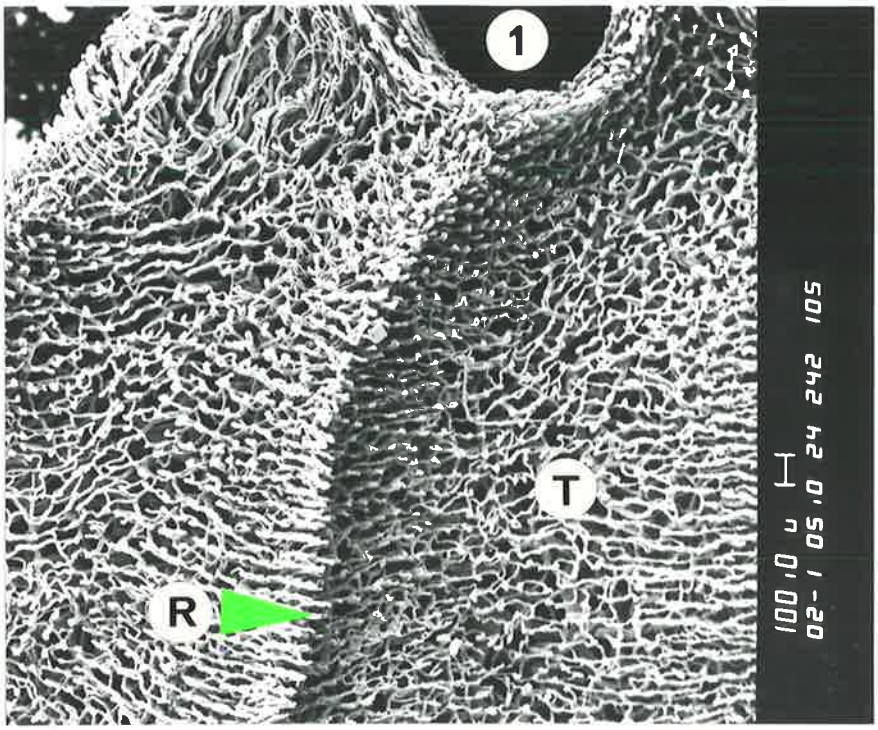

Figure 10. Ruga that runs to the maxillary left first premolar. Note the sagittal orientation of the subepithelial capillary network, which becomes less definite near the tooth sockets.

Papillary loops extend perpendicularly from the subpapillary plexus to the connective tissue papillae. These loops are sagittally orientated and aligned on the crest of the ruga (R) to form a well-delineated spine. Rugal loops are discrete and not interconnected at their peaks. The rugal crest shows the highest density of loops, compared to the slopes of the rugae and inter-rugal troughs.

1 = First premolar socket

T = trough area

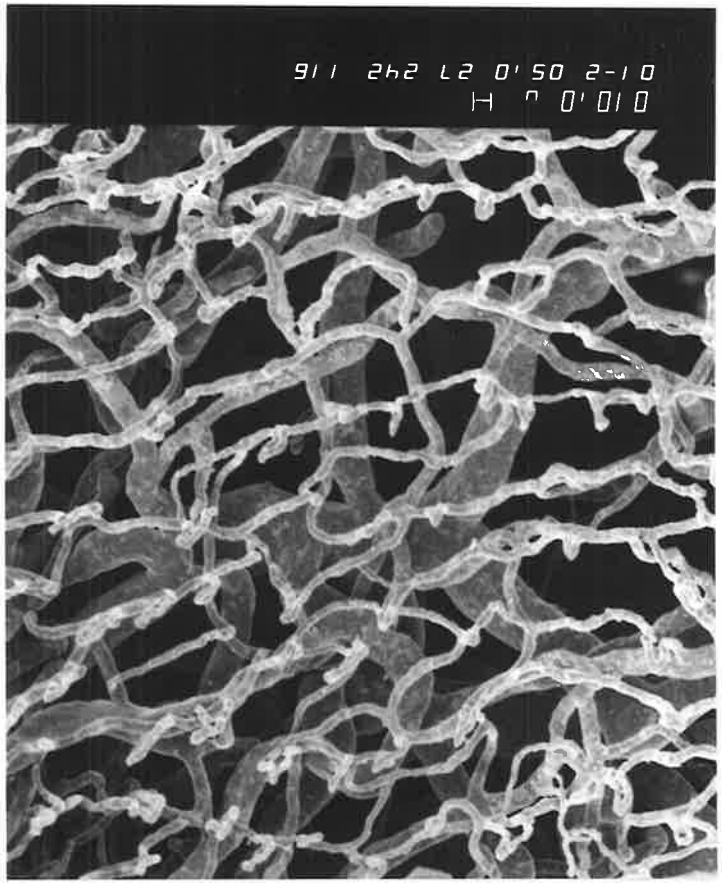
911 2h2 L2 0'50 2-10
H ⁿ 0'010

Anterior

Buccal

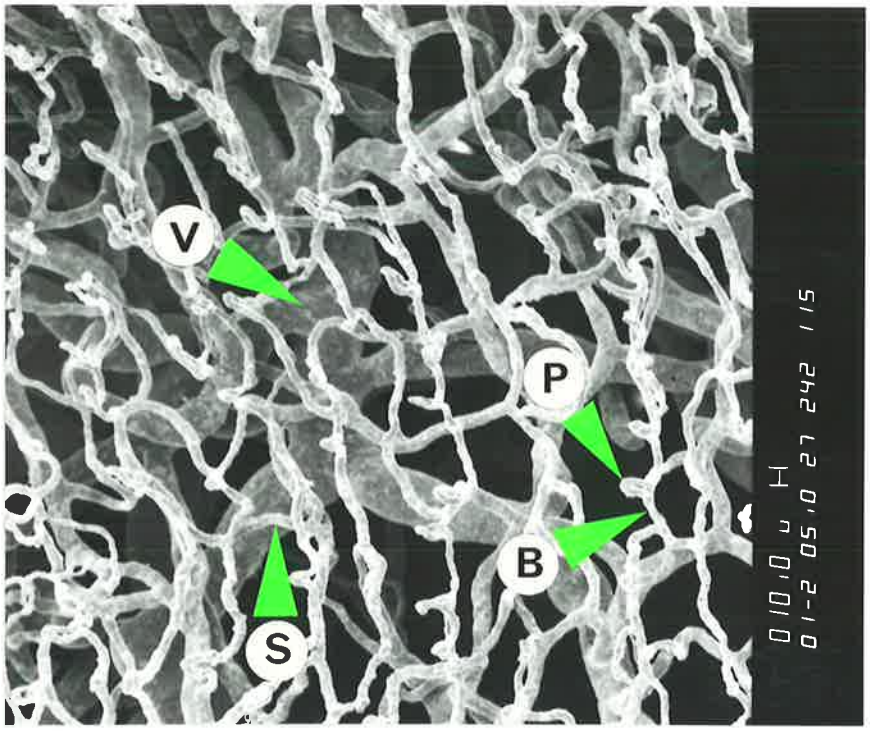

Figure 11. Palatal network in the trough area between the rugae to the maxillary right third premolar and first molar. Papillary loops (P) project from the subpapillary plexus (B) into the connective tissue papillae.

The subpapillary plexus lies over a deeper venous network. Arterioles are less common. Collecting-sized venules (V) coalesce to form a confluence of many vessels. This is an extreme example. Usually, only two or three vessels coalesce together. Short oblique vessels (S) connect adjacent sagittally orientated vessels of the subpapillary plexus.

Superficial subpapillary vessels: 6 - 8 um in diameter

Vessels in the intermediate layer: 10 - 15 um in diameter

Vessels in the deep layer: 30 - 40 um in diameter

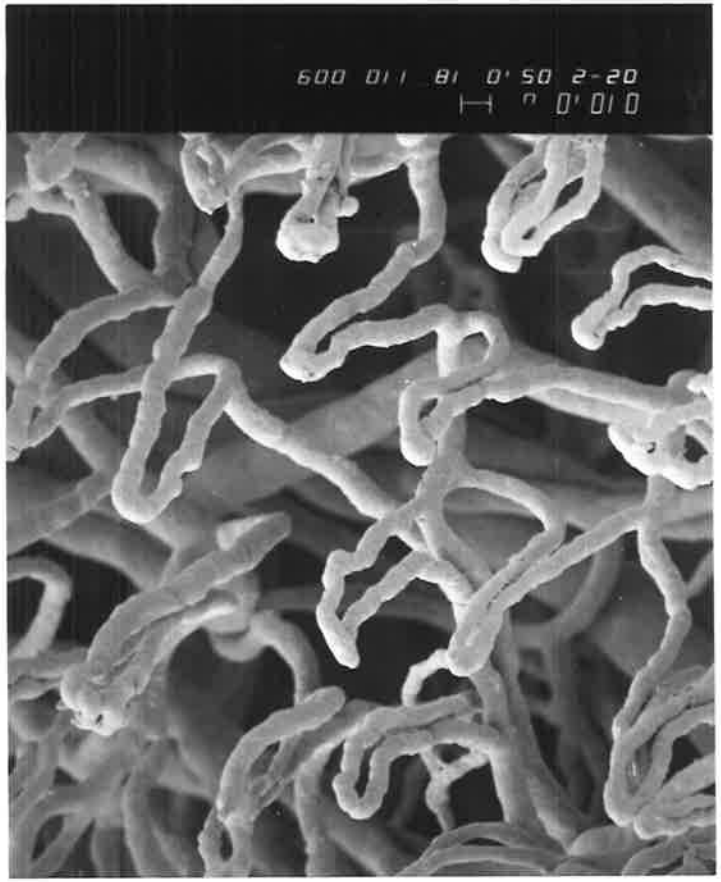
600 011 81 0'50 2-20
H n 0'010

Palatal

Anterior

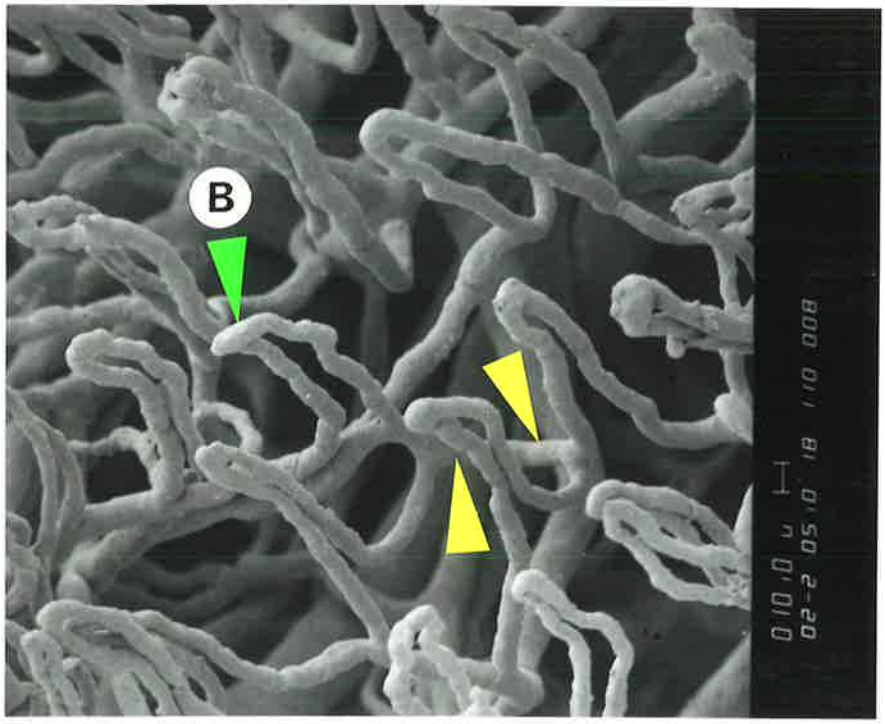

Figure 12. Papillary loops in the inter-rugal trough. Hairpin capillary loops ranging from 70-100um in height extend into the connective tissue papillae. The horizontal capillary (yellow arrows) in the subpapillary plexus connects four adjacent loops at the base. The loops do not bear any distinct imprint patterns. The tip of the loops are sometimes bent (B).

801 242 E2 0'50 2-10
H n 0'010

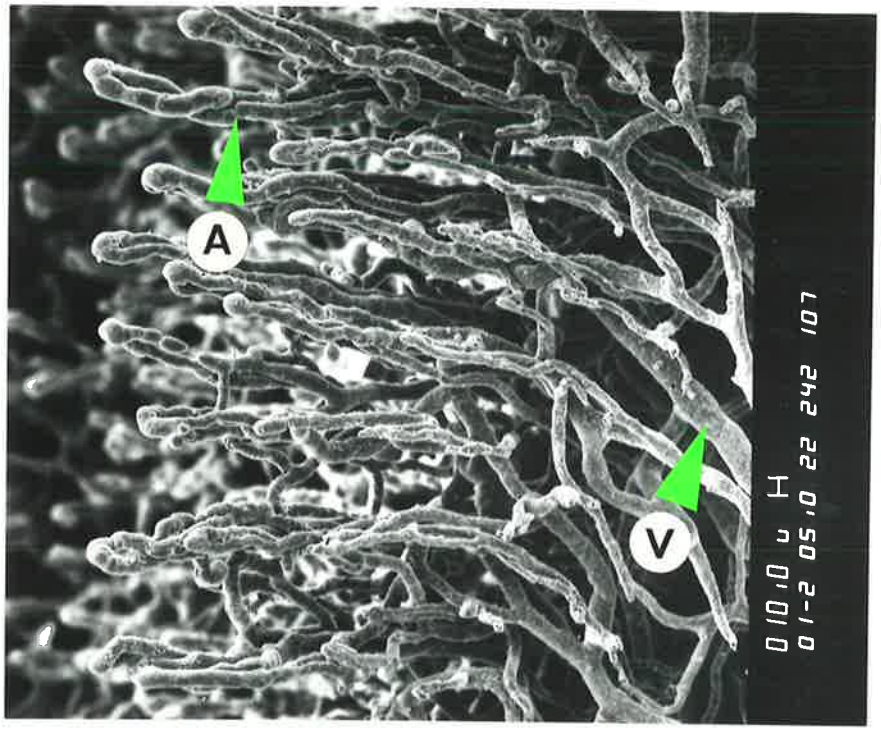

Figure 13. Anterior view of loops at the rugal crest. Each papillary loop makes a hairpin bend at its peak. Localized annular constrictions (A) occur along the papillary loop, giving rise to a linked-sausage appearance. Rugal loops tend to twist upon themselves.

The height of the rugal loops ranges from 150-250*um*. Their diameter ranges from 8-10*um*. Note the lack of connection between adjacent loops at their peaks.

V = Postcapillary-sized venule

4/0 2E2 L2 5.20 I -40
0.00
100

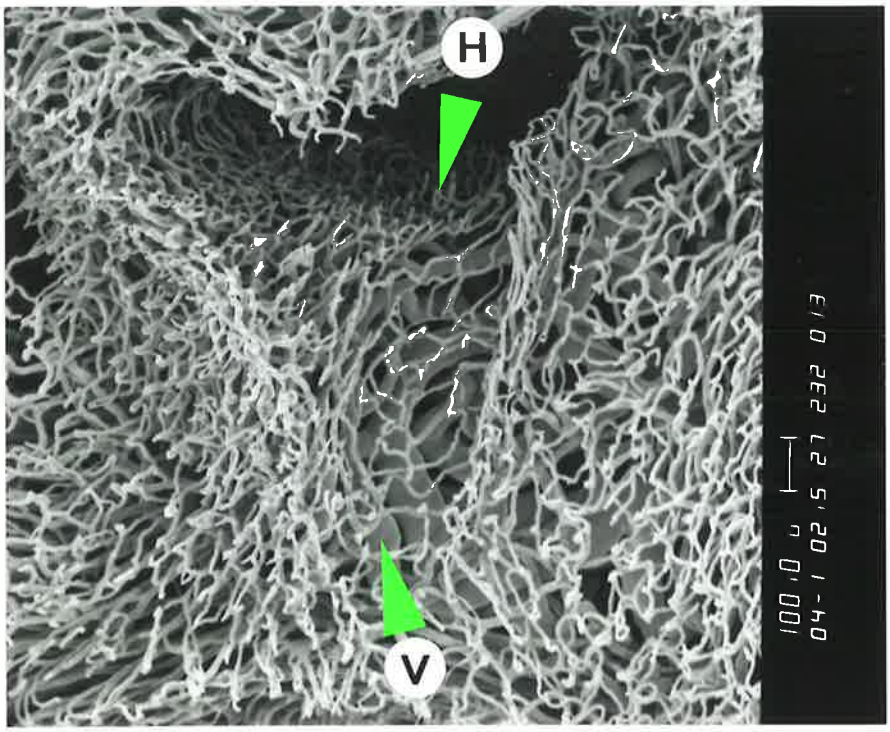

Posterior

Buccal

Figure 14. The right nasopalatine foramen. A capillary network lines the nasopalatine canal. Short hairpin loops (H) can be seen on the lateral wall, projecting into the lumen of the foramen.

V = Collecting-sized venule

811 242 82 0'50 i-10
H n 0'001

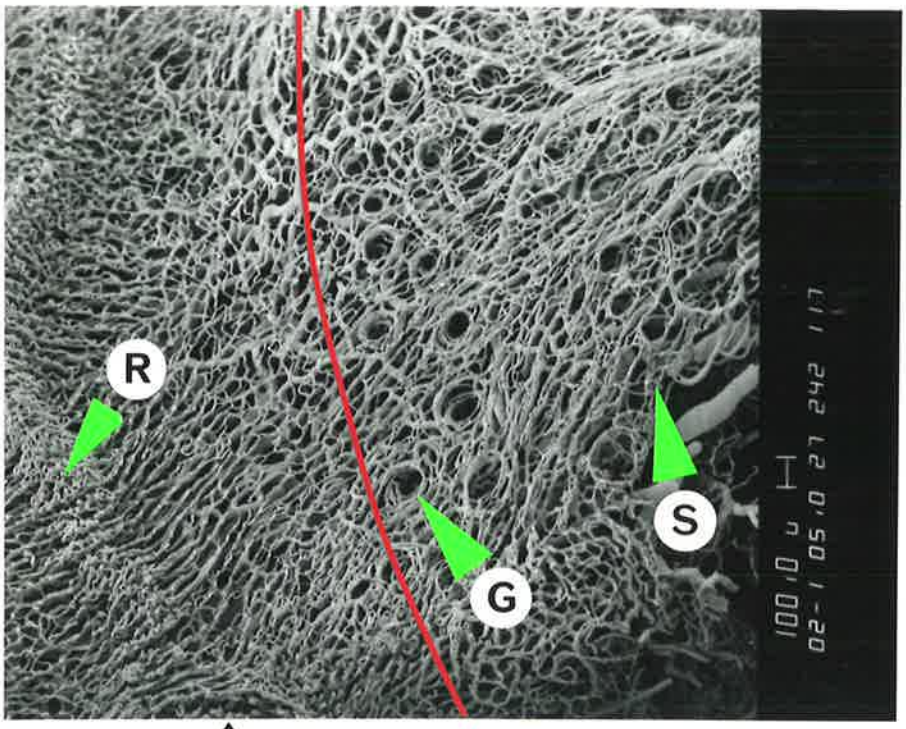

Figure 15. The soft palate in the right maxilla. The red line indicates the approximate junction between the hard and soft palate.

In the soft palate, the capillary network is less dense and it loses its sagittal orientation. Vessels surrounding the minor salivary gland ducts can be seen, with characteristic circular pattern (G). Note the absence of rugae and perpendicularly projecting papillary loops in the soft palate.

R = Ruga to maxillary second molar S = soft palate

E01 2h2 91 0'50 2-E0
0'10'0 n

Anterior

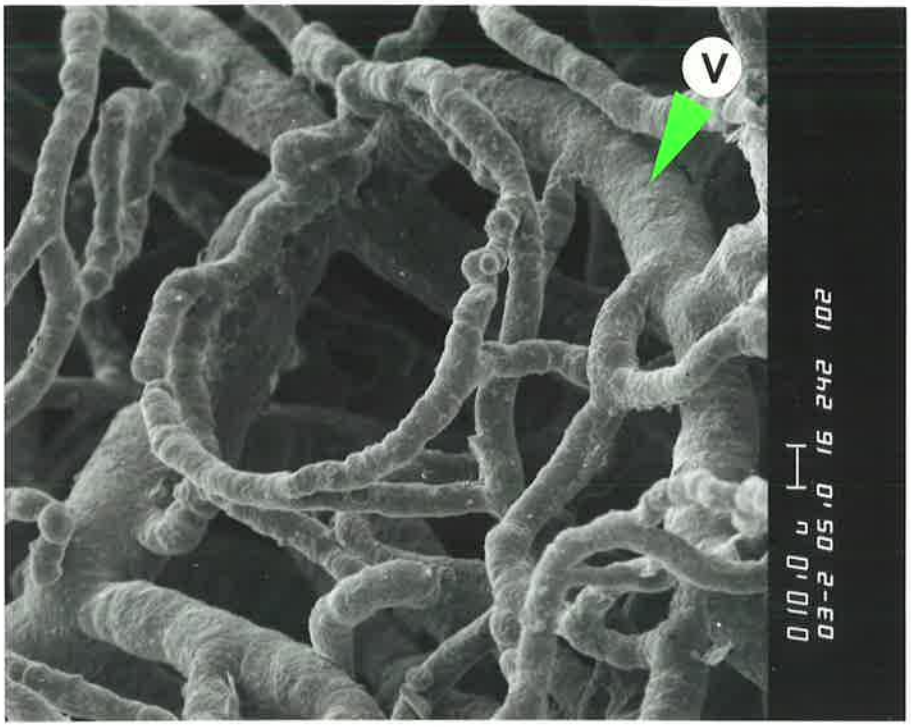

Figure 16. Vessels surrounding the secretory duct of a minor salivary gland. The diameter of this ring is about 110*um*. The ring is composed of capillary-sized vessels about 8*um* in diameter, which do not show any distinct imprint patterns. The direction of blood flow in these ring formations was difficult to estimate.

V = Postcapillary-sized venule

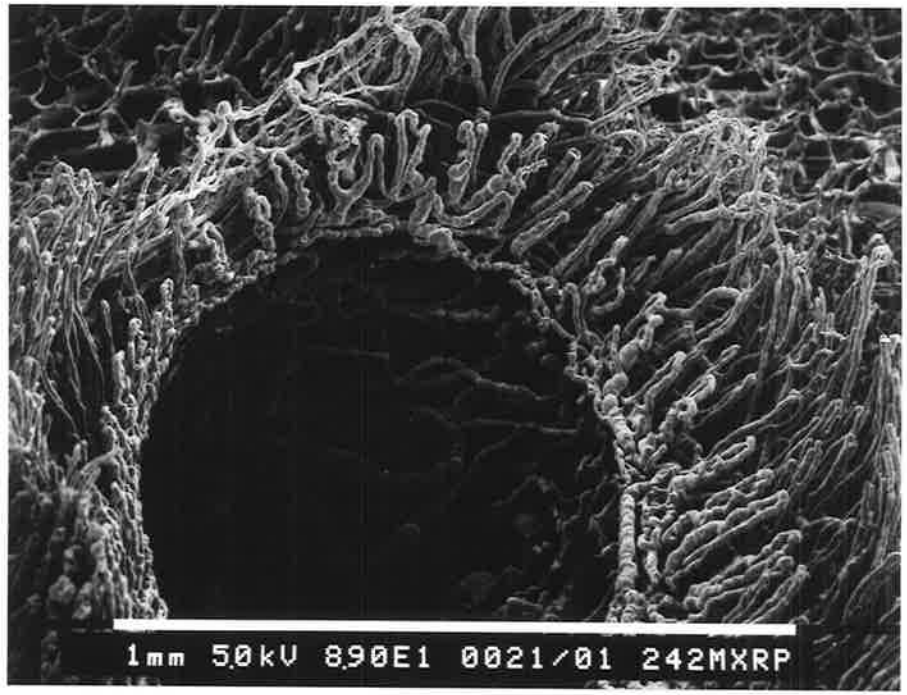
1mm 5.0kV 8.90E1 0021/01 242MXRP

Posterior

Palatal

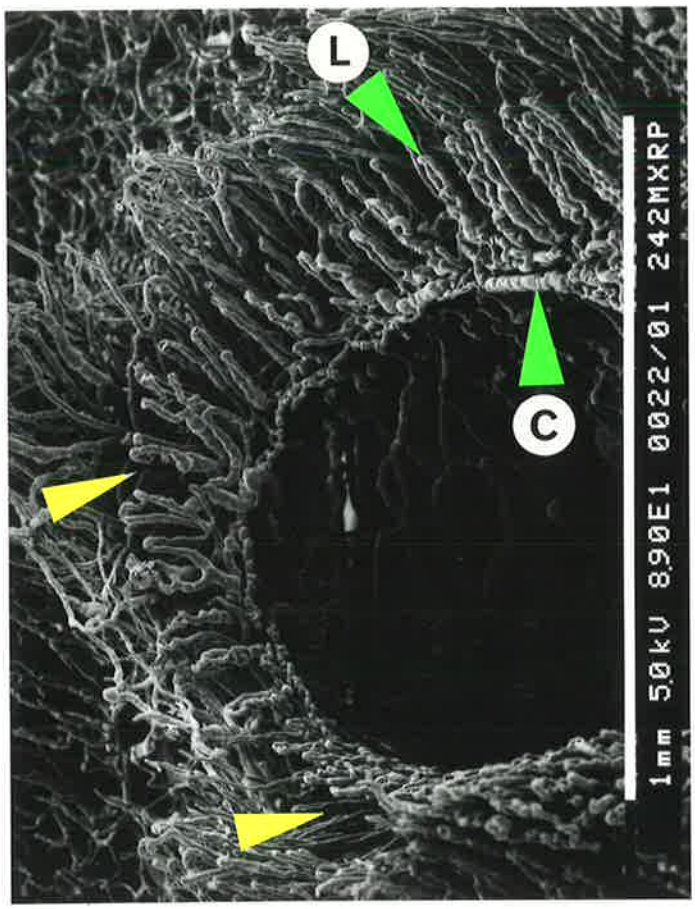

Figure 17. Palatal gingival margin of the maxillary right third premolar. The crevicular plexus completely encircles the tooth, and is separated from the palatal gingival loops, by a distinct gap (yellow arrows). The circular plexus (C) lies at the apical base of the crevicular plexus. Crevicular loops (L) arise from the circular plexus to extend into the connective tissue papillae.

EE1 2h2 L2 0,50 2-10
H n 0,010
0,0 0,010

Anterior

Buccal

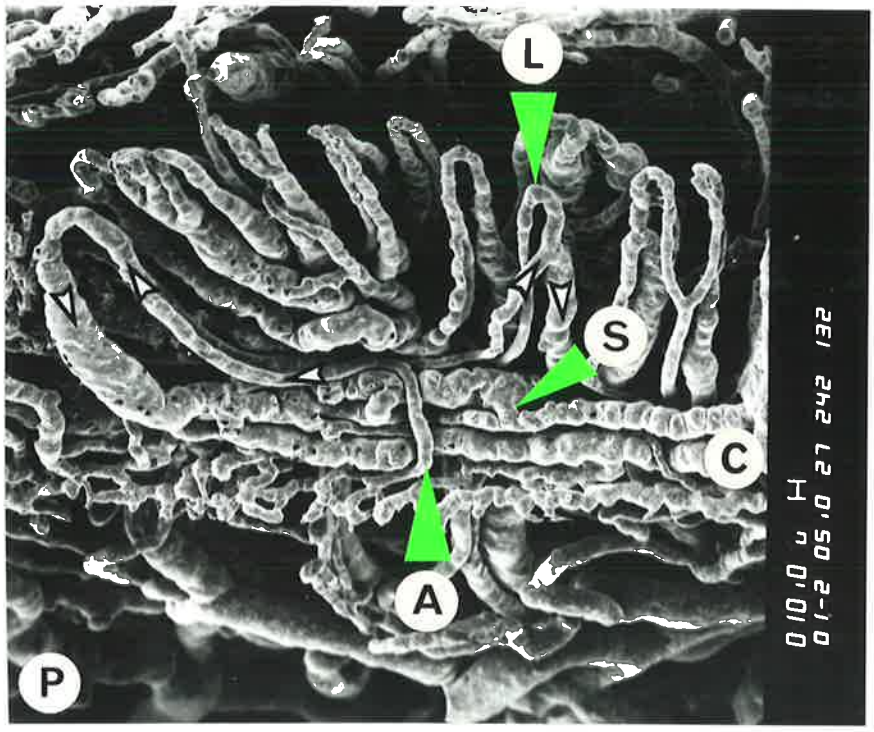

Figure 18. Mesial margin of the maxillary right first molar. The circular plexus (C) is knotted along its length. Vessels forming the circular plexus are 10-25 um in diameter, running almost parallel to each other, and sometimes connected by short communicating links (S). A capillary (A) arising from the circular plexus divides into two ascending limbs to supply the crevicular loops.

Crevicular loops drain into the circular plexus, or deep to it, into the periodontal ligament. White arrows indicate the presumptive direction of flow. The descending limbs of the crevicular loops (L) are distended. Ascending limbs are thinner and more constant in diameter.

P = Periodontal ligament

0,10,0 " H
021 242 52 0,50 2-1 0

Occlusal

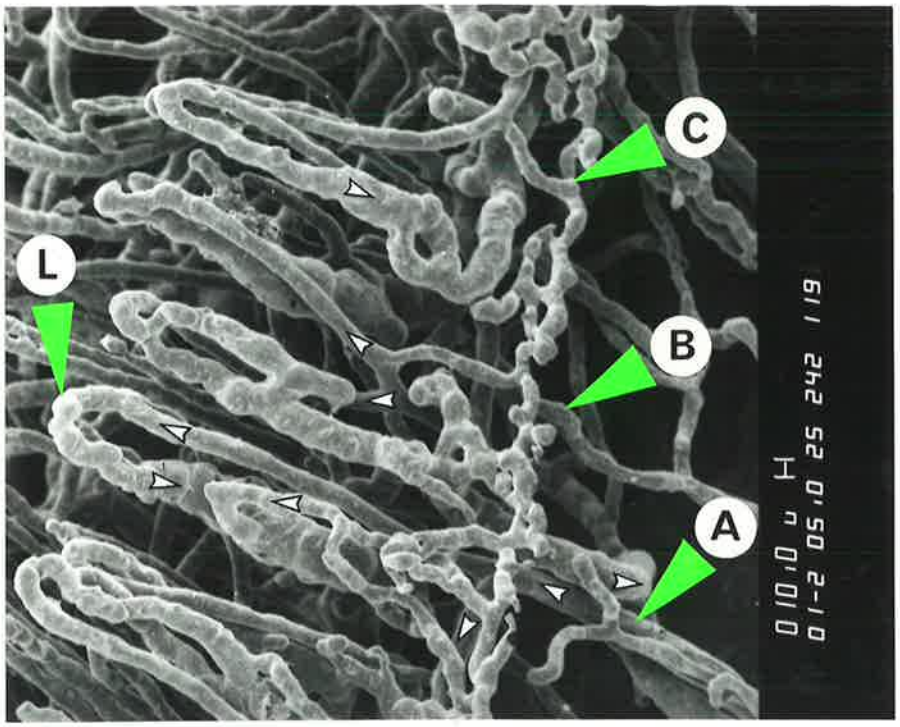

Buccal

Figure 19. Crevicular loops on the maxillary right second molar.

A terminal arteriole (A) from the periodontal ligament by-passes the circular plexus (C) to supply the crevicular loops (L). A capillary (B) from the periodontal ligament supplies the circular plexus. Crevicular loops also derive blood from the circular plexus. Crevicular loops drain into the periodontal ligament, or into the circular plexus. Both the ascending and descending limbs may divide and coalesce as they ascend and descend. White arrows indicate the presumptive direction of flow.

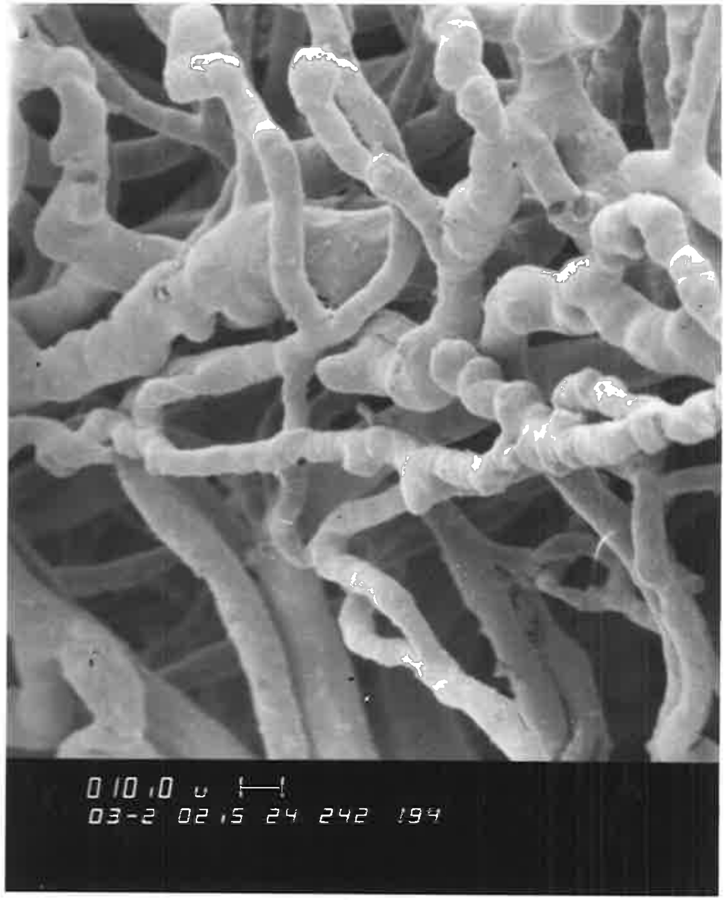
0.010 u
03-2 02.5 24 242 194

Buccal

Occlusal

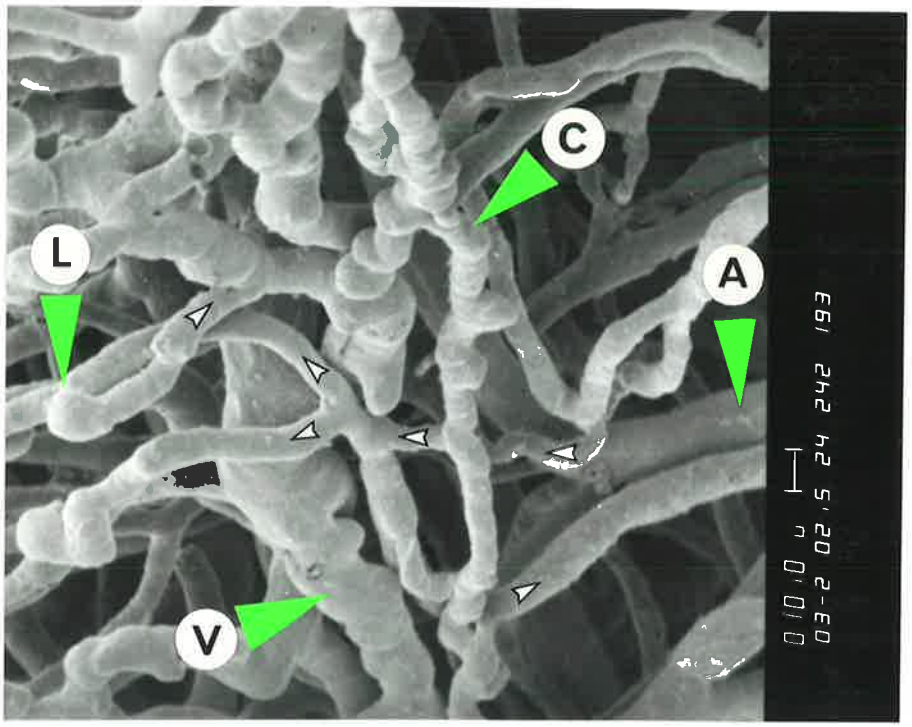

Figure 20. Mesial periodontal ligament and gingiva of the maxillary left first molar.

A capillary from the periodontal ligament supplies blood to the circular plexus, from which arise the ascending limbs of crevicular loops (L). White arrows indicate the presumptive blood supply from the PDL capillary to two crevicular loops, and the presumptive blood drainage from the circular plexus (C) to the PDL.

A = Arteriole V = Postcapillary-sized venule

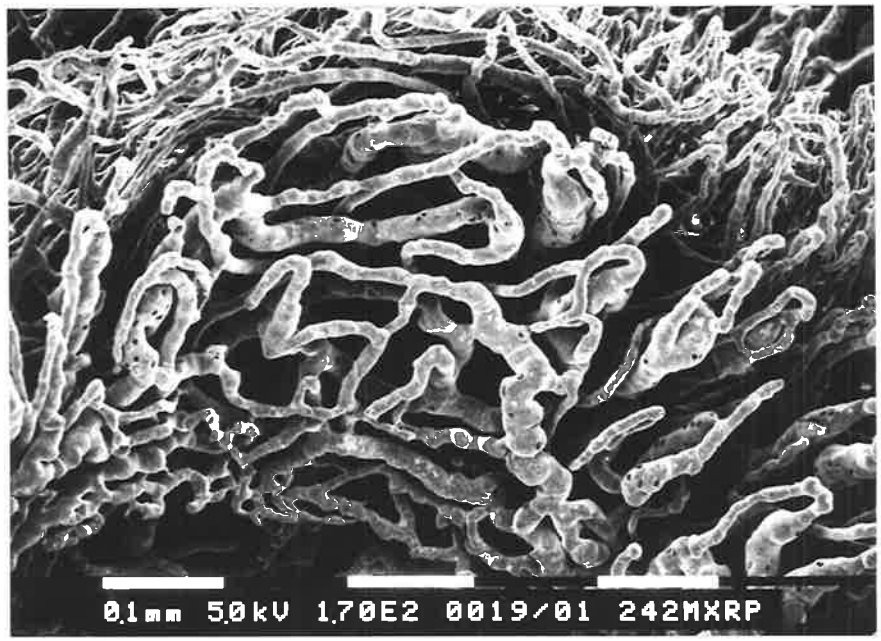
0.1mm 5.0kV 1.70E2 0019/01 242MXRP

Posterior

Palatal

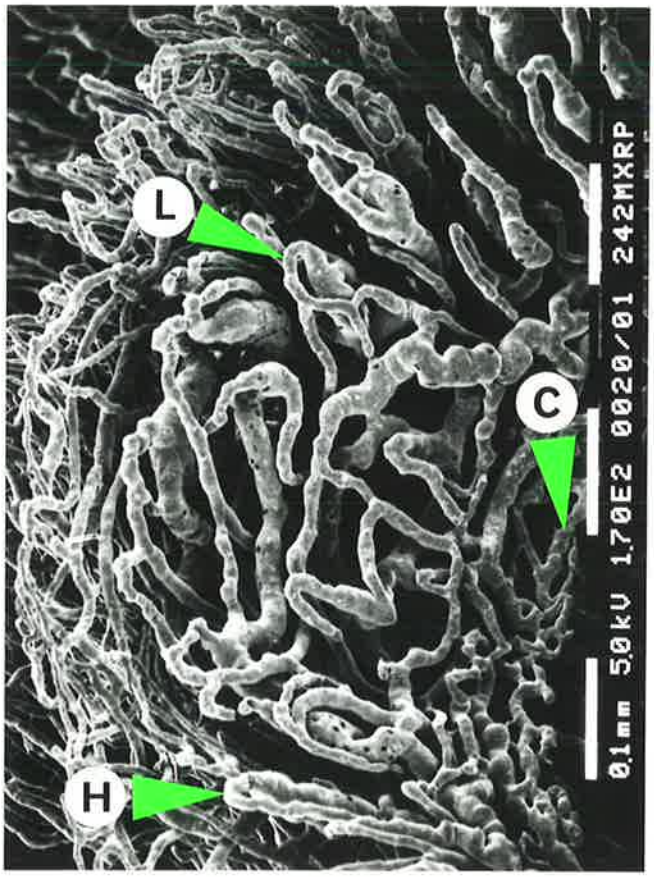

Figure 21. Palatal margin of the maxillary right first molar. Crevicular loops (L) show multiple branching.

C = Circular plexus

H = Hairpin crevicular loop

520 000 25 0,50 1 40
100 0,001 n

Distal

Buccal

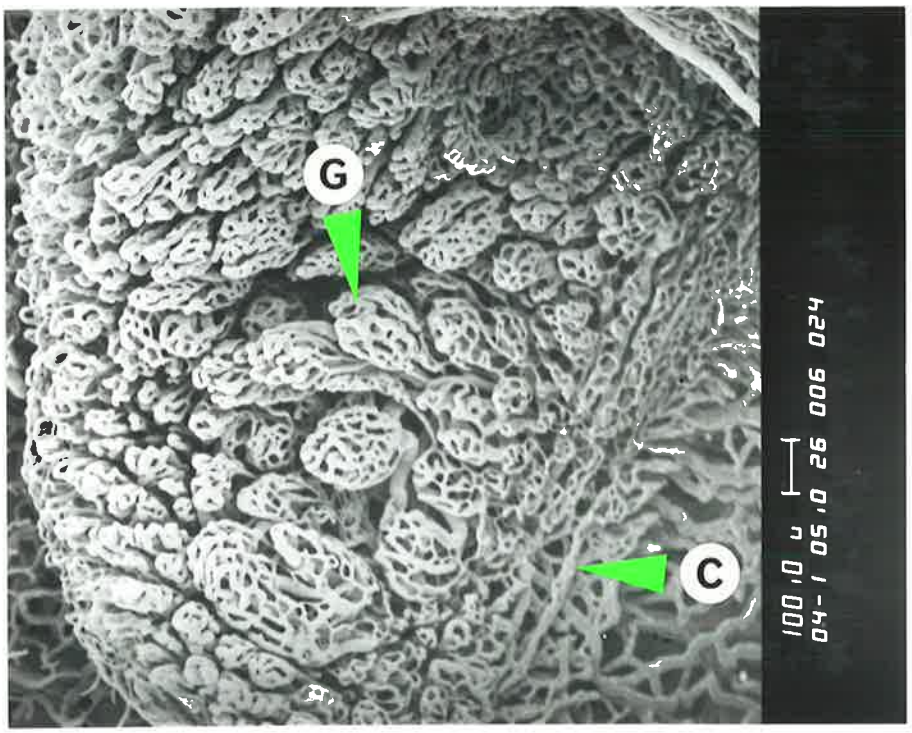

Figure 22. Buccal gingiva of the maxillary left canine.

Glomerular-like structures (G) are abundant in the canine gingiva. These are arranged in multiple tiers above the circular plexus (C).

050 0E2 L2 0'50 2-10
H ⌐ 0'010

Occlusal

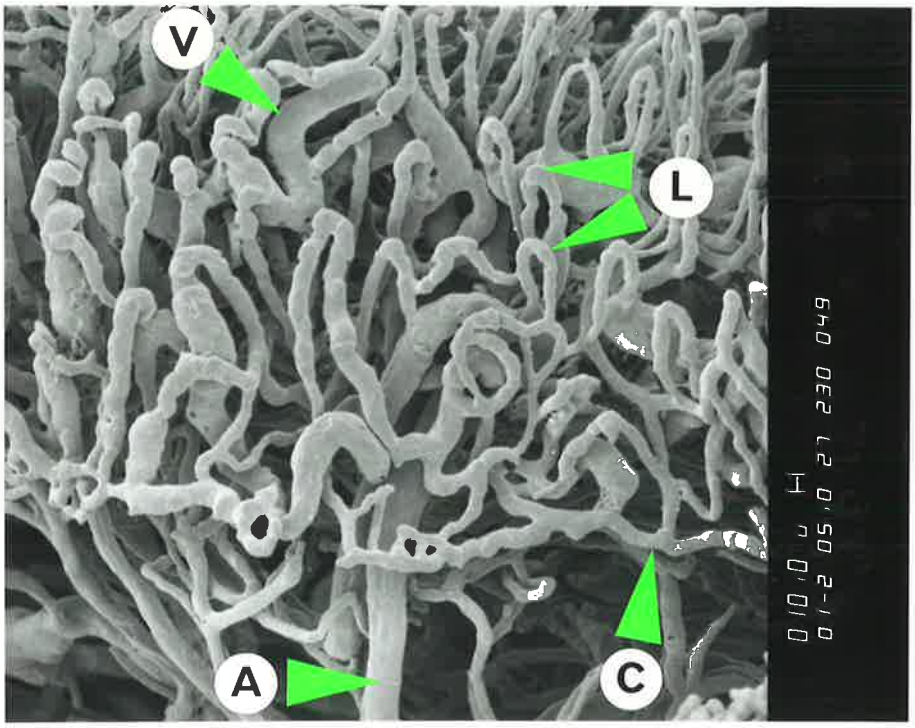

Figure 23. Buccal gingiva of the mandibular left second molar. Crevicular loops (L) in this region are arranged in multiple rows. They arise from and drain into the circular plexus (C).

A = Terminal arteriole V = Postcapillary-sized venule

821 242 26 0,50 2-20
0,0,0 H 0,0,0

Palatal

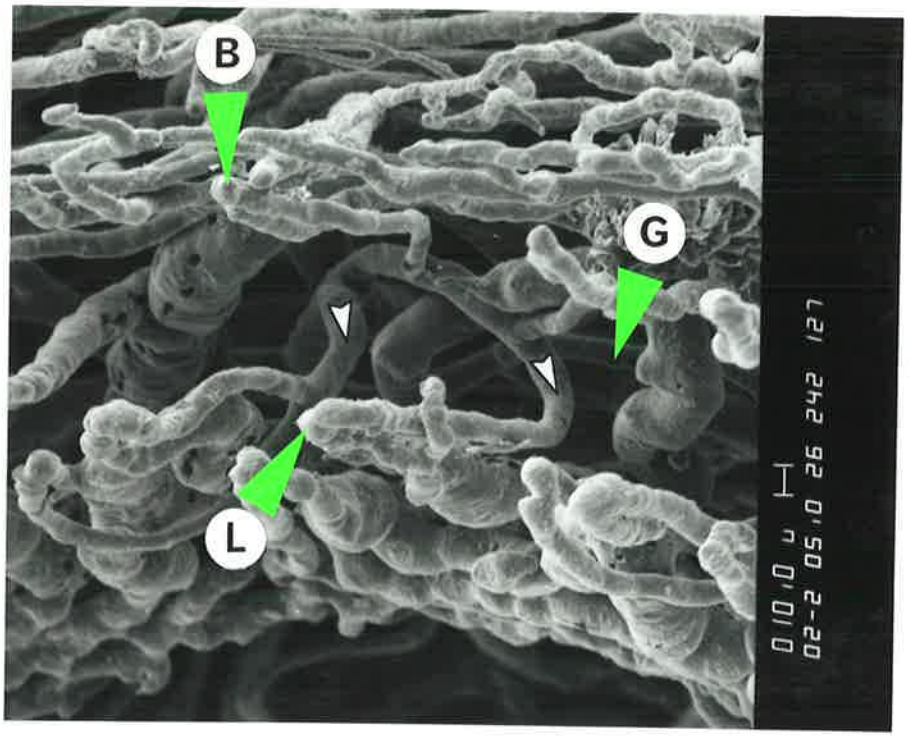

Posterior

Figure 24. Palatal gingival margin of the maxillary right second molar (Occlusal view).

Both crevicular loops (L) and palatal gingival loops (B) are supplied by deep gingival vessels. White arrows indicate the presumptive direction of flow. A gap (G) exists between the crevicular and palatal gingival vasculature.

SH1 2h2 E2 0'50 2-10
H n 0'010

Buccal

Occlusal

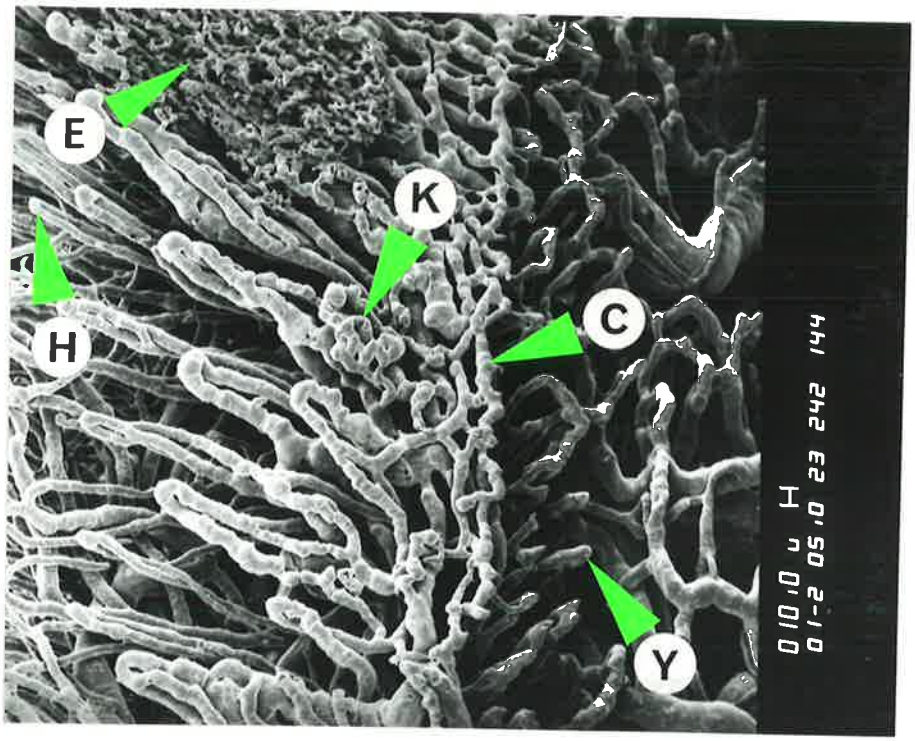

Figure 25. Mesial gingiva of the maxillary left first premolar.

Crevicular loops range from simple hairpin loops to complex twisted and coiled loops (K). Simple hairpin loops (H) supply the interdental col.

Capillary loops (Y) from alveolar bone extend to the periodontal ligament below the level of the circular plexus (C). These capillary loops are mainly found in the cervical PDL.

Extravasated material (E) is seen in association with crevicular loops. The extravasated resin shows a delicate honeycomb pattern, with small spaces between the material. No imprint patterns are seen on the extravasated material.

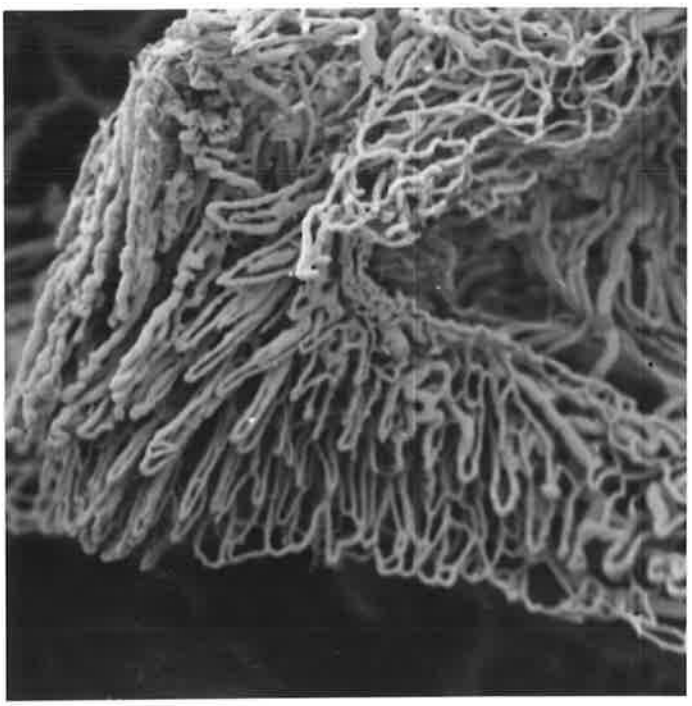

Lingual

Mesial

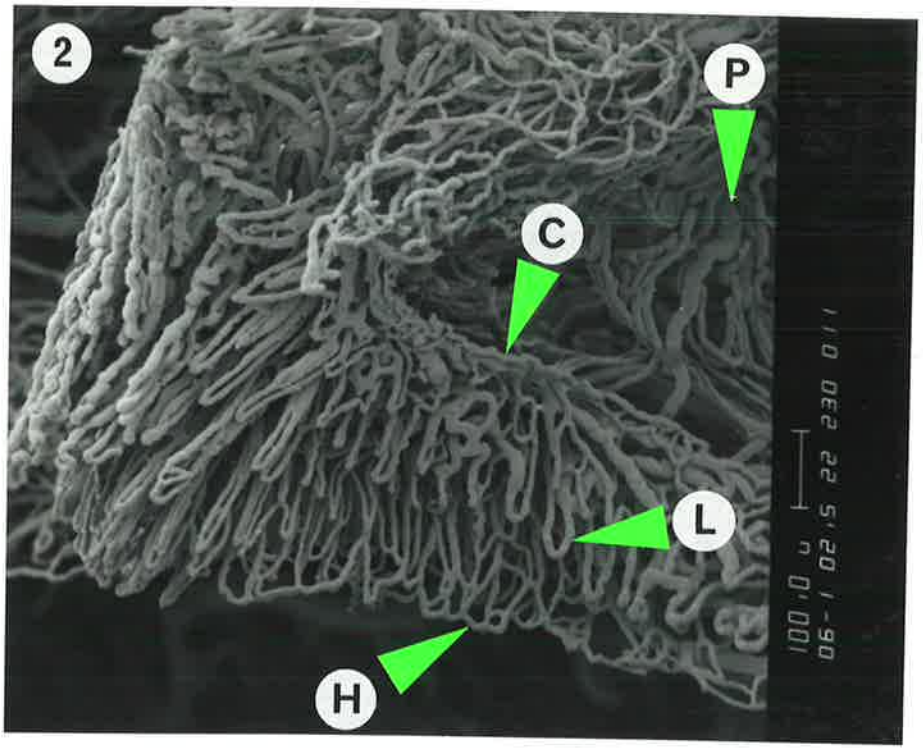

Figure 26. Distal view of the mesial and buccal gingival vasculature of the mandibular left third premolar.

The gingival vasculature on the vestibular aspect is composed of capillary loops which have coalesced to form a continuous network with a horizontal capillary (H) surmounting the crest.

C = Circular plexus

P = Periodontal ligament

L = Crevicular loop

2 = Second premolar

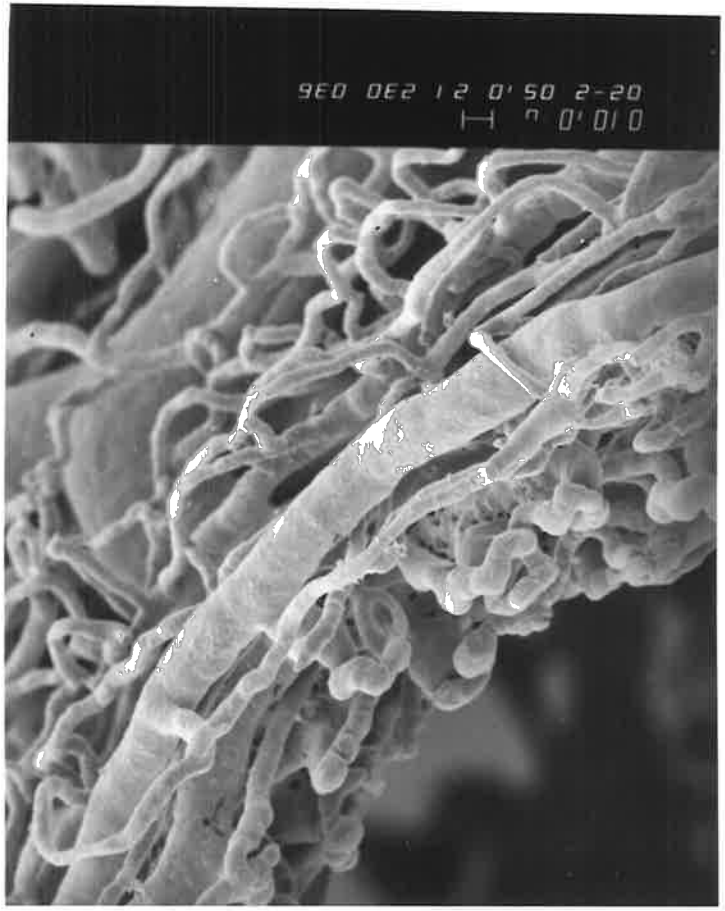
9E0 0E2 12 0'50 2-20
H n 0'010

Buccal

Distal

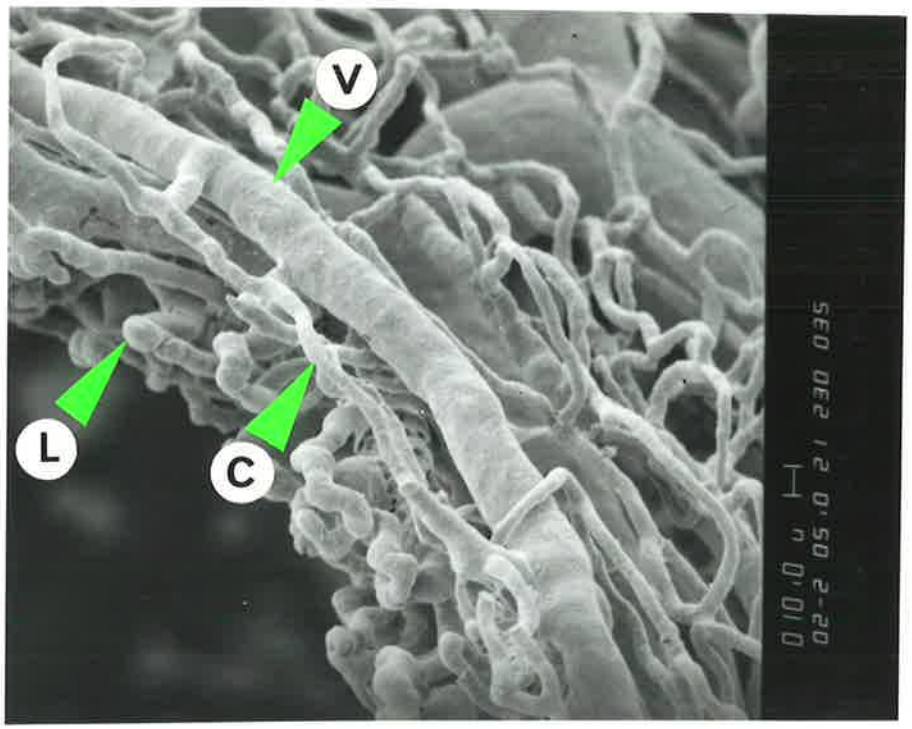

Mesial

Figure 27. Occlusal view of the buccal gingival margin of a mandibular left third premolar.

A capillary (C), 5*um* in diameter, surmounts the gingival crest, and drains into a larger postcapillary-sized venule (V), 20*um* in diameter.

L = Crevicular loop

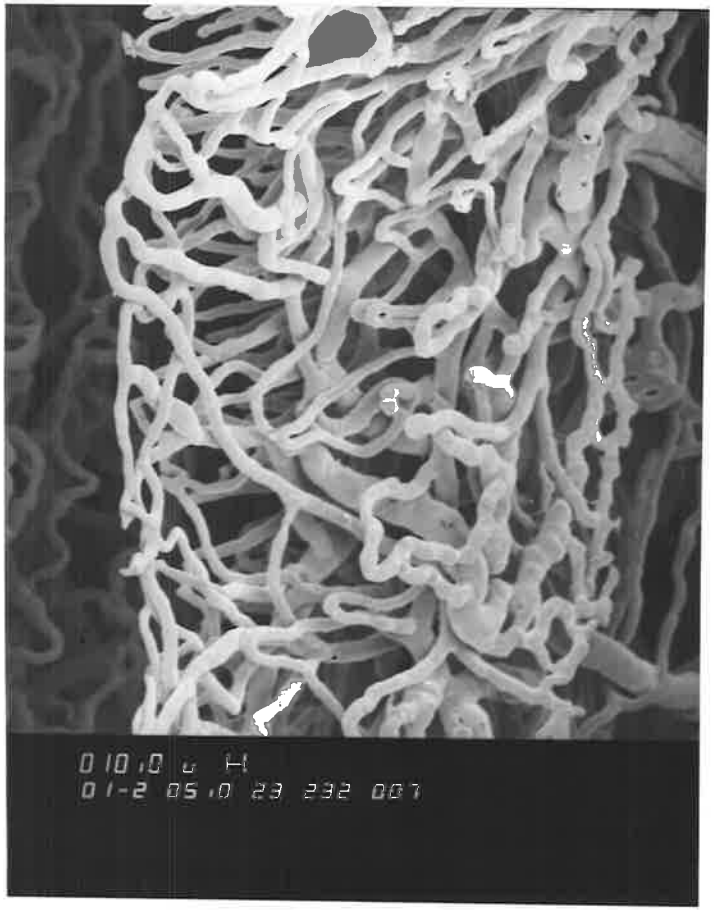
0 10 0 u H
01-2 05 0 23 232 007

Buccal

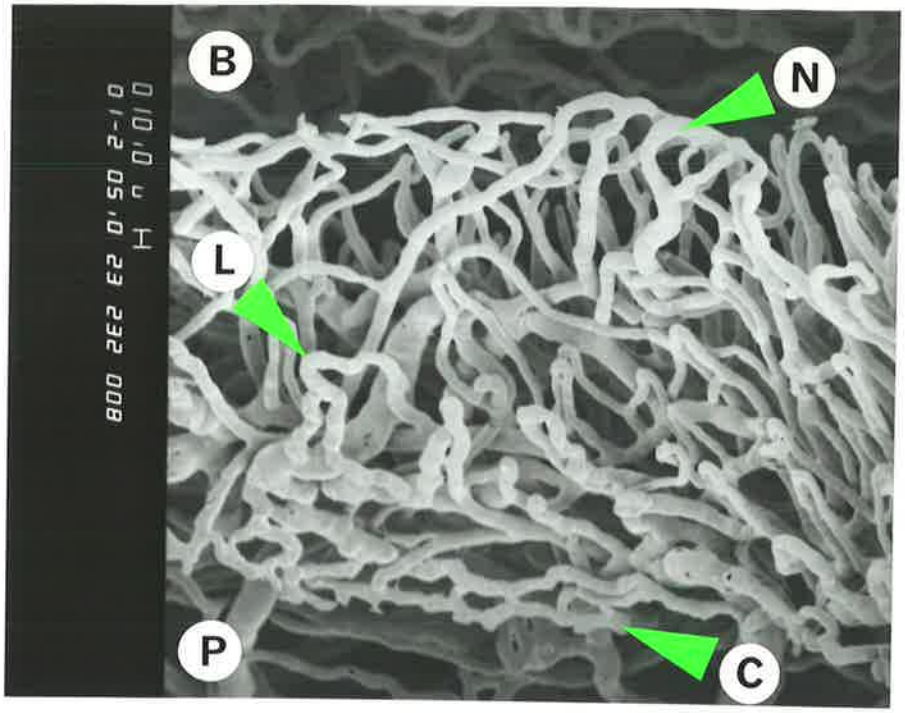

Distal

Figure 28. Occlusal view of the buccal gingiva of a mandibular right second premolar.

The vestibular gingival network (N) is a continuous network and anastomoses with the crevicular loops (L) and the circular plexus (C). The innermost circular vessel is incompletely cast. Anastomoses with the periodontal ligament plexus can also be observed.

B = Cheek vasculature

P = Periodontal ligament

820 01/ L2 0'50 /-E0
n 0'00!

Posterior

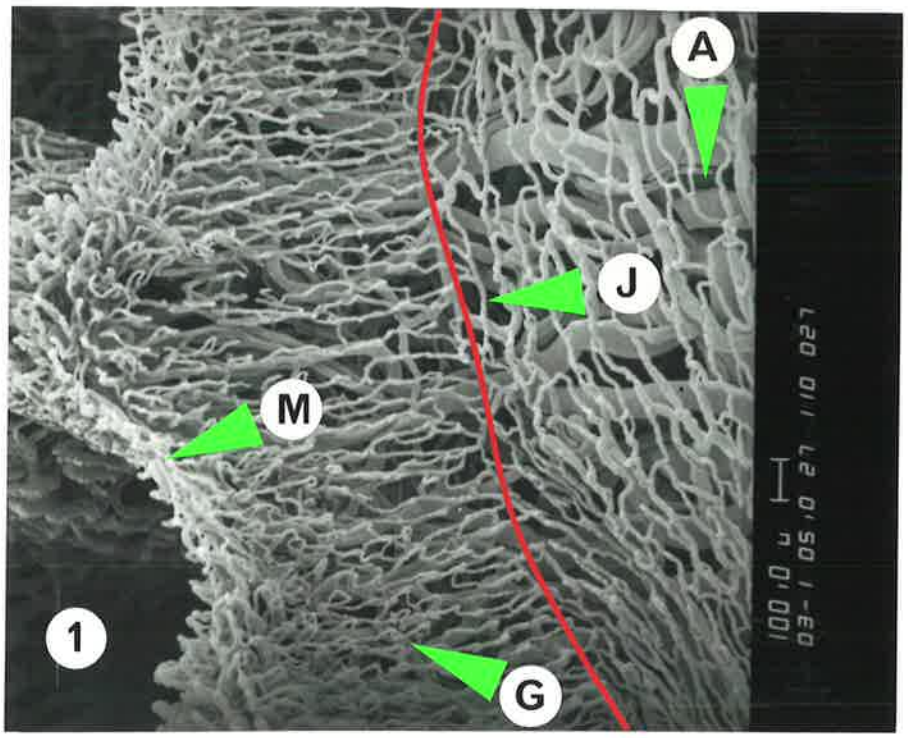

Anterior

Figure 29. Buccal gingiva of the first and second premolars in the right maxilla. Note the horizontal orientation of the vessels below the gingival margin (M) and the occluso-apical orientation further apically.

An occluso-apically orientated venous plexus lies beneath the capillary network. The orientation of the capillary network changes suddenly at the presumptive mucogingival junction (red line), about 800*um* from the gingival margin. J indicates the most occlusally placed vessel of the alveolar mucosa network.

1 = First premolar

G = Gingiva

A = Alveolar mucosa

220 0E2 81 0'50 1-90
100 0'001

Anterior

Occlusal

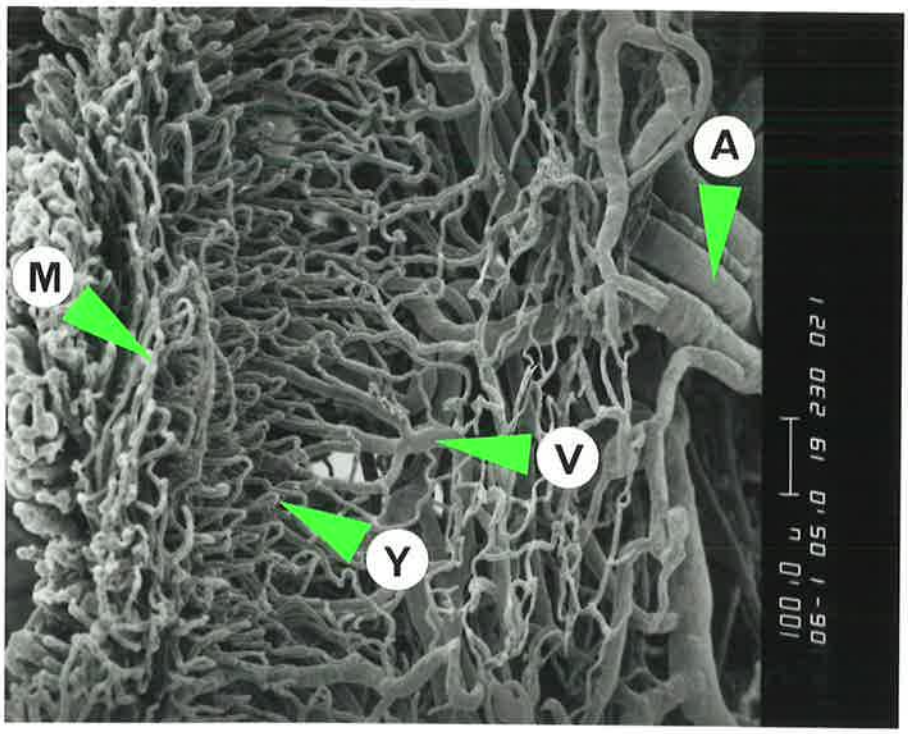

Figure 30. Buccal gingiva of the mandibular right first molar.

Note the horizontal orientation of the vessels below the gingival margin (M). Further apically, venous vessels (V) drain the gingiva occluso-apically towards the vestibular sulcus. As they descend, they coalesce into larger trunks. Papillary loops (Y) are reduced in height as they extend away from the gingival margin.

A = Arteriole

2E0 01' 82 0'50 2-10
H n 0'010

Posterior

Occlusal

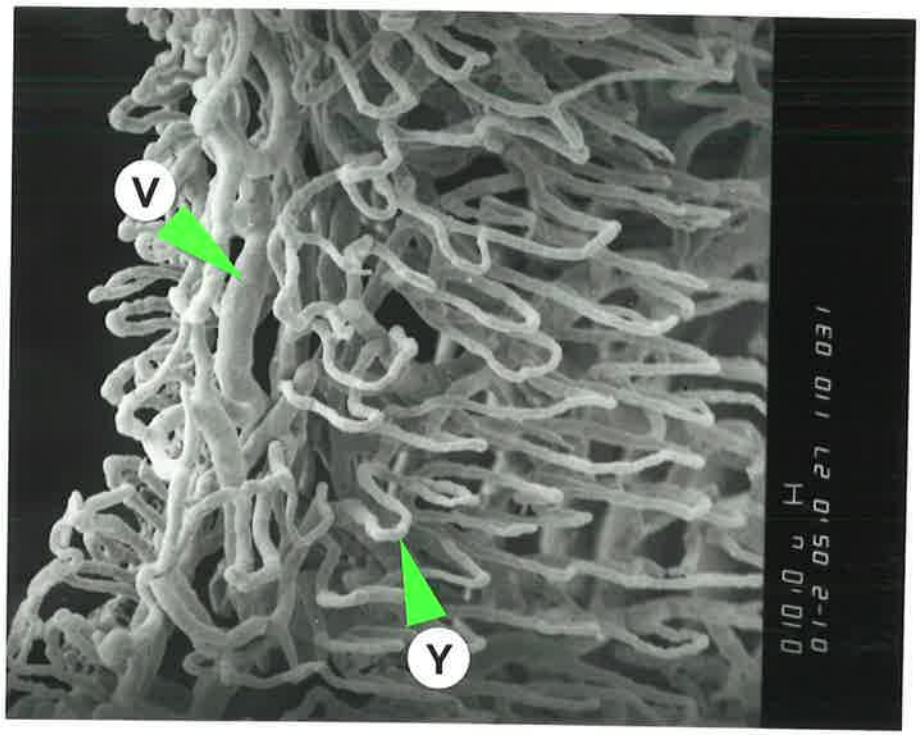

Figure 31. Capillary network on the buccal gingiva of the maxillary right second premolar.

Note the occluso-apical orientation of papillary loops apical to the gingival margin. The height of the papillary loops ranged from 60-120*um*.

Y = Hairpin capillary loop

V = Postcapillary-sized venule

55! 2k2 L2 0'50 I-50
0'00 n
100 0'00

Buccal

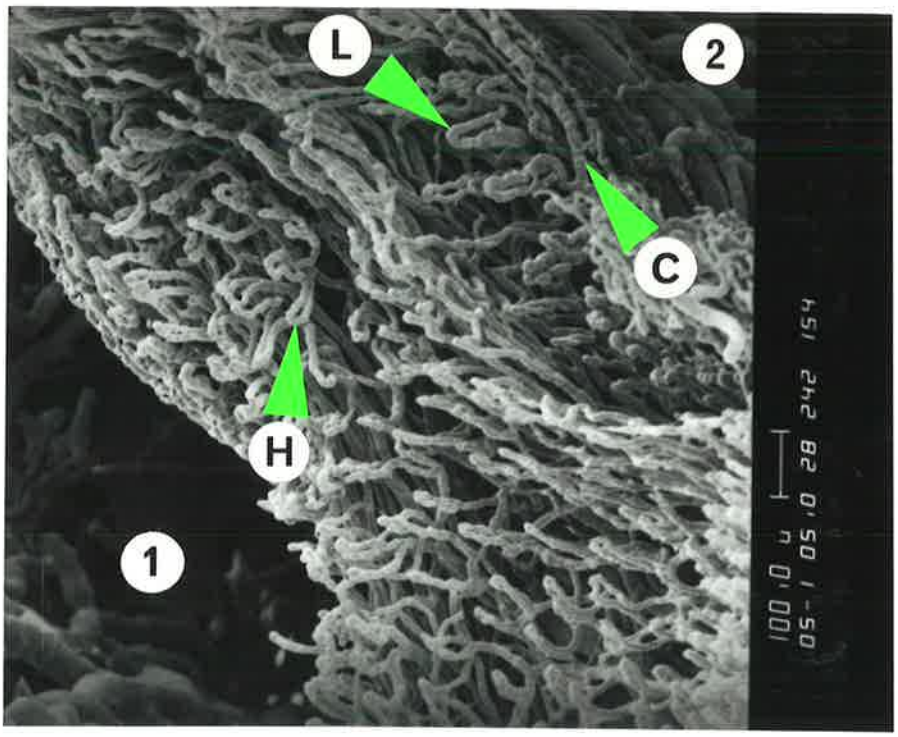

Palatal

Figure 32. The interdental col between the maxillary left first and second premolars.

Bucco-lingually orientated hairpin loops (H) in the interdental col area drain into bucco-lingually orientated venules.

1 = First premolar

2 = Second premolar

C = Circular plexus

L = Crevicular loop

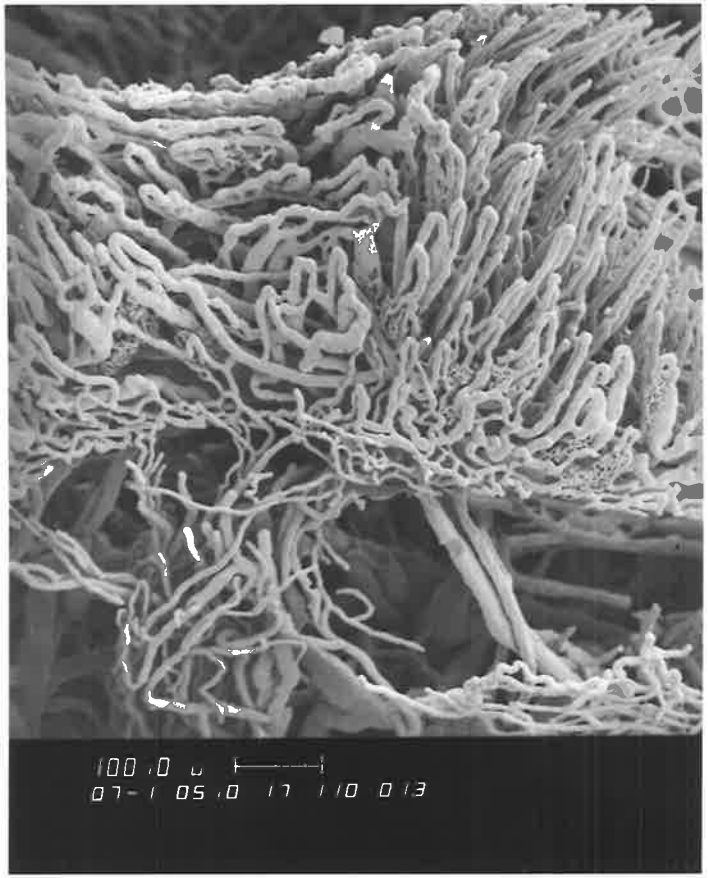

Palatal

Anterior

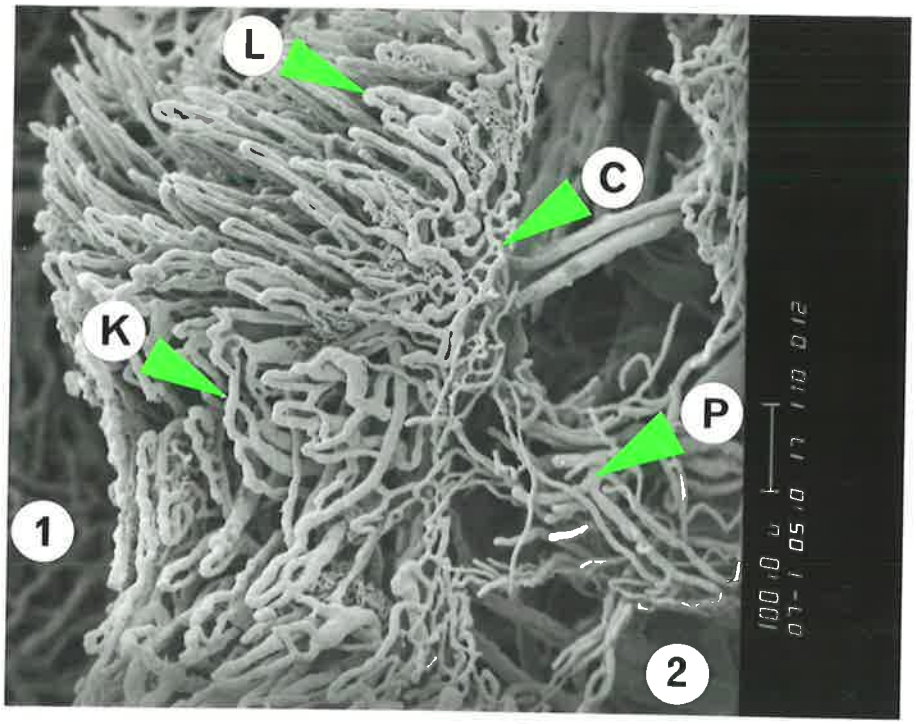

Figure 33. Distal view of the interdental col between the maxillary right first and second premolars.

Papillary loops extend into the col area, orientated sagittally. In this micrograph, col loops (K) show multiple branching. The ligament vessels are incompletely cast.

P = PDL vessels

L = Crevicular loop

1 = First premolar

2 = Second premolar

C = Circular plexus

EEO 011 L2 0'50 1-10
H n 0'001

Occlusal Buccal

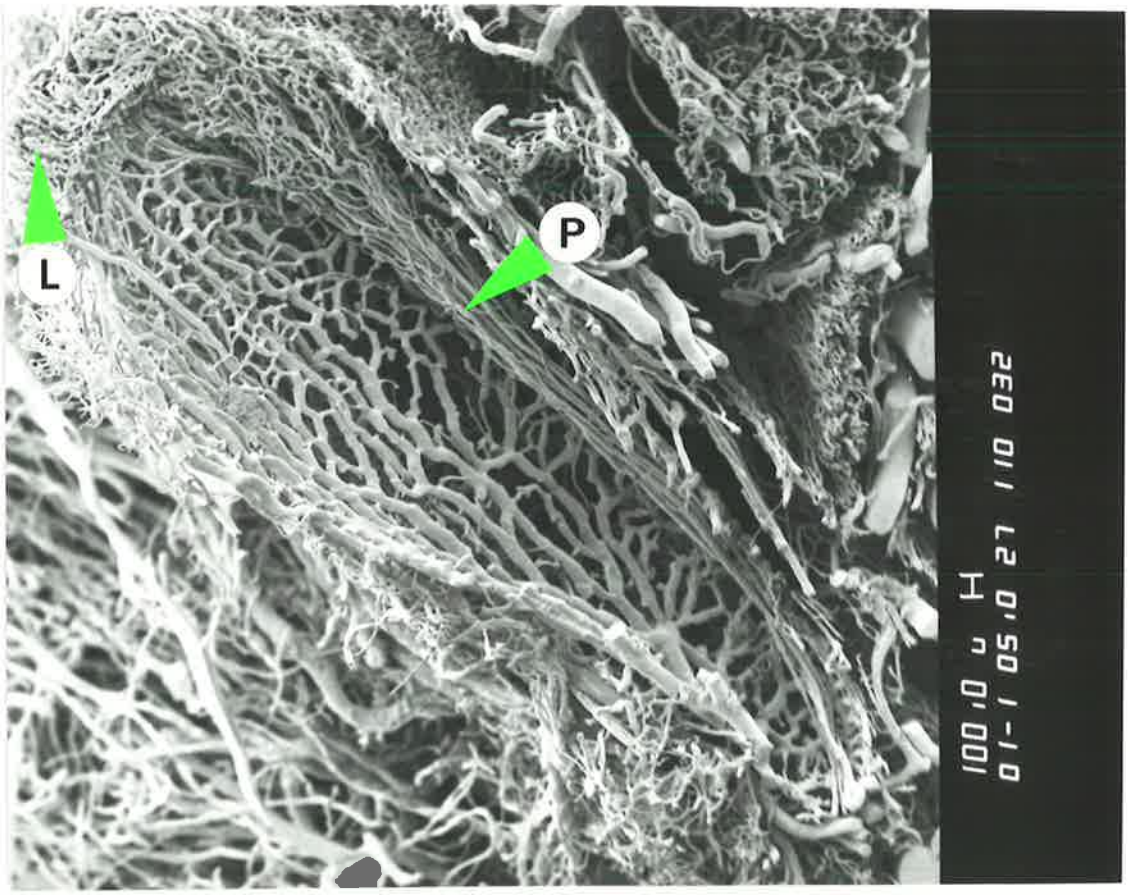

Lingual

Figure 34. Mesial periodontal ligament of the mandibular right second premolar. Posterior view.

The ligament vessels are predominantly postcapillary venules, with occluso-apical orientation, and they frequently anastomose with each other. Compare with figure 35 where the principal ligament vessels are arranged in palisades.

P = Pulp vessels L = Crevicular loops

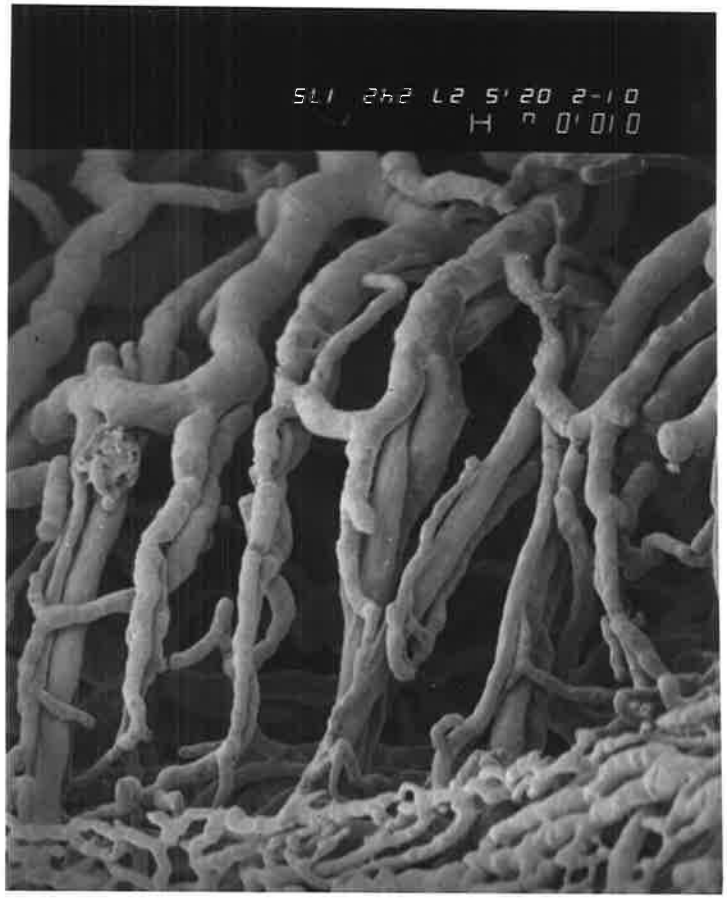
SL1 2h2 L2 5'20 2-10
H n 0'010

Occlusal

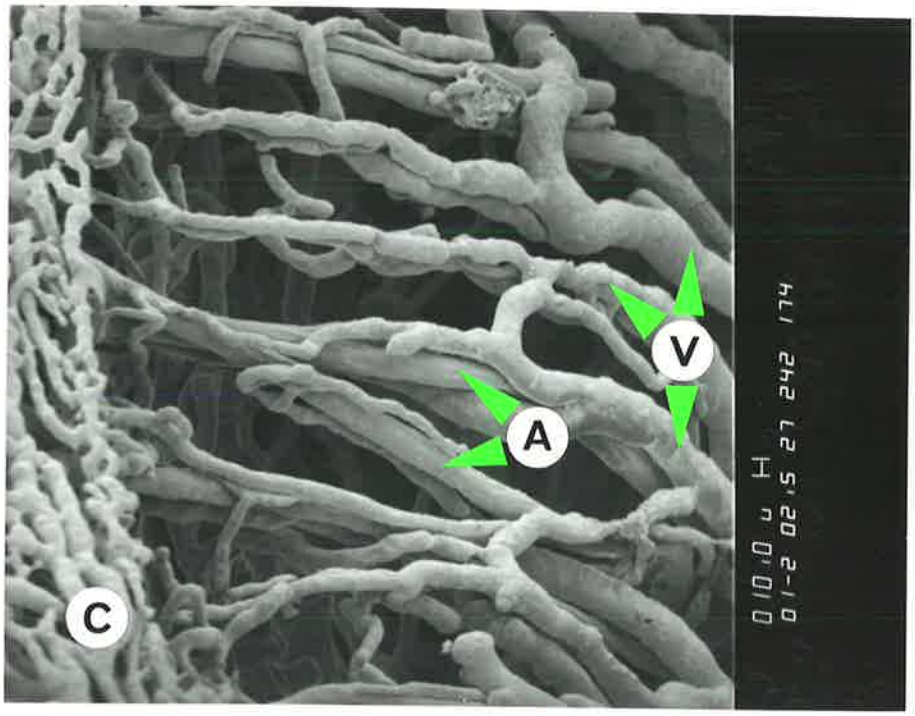

Buccal

Figure 35. Cervical end of the mesial periodontal ligament of the maxillary right second molar. Viewed from the root aspect.

Periodontal ligament vessels are arranged occluso-apically in a palisade. Arterioles (A) are less numerous, tend to have a constant diameter, run a straighter course, and branch less often. Venules are more numerous, have a varying diameter, run a more sinuous course, branch more often, and tend to be closer to the root surface. Compare with figure 37 where the ligament vessels are arranged in a plexiform pattern.

V = Postcapillary-sized venules

C = Circular plexus

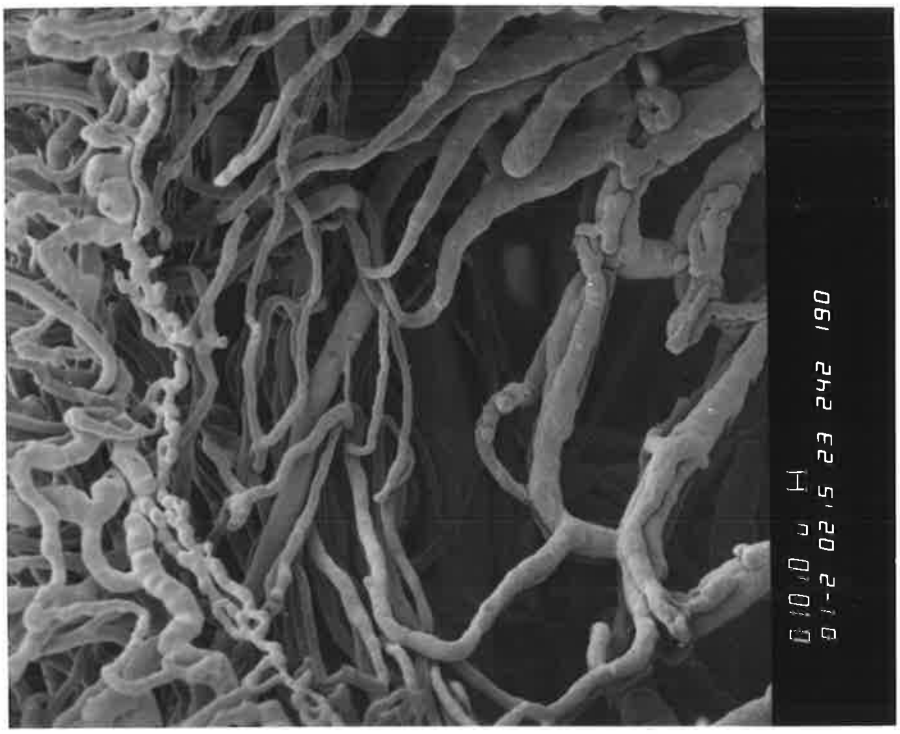

Mesial

Occlusal

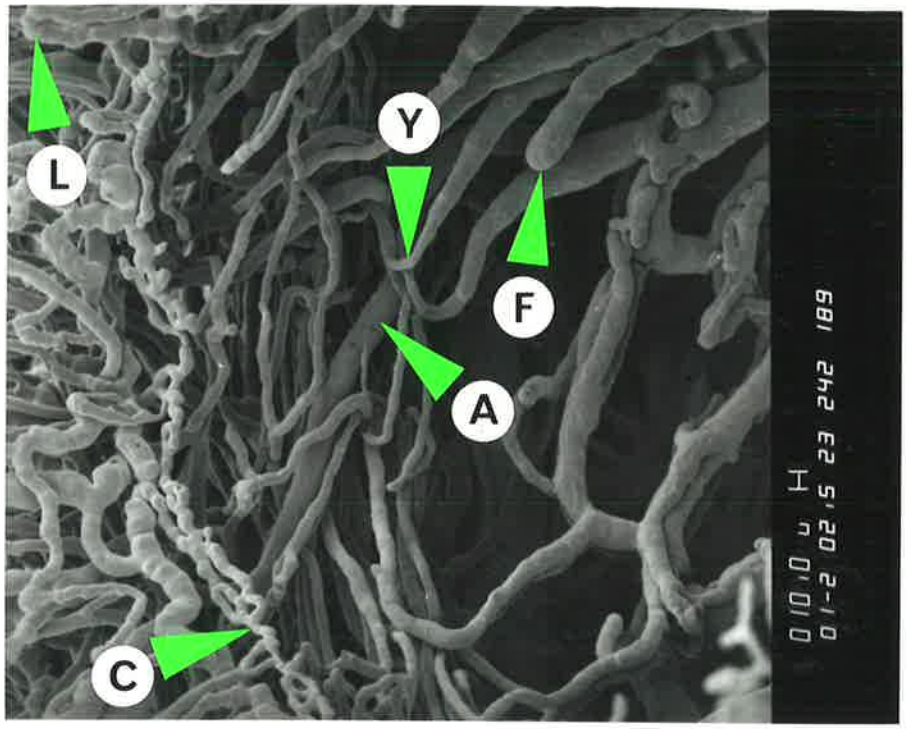

Figure 36. Palatal periodontal ligament of the maxillary left third premolar. Viewed from the root aspect.

In this region, the periodontal ligament vessels run occluso-apically in an oblique direction. Capillaries (Y) enlarge suddenly into postcapillary-sized venules up to 30um in diameter. Capillary vessels (Y) perforate the cribriform plate to pass into the periodontal ligament.

C = Circular plexus

A = Arteriole

L = Crevicular loop

F = Incomplete filling

LEO 01' L2 0'SO 2-20
H n 0'010

Occlusal

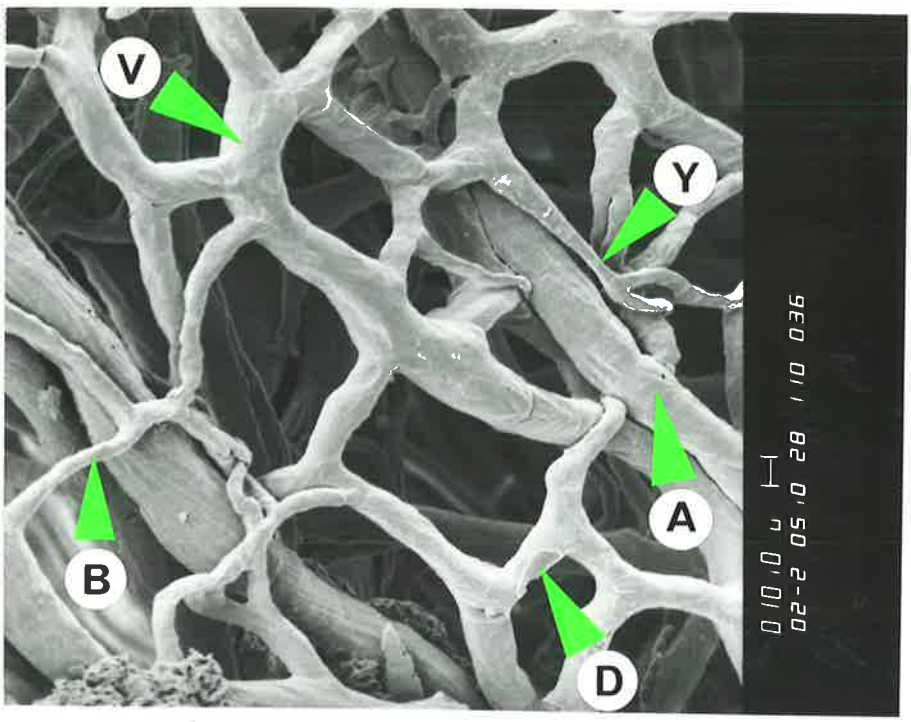

Buccal

Figure 37. Cervical periodontal ligament of the mandibular right second premolar, viewed from the root aspect.

Postcapillary-sized venules (V) drain in an occluso-apical direction. Capillaries (B) link up adjacent postcapillary-sized venules. Some capillaries appear to run in an apico-occlusal direction (Y). Terminal arterioles (A) are clearly demonstrated in the ligament. Voids (D) do not bear any imprint patterns.

H12 2H2 22 5.20 2-20
0.010 n

Occlusal

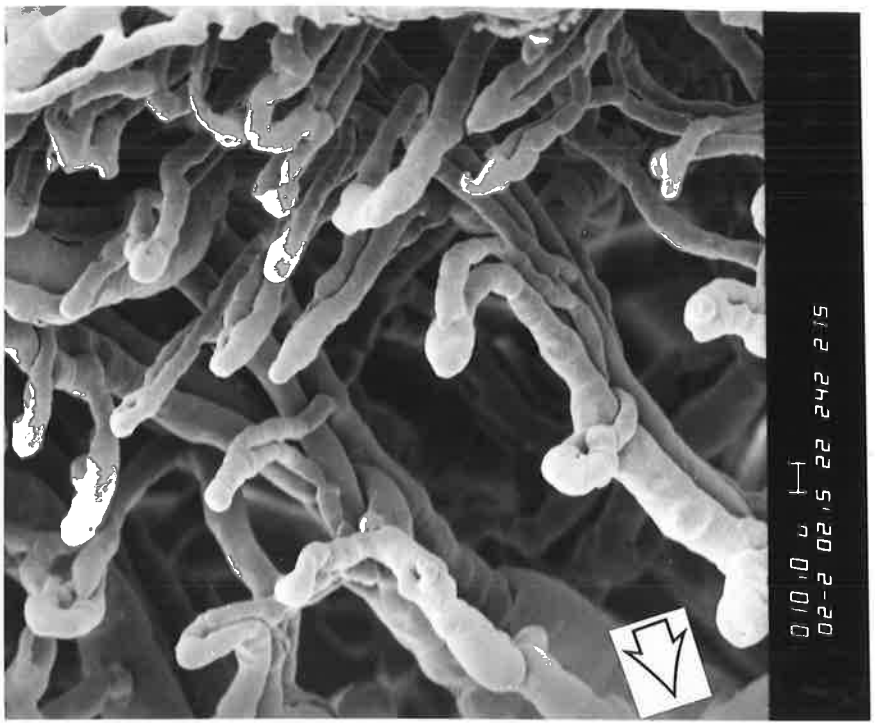

Buccal

Figure 38. Hairpin capillary loops in the cervical third of the distal periodontal ligament in the mandibular left third premolar. Viewed from the root aspect. The arrow points towards the apex.

Capillary loops are orientated in the direction of the root surface.

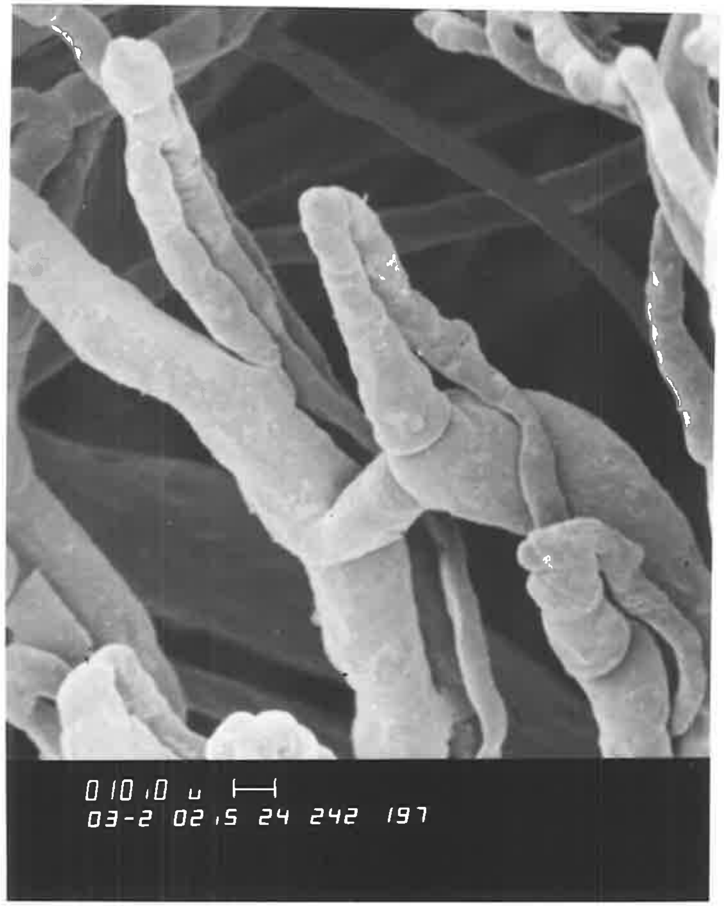
0010.0 u
03-2 02.5 24 242 197

Buccal

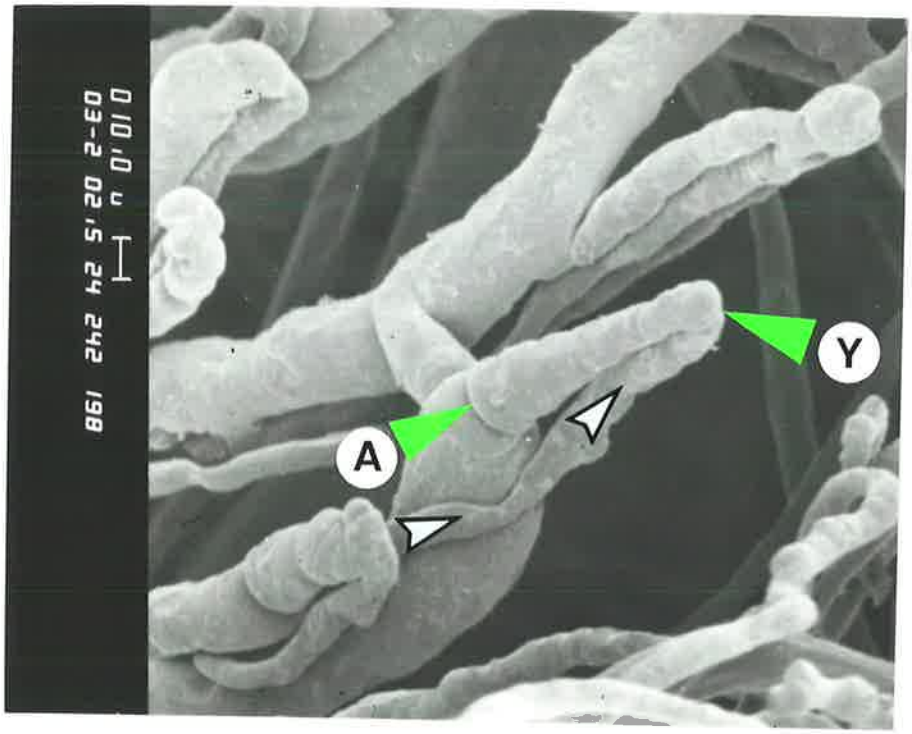

Occlusal

Figure 39. Cervical third of the distal periodontal ligament of the maxillary left second premolar, in the disto-palatal corner. Viewed from the root aspect.

The descending limb of the capillary loop (Y) expands suddenly and drains into a postcapillary-sized venule. An annular constriction (A) is seen at the base of the descending limb, before it joins the postcapillary-sized venule.

White arrows indicate the presumptive direction of flow.

SEO 011 82 0'50 I -40
n 0'001

Occlusal

Buccal

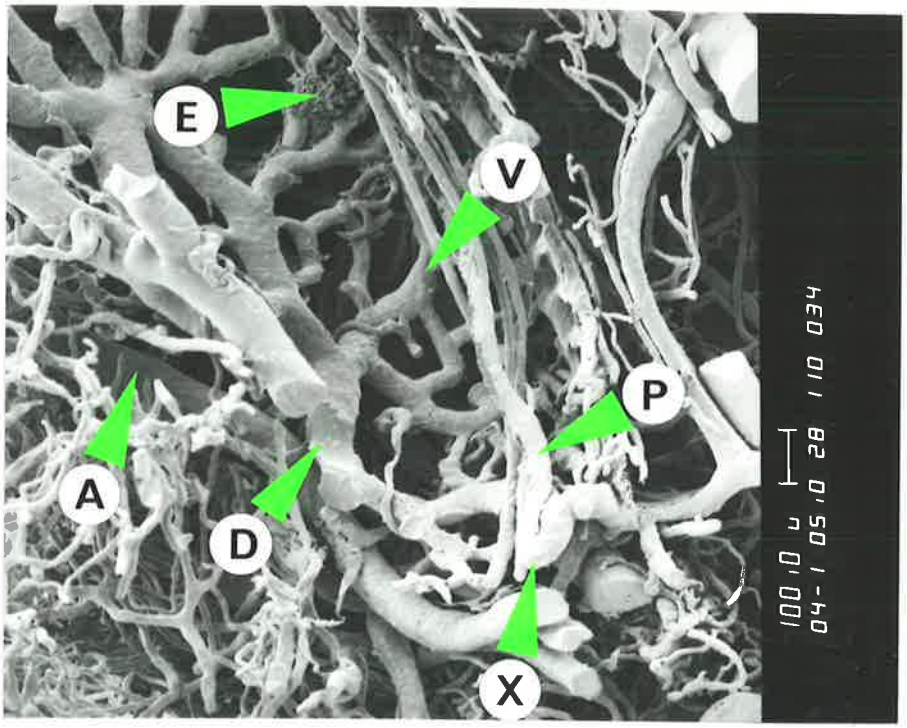

Figure 40. Distal view of the apex of the mandibular right second premolar. Periodontal ligament vessels converge at the apex. Anastomosis (X) between periodontal ligament venule and pulp venule (P) occurs at the apex.

E = Extravasated resin

A = Arteriole

V = Collecting-sized venule

D = Void in the cast (incomplete filling). Note the absence of imprint patterns in the void.

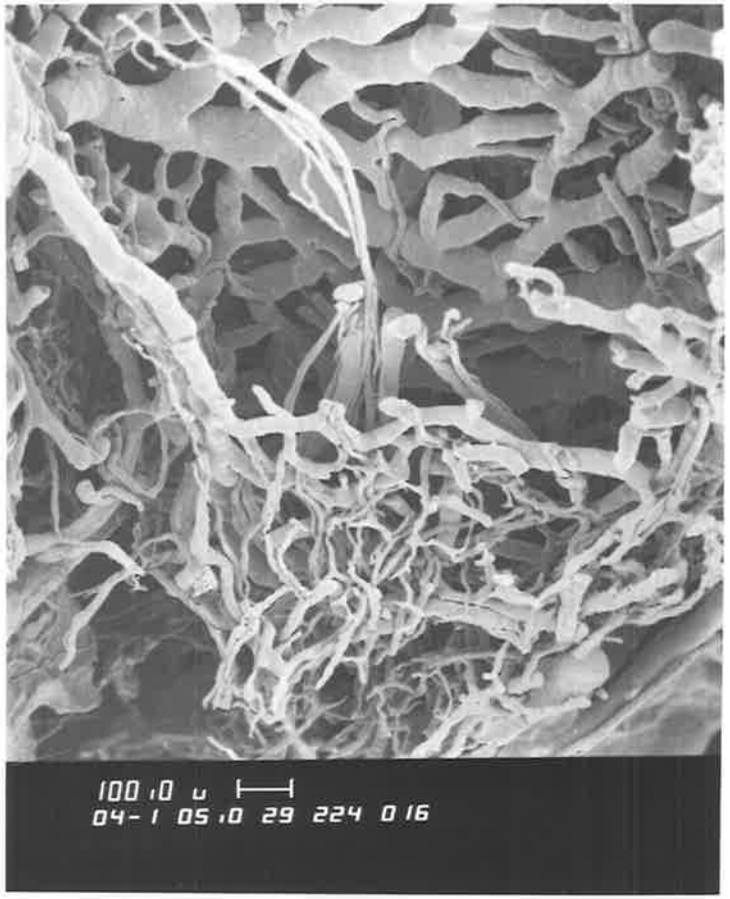
100.0 u
04-1 05.0 29 224 016

Palatal

Occlusal

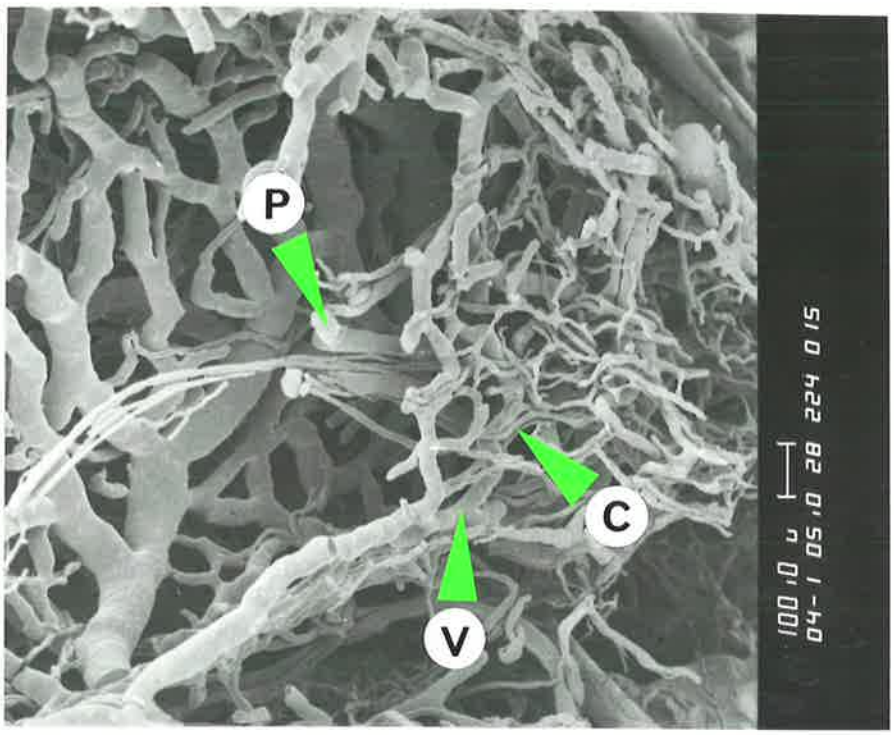

Buccal

Figure 41. Distal view of the apex of the maxillary right first premolar. Postcapillary-sized venules and collecting-sized venules form a network closer to the root surface. Capillary vessels (C) form another network closer to the alveolar bone.

P = Pulp vessels

V = Collecting-sized venule

DISCUSSION

TECHNICAL CONSIDERATIONS

Corrosion casting is a technically difficult procedure, often with unpredictable results. Incomplete casting is a common problem and has often been attributed to vasospasm, blockage, or insufficient perfusion pressure.

Production of good castings depends on the control of the following factors, which ensure adequate flow of the resin to the smallest vessels of the oral microvascular bed.

Perfusion procedure

The animal can be perfused from the heart, but a better casting is produced if the cannulation is as close to the target organ as possible (Tompsett, 1970; Lametschwandtner *et al.*, 1984). Therefore, the common carotid arteries were selected for cannulation.

After saline washout, some other investigators (*e.g.* Murakami, 1971) would further rinse the vasculature at 50-55°C to warm up the vessels so as to accelerate the polymerization of the casting medium. This procedure was omitted as the effect on the vasculature is not known.

Tompsett (1970) advised against the use of excessive pressure during perfusion as this can cause tissue swelling and waterlogging. It may be argued that it is important to perfuse the animal at physiologic pressure. However, the bottle pressure is not equal to the intra-vascular pressure, which is the important parameter (Lametschwandtner *et al.*, 1984). Furthermore, the purpose of this experiment was to demonstrate the anatomic relations of the total microvascular bed, as distinct from the functional microvascular bed which

may include dormant areas. Consequently, vasodilators and hand perfusion were employed to ensure adequate perfusion.

One criterion to assess intravascular pressure is the "dry nose criterion" (Hodde *et al.*, 1977; Hodde and Nowell, 1980). According to these authors, as long as there is no outflow of transudate from the nose of the animal, the injection pressure would not be excessive. This guideline was observed in this experiment, although it can be argued that the periodontal microvasculature may react differently from nasal mucosal microvasculature to the same intravascular pressure.

Prolonged blood washout should be avoided, since prolonged saline perfusion produces progressively more oedema in the tissues so that extensive changes may occur in the vascular cast (Gannon, 1978). This was avoided by the addition of PVP-40 in the washout solution to increase the colloid osmotic pressure.

Fixation with glutaraldehyde

Prior fixation before the introduction of the casting medium was found to improve replication of the luminal surface and clarity of detail of the resulting cast (Hodde *et al.*, 1977; Hodde, 1981).

On the other hand, prior fixation sometimes made it more difficult to macerate the specimen. Furthermore, the vasoactive effects of the fixative on the vessel wall are not known (Hodde and Nowell, 1980).

Incomplete Casting

Incomplete casting can be due to:

1. Vascular spasm. Such spasm can limit the distribution of the resin. Papaverine and sodium nitrite were added to the washout solution to promote vasodilation and reduce vasospasm.

2. Blockage. Fine vessels can be blocked by particulate matter if the washout solution, fixative, or resin, are not filtered. Also, air bubbles accidentally introduced into the tubing can lead to blockage by the emboli. It is important to rinse out all the blood before casting as blood cells can cause blockage (Lametschwandtner *et al.*, 1984).

3. Insufficient perfusion pressure. If the infusion pressure is not high enough, the resin will not flow well. It may be helpful to intermittently clamp the drainage tube and allow the intravascular pressure to build up during perfusion, thereby opening up dormant vascular beds. If the pressure at the exit of the tubular system (the inferior vena cava) is too high, flow will be impeded. Therefore, a large tubing was inserted into the inferior vena cava to allow unimpeded flow. Blood clot in the venous system, or drainage tube, will also impede the flow. Excessive pressure, on the other hand, can lead to rupture of the capillaries (Lametschwandtner *et al.*, 1984).

4. High viscosity. The viscosity of the fluid should be low enough to fill the smallest vessels. The viscosity of Mercox increases immediately upon mixing with the catalyst. Premature polymerization of the Mercox resin can result if too much catalyst is added, if the temperature of the resin

is too high, or if there is prolonged mixing of the catalyst with the Mercox resin.

There is a limit to which the viscosity of the fluid can be reduced, as too fluid a mixture tends to rupture fine vessels (Gannon, 1978). Whether such reduction in viscosity can lead to extravasation in vessels has been questioned by Castenholz (Lametschwandtner *et al.*, 1984). The findings in this investigation indicate that extravasations, due to reduced viscosity or other factors, do indeed occur.

Too viscous a resin will not penetrate the capillaries. On the other hand, viscosity should be high enough to obtain minimal polymerization shrinkage (Lametschwandtner *et al.*, 1984). A viscosity of 36 centistokes was found suitable for the method employed in this experiment.

5. Small cannula size. This was the major reason why initial attempts at vascular casting failed. The largest cannula possible must be used. This is the most important factor to consider, as flow rate is related to the fourth power of the radius. Doubling of the radius leads to a sixteen-fold increase in flow rate.

6. Inadequate mixing of catalyst and resin can result in incomplete polymerization of the cast.

7. Breakage. The delicate casts are easily broken during processing and many fine branches are broken in this way.

8. External pressure on the vascular bed can lead to vascular occlusion, preventing complete filling.

9. Rupture or blowout of vessels can occur if excessive pressure is used, or if the animal is handled roughly.

10. Cannulation too far from the target organ. This was not a problem in this experiment, but it can be a problem in perfusing other tissues if the resin has to pass through an intervening capillary bed.

11. Insufficient perfusion time. Perfusion should not be stopped until resin appears at the egress site.

Dimensional stability of the replicating medium

According to the manufacturer, there is a shrinkage of 0.9% measured following the Japanese Industrial Standards method K 6911 (Hodde *et al.*, 1977). However, Weiger (1981) and Weiger, Lametschwandtner and Adam (1982) have found a shrinkage of 6%, despite the manufacturer's claims. This factor should be considered when dimensions of the casts are estimated. In this experiment, the cast dimensions stated were not corrected for polymerization shrinkage.

Tissue Corrosion

Tissue corrosion takes a long time. The larger the piece of tissue, the longer it takes to corrode the specimens and clean the cast. Hence, it is a good idea to section the tissue into small blocks for corrosion. On the other hand, if the casts are too small, the delicate casts can be damaged as they are not protected by the surrounding vascular network against accidental knocks during handling.

The concentration of KOH is not critical for corrosion and sodium hydroxide can also be used (Gannon, 1978). Specimens can be placed in phosphate-buffered pancreatin or sodium hypochlorite for further cleaning (Gerszberg, Roa and

Korte, 1985). In this experiment, KOH proved adequate for most of the specimens.

Higher incubation temperatures accelerate the tissue digestion, but temperatures above 50°C should be avoided since the acrylic casts may soften at higher temperatures (Gannon, 1978). Some investigators (*e.g.* Murakami, 1971) have used ultrasonic cleaning to clean the casts but this was not found to be necessary.

Trimming of casts

Methods of trimming casts used by other investigators include fine trimming with forceps in a warm alcohol bath (Murakami, 1972), sectioning on the dry and mounted cast (Murakami, 1975), sectioning casts embedded in water soluble wax, cutting dried mounted casts with a laser beam (Hodde and Nowell, 1980; Hodde, 1981), using a light microscope micromanipulator (Nowell and Tyler, 1974) or an SEM micromanipulator (Pawley and Nowell, 1973).

The SEM micromanipulator appears to be most promising, but unfortunately was unavailable for use in this investigation.

Artifacts

Artifacts can be recognized by the lack of endothelial cell imprints (Hodde, 1981). Incompletely filled vessels appear as blind-ended finger-like processes (5.46/fig. 36). Voids appear in the cast as hollowed-out craters (5.47/fig. 37). These can be due to improper mixing of the resin, or the inadvertent introduction of air bubbles during perfusion.

Spots, blemishes or particles on the cast surface can be due to incomplete cleaning, dust contamination, or fragments of uncorroded tissue.

White spots in the micrographs are due to charging of the specimen, when there is a build-up of electrons on the specimen surface. Charging is prevented by proper mounting and coating of the specimen, using low accelerating voltages for SEM examination, and the use of conductive bridges (Lametschwandtner, Miodonski and Simonsberger, 1980). These bridges were used in some of the specimens.

Murakami *et al.* (1973) said that specimens could be viewed under the SEM by exposing to vapourized osmium without further coating with metal. Charging effect was claimed to be minimal. However, all the casts in this experiment were further coated with carbon and gold/palladium alloy.

Constrictions in corrosion casts have been demonstrated by Duvernoy, Delon and Vannson (1981) in the human cerebral vessels, and by Motti *et al.* (1987) in rat cerebral vessels. Constrictions in the cast may be due to incomplete filling, or alternatively, represent sphincters. Sphincters could be differentiated by the occurrence of a high density of nuclei imprint patterns. Absence of nuclei imprints suggested incomplete filling. Vasoconstrictive reactions of the vessels to various casting media have been cited by Hodde and Nowell (1980). Motti *et al.* (1981) have suggested that the vasospastic phenomenon is due to the myogenic response of blood vessels to the high pressure used when the casting medium is injected, while Duvernoy *et al.* (1981) have suggested that they may be due to vascular sphincters which regulate cortical blood flow.

Sphincters have not been described in the periodontal ligament blood vessels but the possibility of a vascular response should be considered. Pericytes and endothelial cells may have contractile properties, resulting in a reduction in luminal diameter (Rhodin, 1968).

Broken casts are easily identified as they have sharp jagged edges. Breakages are common as the casts are extremely delicate and specimen preparation requires a lot of handling and movement which often introduce vibrations.

Sometimes, a mass of resin can be seen which bears no resemblance to any anatomic structure. This is due to extravasation of the resin into tissue spaces. The amorphous mass may bear a resemblance to uncorroded tissue, but when occurring isolated in an otherwise clean area, it suggests that extravasation may be a more likely cause. This extravasated material was often found in the marginal gingiva in close association with complex convoluted crevicular loops in this study. Kindlova (1967a) also found extravasation related to dilated gingival capillaries and attributed it to vascular changes due to inflammation.

Extravasation of resin can occur at high perfusion pressures. Casley-Smith and Vincent (1978) have shown that semi-polymerized methyl methacrylate molecules could pass through vascular fenestrae into interstitial tissue channels in the rat in areas of high intravascular pressure. Such high pressures may have resulted from hand injection of the resin, in conjunction with a localized weakness in the vascular endothelium, resulting in rupture through the vessel wall.

It is possible that the morphological appearance of the extravasated resin in this project reflected interstitial

channels in the gingival vasculature. The limited areas in which this extravasated material was found could be because the blood vessels in those regions have increased permeability. This increased gingival permeability may be related to a functional requirement, for example, in the production of crevicular exudate (Cimasoni, 1983).

The administration of even small amounts of heparin makes the capillary susceptible to minor environmental changes and leads to petechial haemorrhages during simple reactive hyperemia (Zweifach, 1961). This effect may be another factor related to the extravasations.

The use of the SEM and stereopair micrographs

Recording the SEM images of the casts on single unpaired micrographs gives far less information than could be provided from stereopair micrographs. According to Gannon (1978), stereopair images can convey ten times as much anatomical information as a single micrograph.

In this project, stereopair micrographs were used to provide three-dimensional images. With this method, the field of view was first selected, and the stereopair was then taken. Other areas of the cast that might have been more interesting could possibly be missed as the three-dimensional aspect of the cast was not recognized. A definite advantage exists in the use of dynamic stereoscopy with the SEM, viewing three-dimensional images of the cast in real-time (Chatfield, 1978). However, such facilities were not available to the author.

Limitations of the corrosion cast technique

1. The direction of blood flow cannot be ascertained from a short section of the cast (Lametschwandtner *et al.*, 1984). However, by following the path of one vessel as it enlarges, branches or coalesces with other vessels, the direction of flow can be inferred.

2. Casts offer no information about the physiologic state of the vascular bed. Some vessels may be opened artificially by the perfusion.

3. The chemical effects of the casting medium on the luminal surface and the vessel wall are unknown.

4. There is insufficient information presently available regarding the physico-chemical properties of the casting medium, such as resistance to drying and heat, corrosion, polymerization characteristics *etc.*

5. Luminal diameters cannot be accurately measured using this method as the injection pressure produces expansion of the vessel wall (Rhodin, 1973). Irino, Ono and Shimohara (1982) noted vascular spasm in the early stage of resin injection, followed by marked dilatation at a later stage. The thinner-walled vessels dilated more than the thicker-walled ones.

   Vascular smooth muscle tone can be altered by changes in the chemical milieu, such as ionic activity, pH, availability of metabolites, *etc.* (Olson, 1980). In addition, the amount of stretch is not consistent throughout the vasculature.

6. Morphological relationships of the blood vessels to adjacent structures cannot be determined precisely.

7. According to Hodde (1981), the cast cannot replicate the fenestrations in vessels. Fenestrated and non-fenestrated vessels look identical in cast form.

8. Since the magnification given in the micrograph only represents an approximation, the interpretation of lateral distances on a micrograph can be grossly in error without three-dimensional analysis (Chatfield, 1978). The measurement of three-dimensional data from two-dimensional pictures has been discussed by Boyde (1973, 1979).

MORPHOLOGICAL CONSIDERATIONS

Palatal vasculature

A subepithelial capillary network arrangement in the marmoset is also reported in the mouse, rat and dog (Wong, 1983; Weekes, 1983; Takahashi *et al.*, 1985). The sagittal orientation of capillaries on the rugal crest and slopes found in the monkey is consistent with a similar orientation in the rat (Weekes, 1983) and mouse (Wong, 1983). In the marmoset, these palatal capillaries were thrown into a series of loops, whereas no loops were mentioned by Weekes (1983). In the rat (Weekes, 1983), the capillaries only displayed a sinuous course.

There appears to be a qualitative difference in the extent of looping of palatal capillaries between the monkey and the rat, which may be related to a functional adaptation

of the monkey palate to higher masticatory shearing forces (*vide infra*: 6.13) or differences in diet.

The rugal loops were aligned laterally along the rugae in the marmoset, as in the mouse and the rat. The high density of vessels on the marmoset rugal crest was also reported for the rat (Weekes, 1983). A higher concentration of papillary loops on the rugal crest may be a necessary adaptation for nutritive needs of sensory receptors on the rugae, or for an increased number of connective tissue papillae on the rugae. The palatine rugae are thought to assist in grasping the nipple during suckling and, in the adult, assist in mastication (Scott and Symons, 1982). It has been shown that some of the rugae found on the rat palate contain numerous touch corpuscles so that tactile information is conveyed when food is brought into the mouth (Scott and Symons, 1982). It is possible that the rugae have a similar function in the monkey.

In the mouse, Wong (1983) found a single, transversely orientated capillary surmounting the rugal crest and connecting adjacent sagittally orientated capillaries. Subsidiary transverse vessels were also found in the inter-rugal troughs. However, no such vessels were found in the marmoset, except at a subpapillary level. In contrast, capillary loops on the marmoset rugal crest were discrete and not interconnected with adjacent vessels. It does not appear that functional needs of the tissues will be compromised by the discrete loop arrangement in the marmoset since anastomoses are present at a subpapillary level.

Wong and Sims (1987) described looped capillaries on the rugal slopes of the mouse, which changed to a flattened

plexus where they crossed the inter-rugal venous system. In contrast, the inter-rugal trough in the marmoset still consisted of capillary loops, although the height of the loops was reduced, and the capillaries were less distinct in their sagittal orientation. In the rat, the inter-rugal network showed no orientation at all, forming a random plexus (Weekes, 1983). In the mouse, the rat, and the marmoset, there is a reduced tendency for sagittal orientation away from the rugal crest. No explanation can be found for this trend.

Wong (1983) found that some of the inter-rugal areas in the mouse lacked a capillary network, but revealed large venous vessels more than 100*um* in diameter. No reason was suggested for the absence of the capillary network. The possibility of incomplete casting cannot be ignored. Absence of the palatal subepithelial capillary network was also a feature in the old animals in this study. Possible reasons are suggested on page 6.36 (Age changes).

Wong (1983) suggested that the wavy vessels on the slopes of the rugae are functionally arranged to withstand masticatory shearing forces. The wavy pattern would allow stretching of these vessels in the rugal tissues similar to those in other gingival structures and in the periodontal ligament. The large venous-type vessels lying at the base of the inter-rugal troughs may also provide the means for the palate to absorb high compressive functional forces.

Cutright and Hunsuck (1970) found that capillary loops of the macaque soft palate were longer than those of the hard palate in all areas. However, loops were not commonly found in the marmoset soft palate. This apparent contrast requires

further study as some of the casts in this study did not extend throughout the entire soft palate.

Takahashi *et al.* (1985) demonstrated the presence of bicuspid venous valves in the dog palate, in large collecting veins more than 200*um* in diameter. These valves were located mainly in the soft palate. No venous valves have so far been found in the monkey palate. This difference needs to be further investigated with deep dissection of the marmoset cast, since the valves in the dog were found in the submucous venous plexus.

The monkey palate in this study was found to have a venous plexus lying underneath a capillary network canopy. The venous plexus lacked a definite sagittal orientation. Takahashi *et al.* (1985) did not state the orientation of the venous plexus or capillary network in the dog lamina propria, but said that the submucous venous plexus ran "longitudinally". Removal of superficial venous vessels in the marmoset palate is required to study the orientation of deep vessels in the submucosa.

It was inferred from the cast topography that the junction between the epithelium and the lamina propria was not smooth, but thrown up into folds, so that the surface contact between the lamina propria and epithelium was increased. This topography allowed for better mechanical support and a greater opportunity for the passage of nutrients from the blood vessels of the lamina propria to the non-vascular epithelium. This feature was more developed in the hard palate to support its masticatory function.

The three-dimensional vasculature of the nasopalatine foramen has never been demonstrated, except in the dog by

Takahashi *et al.*, (1985). However, in their study, the micrographs were not illustrated in stereopairs, and the capillary network was not illustrated.

The marmoset nasopalatine foramen was triangular in outline, whereas that in the dog appeared oval without the capillary network. Takahashi *et al.* (1985) noted vessels of the nasal mucosa connecting with vessels of the palatal mucosa and palatal gingiva, through the nasopalatine canal in the dog. This region of the marmoset palate requires further dissection for evaluation of deeper vascular connections. It would be interesting to see if there are any differences in the microvasculature between tissues derived from the primary palate and those derived from the secondary palate.

Soft Palate ring vessels

These ring vessels were related to the minor salivary gland ducts found by Wysocki *et al.* (1978) in the hamster soft palate. Although Wysocki *et al.* did not describe in detail the dimensions and density of these ducts, their illustrations indicate an average diameter of 52*um* for the connective tissue channels in which the ducts lie. Vessels lining these channels would have to have a larger mean diameter. The diameter of the vascular rings found in the marmoset soft palate ranged from 100-200*um*, corresponding in size to the channels found by Wysocki *et al.*

The possibility that these ring vessels were associated with taste buds was considered. Klein, Weilemann and Schroeder (1979) studied the taste buds in the macaque soft palate. These buds were composed of epithelial islands, 150-300*um* in width, completely surrounded by epithelium. No blood

vessels were seen surrounding the taste buds. However, secretory ducts of salivary (mucous) glands were found surrounded by blood vessels. These glands decreased in density from medial to lateral, a distribution similar to that found in the marmoset.

Klein *et al.* (1979) stated that in the macaque monkey, many lymph follicles were found associated with the secretory ducts just as they entered the epithelium. The ring vessels in the marmoset may participate in regulating the blood flow to the ducts as well as to the lymph follicles.

In the dog tongue, similar ring-like vessels, measuring 50-70*um* in diameter, have been demonstrated in pictures by Kishi *et al.*, (1986b). These ring vessels represent the periductal plexus described by Cutright and Hunsuck (1970) in the rhesus monkey, which formed a sleeve around the duct and anastomosed with the vessels of the subpapillary plexus. Cutright and Hunsuck (1970) suggested that this periductal plexus could play a role in the secretory function of the gland.

Gingival vasculature

Frequent anastomoses between the periodontal ligament vasculature and gingival plexus were demonstrated in the marmoset. This observation contrasts with the findings of Kennedy (1974) and Carranza *et al.* (1966) that vascular connections between gingival and periodontal ligament blood vessels were rare in squirrel monkeys, rats, mice, hamsters, guinea pigs, cats and dogs. This apparent contrast may result from limitations in technique of the earlier studies. Carranza *et al.* (1966) used a histochemical technique for the

demonstration of adenosinetriphosphatase activity to detect blood vessels. Kennedy (1974) studied 80*um* serial sections of monkeys perfused with India ink. These methods provided limited depth of view, and could not establish the three-dimensional connections of the vasculature.

However, Kennedy (1974) observed that when inflammation was induced, the number of vascular connections between the periodontal ligament and gingiva was increased. This difference in the number of anastomoses was not observed in the marmoset, perhaps because of the small number of animals used, and the absence of proper quantification of anastomoses.

The marmoset circular plexus consisted of one to four rings of capillary vessels, 8-10*um* in diameter. The capillaries frequently anastomosed with each other throughout the circular ring. The circular plexus is also found in the mouse (Wong, 1983; Wong and Sims, 1987) and the rat (Weekes and Sims, 1986b). However, in the rat, it was composed of only one continuous vessel (Weekes and Sims, 1986b). This difference may be related to the width of the epithelial attachment which the circular plexus supplies, accounting for the variation in the number of circular vessels in different sites in the marmoset.

In the present investigation, the circular plexus was related to the epithelial attachment; the crevicular loops extended from this plexus into the crevicular gingiva. The "tenuously looped capillaries" of Kindlova (1965) (*vide supra*: 3.13) would correspond to the crevicular loops of this study.

Kindlova and Matena (1962) stated that "coiled periodontal loops" (*vide supra*: 3.24), corresponding to

crevicular loops, did not form part of the gingival circulation, and were considered as part of the periodontal ligament. However, the casts in this study convincingly demonstrated the crevicular loops supplying the crevicular epithelium. The gap between the vasculature beneath the crevicular and oral gingival epithelium, demonstrated in this study, confirms the findings of Kindlova and Matena (1962), of a separate network (*vide supra*: 3.24). However, the authors mistook crevicular loops for periodontal ligament loops.

The circular plexus in the marmoset corresponded with the "horizontal circulus" in the rat (Kindlova and Matena, 1962), or the narrow band of the flat capillary network at the coronal extremity of the periodontal ligament in the *Macaca rhesus* (Kindlova, 1965). A circumferential/circular arrangement of vascular loops closely applied to the epithelial cuff was also described by Carranza *et al.* (1966) in rats, mice, hamsters, guinea pigs, cats and dogs. This arrangement has been confirmed in the marmoset.

The functional significance of the circular plexus is not clear. It was difficult to estimate the direction of blood flow in the circular vessels. The circumferential arrangement of the circular plexus, with multiple anastomoses with the periodontal ligament and crevicular loops, could provide a means for rapid re-distribution of blood when the tooth is under functional load. When masticatory load is released, the circular plexus can be quickly refilled with blood from the surrounding vessels, ensuring the viability of the epithelial attachment.

Crevicular loops were quite variable, ranging from hairpin loops to complex convoluted loops. This variability was not recognized by Kindlova and Matena (1962). These crevicular loops were found on all aspects of the marmoset premolar and molar teeth. The direction of blood flow could be deduced by following the path of the vessels. However, vital microscopic studies by Hansson, Lindhe and Branemark (1968) have shown that vascular flow can be reversed. Flow reversal has important implications in the distribution of blood during physiologic function and in pathologic states. The true direction of flow at any instant in the microvascular bed can only be determined from *in vivo* observations using vital microscopy.

The morphology of the gingival vasculature in the anterior teeth was quite different from that of premolars and molars. Examination of canine and incisor gingiva showed bulb-shaped, complex, crevicular loops resembling renal glomeruli. Weekes and Sims (1986c) recently reported finding these glomeruli in the gingiva, but did not state which teeth they examined. The vasculature of the anterior teeth requires further study. This stark contrast in vascular morphology in different teeth suggests caution when reviewing the literature, as sometimes the site studied is not specified. Differences in physiologic response in various sites may be explained by these morphologic differences.

Glomerulus-like structures can also be found in the mouse (Wong and Sims, 1987), rat (Kindlova, 1967b; Weekes and Sims, 1986b), dog (Egelberg, 1966; Ichikawa, Watanabe and Yamamura, 1977), squirrel monkey (Folke and Stallard, 1967), and man (Wedl, 1881; Schweitzer, 1909; Hayashi, 1932;

Provenza, Biddington and Cheng, 1959; Provenza, Biddix and Cheng, 1960; Ishimitsu, 1960). However, the three-dimensional architecture of these structures can only be fully appreciated using microcorrosion cast techniques.

In the macaque monkey, Kindlova (1965) describes glomeruli as being located apical to the epithelial attachment (*vide supra*: 3.13), but Weekes and Sims (1986b) show them between the epithelial attachment and the gingival crest. Wong and Sims (1987), and findings from the present study, have also shown that they lie occlusal to the epithelial attachment. In this study, no glomeruli were found apical to the epithelial attachment.

The function of these glomeruli remains unresolved. Wedl (1881) stated that in pathological processes, these coiled capillaries are the seat of atrophic changes which resemble those found in the renal glomeruli. He suggested that, in the periodontium, these structures function as coil springs (*Sprungfeder*) acting against the masticatory pressure.

Gasparini (1949) is of the opinion that these glomerular structures act as arterio-venous anastomoses in the healthy periodontium, regulating the flow of blood through the periodontium.

These curious coiled capillary loops are not present in all teeth, as they are not found in the continuously erupting rat incisor (Kindlova and Matena, 1959) and in continuously erupting rabbit molars (Kindlova, 1967b).

According to Ishimitsu (1960), as many arterio-venous anastomoses exist in these glomerulus-like structures, the glomeruli may be capable of regulating the flow of blood through the periodontal ligament. Such a mechanism may also

be related to the intermittent and compressive pressures that occur during mastication and therefore may well be essential to the vascular maintenance of the regional supporting tissues.

Provenza *et al.* (1960) suggest that the glomeruli act to ensure adequate blood supply, as a form of compensation in the periodontium in periodontitis. The heavier walls and larger diameters of the glomeruli, compared with capillaries, render them less susceptible to strangulation by disorientated connective tissue fibres in periodontitis. Provenza (1964) stated that the glomeruli are present throughout the periodontium but he did not demonstrate their three-dimensional structure. Hence, their interpretation should be viewed with caution.

Egelberg (1966) and Hock and Nuki (1970, 1971, 1975) state that the vasculature of non-inflamed free gingiva is composed of a regular network, and that loops develop in response to gingival inflammation. Egelberg (1966) suggested that venules in the crevicular plexus are more superficially situated than venules under the vestibular gingival epithelium, and may be associated with the production of gingival fluid from the gingival crevice.

Kindlova and Trnkova (1972) noted a relationship between the degree of inflammation and crevicular loop formation. However, they also observed considerable variability in the crevicular capillary beds, and suggested that variability may be a feature of dog periodontium.

Sims *et al.* (1988), however, demonstrated the presence of glomerular structures in germ free rats in the absence of

leukocyte infiltration, which suggests that the glomeruli may be a feature of normal healthy gingiva.

Since the loops of the gingival crevice in rats and dogs are considered to comprise mainly exchange vessels (Kindlova and Matena, 1962; Egelberg, 1966; Nuki and Hock, 1974; De Almeida and Bohm, 1979), it is possible that they may play a role in the production of crevicular exudate.

It is interesting to note that SEM microcorrosion cast studies of mice (Wong, 1983), rats (Weekes, 1983) and marmosets have all demonstrated glomeruli related to the gingival crevicular epithelium, but not in the periodontal ligament. These glomeruli were not found beneath the oral gingival epithelium. Their location suggests that they may play a role in the production of crevicular exudate, as suggested by Cimasoni (1983). Also, the convolution of the crevicular loops may be induced by some as yet unknown epithelial vasogenic factors suggested by Ryan (1973b).

The vasculature of the marmoset gingival margin was often composed of capillary loops, although in some areas, these loops coalesced to form a continuous capillary network, surmounted by a single horizontal vessel. In contrast, the outer circular system beneath the gingival margin in the mouse was described as a single vessel (Wong, 1983). Some variability was recognized by Forsslund (1959), who observed both an anastomosis (network) pattern and a loop pattern in healthy gingiva, with the former predominating in inflamed gingiva. The anastomosis pattern changed to a loop pattern when inflammation subsided following periodontal therapy. Forsslund's observations are in contrast with those of

Egelberg (1966) and Nuki and Hock (1970, 1971, 1975), *vide supra*: 6.21.

Cutright and Hunsuck (1970) and Carranza *et al.* (1966) stated that the gingiva derived its blood supply mainly from mucosal/supraperiosteal vessels, and received only minor contributions from the alveolar bone. However, they did not distinguish between the supply to the vestibular network and that to the crevicular network of the gingiva. This distinction is important because the crevicular and oral gingival epithelium have very different functions.

The functional independence of the gingival and periodontal ligament blood supplies has been demonstrated (Goldman, 1956; Kennedy, 1969). Occlusion of vessels in the periodontal ligament does not affect the blood supply of the gingiva (Goldman, 1956) and occlusion of the arterioles supplying the gingiva does not appear to alter the blood supply of the periodontal ligament (Kennedy, 1969). However, in the latter study, the initial revascularization of the gingiva was derived from vessels of the periodontal ligament, thus demonstrating a potential for extensive collateral circulation to the gingiva from the periodontal ligament. Also, Nobuto *et al.* (1987) showed that revascularization of gingival wounds was faster from the occlusal edge compared to the apical edge. Kennedy (1974) showed that when specific needs arise, a compensatory blood supply can be provided easily. Thus, it can be seen that the periodontal ligament is important not only for the crevicular gingiva, but for the oral gingiva as well.

In the marmoset, it appeared that the crevicular gingival vasculature derived its blood supply mainly from the

periodontal ligament and alveolar bone, whereas the vestibular gingival vasculature derived its blood supply mainly from the mucosal/supraperiosteal vessels approaching occlusally from the sulcus.

This apico-occlusal supply to the vestibular gingiva is supported by *in vivo* fluorescein angiography studies of Mormann, Meier and Firestone (1979) in human gingiva. Punch wounds in the mandibular labial attached gingiva resulted in ischemia only in the area occlusal to the wounds.

In the marmoset, it could not be determined whether the occluso-apically orientated arterioles and venules were more abundant in the mid-axial region (along the long axes of the teeth), or in the mid-papillary region. Mormann *et al.* (1979) found significantly greater areas of ischemia resulting from gingival punch wounds in the mid-axial region than in the mid-papillary region. This suggests that the mid-axial region has less potential for collateral circulation and revascularization. This is not surprising, since anastomoses exist between the mid-papillary vessels of the buccal and lingual interdental papillae, via bucco-lingually orientated vessels of the interdental col.

Nobuto *et al.* (1987) also showed that revascularization of denuded bone arose from the subpapillary plexus of adjacent tissues, with the supraperiosteal network developing later, and contributions from the alveolar bone via Volkmann canals occurring much later. This emphasizes the importance of the subpapillary and supraperiosteal network in the repair of gingival wounds.

Studies of the revascularization of gingival tissues following gingivectomy in the dog suggest that blood vessels

of the periodontal ligament play the most important role in the blood supply for newly formed gingivae (Watanabe and Suzuki, 1963; Cutright, 1969).

According to Stahl (1965), epithelialization of gingiva occurs from 4-9 days after surgery. This period corresponds approximately to the formation of the first mature capillary loops found by Cutright (1969). Cutright suggested that the gingival epithelium plays an important role in the maturation of healing capillary loops.

The occluso-apical orientation of the capillaries, arterioles and venules on the vestibular aspect of the marmoset gingiva suggests that surgical incisions in the gingiva should also be occluso-apically orientated, to minimize disruption of the blood supply to the gingiva.

Also, since arterioles branch as they ascend apico-occlusally, buccal flaps should have a broad base. This will ensure better blood supply and maintain the viability of the flap (Mormann and Ciancio, 1977).

Cutright (1969) described the blood supply from the dog alveolar mucosa running anteriorly and occlusally, giving off branches to the gingiva. However, he did not mention the orientation of the capillary network or define the regions of the mouth where this anterior-occlusal orientation applied.

The antero-posterior orientation of the network in the alveolar mucosa of the marmoset was also reported for the macaque monkey (Cutright and Hunsuck, 1970), and the dog (Kishi *et al.*, 1986a). However, in the latter study, they found capillary loops in the alveolar mucosa, which were low in height and few in number. In the marmoset, capillary loops were not found in the alveolar mucosa in the premolar-molar

regions. This may be related to the function of the alveolar mucosa epithelium, which is not as exposed to masticatory shearing forces as the gingival epithelium.

Karring and Loe (1970) described the connective tissue at the human gingival margin as arranged in parallel rows of short papillae or ridges when these papillae fused. In the present investigation, the loop arrangement below the gingival margin was seen in clinically healthy gingivae as well, and may represent anatomic variation rather than an inflammatory change. However, according to Hock and Nuki (1971), once transformed, the gingival vessels do not revert to their original network arrangement, despite the resolution of inflammation. They suggest that when loops are found, it indicates current or a previous episode of inflammation.

The interdental col vasculature

The interdental col area in the marmoset had capillary loops of varying pattern ranging from simple hairpin loops to complex branching loops. However, Weekes and Sims (1986b) found most of the loops were glomerular-like, complex, twisted vascular loops in rats.

Kindlova and Matena (1962) stated that the interdental col of the rat molar region is supplied only by coiled loops of the periodontal ligament. They said that the gingival plexus does not reach into the area below the contact point of adjoining teeth. In contrast, Garfunkel and Sciaky (1971) reported blood supply to the col region as being derived from the lingual and buccal periosteal blood vessels, as well as from both the adjacent periodontal network. Boyer and Neptune (1962), Folke and Stallard (1967), and Kennedy (1974) also

found communicating blood vessels coming from the crestal bone.

In the marmoset, gingival loops could be seen extending into the col area. The arterial supply to the col arose from the gingival plexus of the buccal or lingual interdental papillae. Loops extended into the connective tissue papillae of the lamina propria, as in the palate. The multiple source of blood supply ensured viability of the col tissue.

A tract of capillary vessels could be seen running mesio-distally in the primate space between the upper lateral incisor and canine. This interesting feature needs to be investigated further.

Periodontal ligament vasculature

The periodontal ligament vessels in the monkey were composed mainly of occluso-apically orientated postcapillary-sized venules, 20-35*um* in diameter. Similar axial orientation of the periodontal ligament plexus is also found in rats, mice, hamsters, guinea pigs, cats, dogs, macaque monkeys and man (Garfunkel and Sciaky, 1971; Nakamura *et al.*, 1983; Weekes, 1983; Wong, 1983; Carranza *et al.*, 1966; Goldman, 1956; Kindlova and Matena, 1962; Kindlova, 1965, 1967a, 1967b; Castelli, 1963; Castelli and Dempster, 1965; Rohen *et al.*, 1984; Hayashi, 1932).

The predominance of venous vessels in the marmoset periodontal ligament microvascular bed is supported by studies in the rat (Weekes and Sims, 1986a), mouse (Wong and Sims, 1987), rabbit and macaque monkey (Rohen *et al.*, 1984).

Freezer and Sims (1987) found that in the mouse, 88% of the total periodontal vascular pool was contained in

postcapillary-sized venules. Capillary-sized vessels, on the other hand, contained 12% of the periodontal blood volume. No postcapillary-sized venules were found in the tooth-third of the periodontal ligament.

The main periodontal ligament vessels in the marmoset, 20-35um diameter, were generally larger than the 21um diameter vessels found in the mouse molar (Wong and Sims, 1987). A higher proportion of larger diameter vessels was noted in the apical third of the marmoset ligament. Kindlova and Matena (1962) also observed that vessels were larger towards the apex. This was not surprising, since the periodontal ligament venules drained in an occluso-apical direction.

Arterioles were less abundant in the periodontal ligament, and could be found on both sides of the venous network. This is in contrast to the findings of Weekes and Sims (1986a), who claimed that arterioles were not found coursing in the ligament on the buccal, lingual and proximal walls of the socket. In the rat, arterioles perforating the cribriform plate from the marrow space immediately drain into postcapillary-sized venules, orientated occluso-apically. Arterioles were clearly demonstrated in the marmoset periodontal ligament and, although not numerous, were certainly not uncommon.

The ligament vessels in most areas in the marmoset formed a network, but in some areas, they were arranged in a palisade. A network arrangement was also described for the mouse (Wong and Sims, 1987) and the macaque monkey (Kindlova, 1965). In the rat, however, the ligament vessels are arranged in palisades or longitudinal tracts (Kindlova and Matena,

1962; Weekes and Sims, 1986a). The functional significance of the type of arrangement is not understood.

According to Weekes (1983), there is no capillary bed between the arteriolar supply and the venous side of the periodontal ligament circulation. In the marmoset, capillaries were not so numerous as to form an extensive capillary bed. However, a capillary bed could be observed in the apical region, situated closer to the alveolar bone than the venous network.

Perforating branches from the alveolar wall seen in the rat (Garfunkel and Sciaky, 1971; Weekes, 1983), mouse (Wong and Sims, 1987), squirrel monkey (Folke and Stallard, 1967) and rhesus monkey (Kindlova, 1965; Castelli and Dempster, 1965), were also seen in the marmoset. Anastomosis of periodontal ligament vessels with medullary vessels also occurs in the rabbit, the opossum (Boyer and Neptune, 1962), the hamster, the guinea pig, the cat and the dog (Carranza *et al.*, 1966).

It could not be ascertained whether the periodontal ligament network was closer to cementum or to bone in this study. Carranza *et al.* (1966) state that the periodontal ligament plexus in rats, mice, hamsters, guinea pigs, cats, and dogs occurs closer to bone. Kindlova (1965), Folke and Stallard (1967) and Levy *et al.* (1972a) also state that the periodontal ligament plexus is closer to bone in macaques, squirrel monkeys and marmosets, respectively.

Khouw and Goldhaber (1970), in a study of rhesus monkeys and dogs, said the middle third had the greatest vascularity and the tissue next to the bone was more vascular than that lining the cementum. This finding was confirmed by

Douvartzidis in 1984 in her morphometric study of the marmoset molar periodontal ligament vasculature. Douvartzidis (1984) and Gotze (1976) found the vascular proportion to increase apically. This change correlated with an increased number of larger diameter vessels, and closer packing of vessels in the apical third in this study. However, the increased vascularity does not show a constant trend from the coronal to the apical end, as shown by Sims (1987b) in the mouse.

Anastomoses between the periodontal ligament vessels and the gingival network have been reported by Hayashi (1932), Kindlova and Matena (1962), Kindlova (1965), Castelli and Dempster (1965), Levy *et al.* (1972a), Weekes (1983), Wong (1983) and others. These anastomoses were also seen in the marmoset, although Carranza *et al.* (1966) stated that anastomoses were rare in the various laboratory animals that they studied (*vide supra*: 6.16).

The principal vessels of the periodontal ligament communicate with each other by lateral branches (Kindlova and Matena, 1962; Kindlova, 1965; Castelli and Dempster, 1965; Carranza *et al.*, 1966; Garfunkel and Sciaky, 1971; Kishi and Takahashi, 1977). Weekes and Sims (1986a) reported few connecting branches between the principal vessels of the rat periodontal ligament. However, in this study, the principal vessels were seen to communicate frequently as they traversed the periodontal ligament. The multiple anastomosis pattern may be important in the re-distribution of blood when the tooth is under functional loading.

In the marmoset, loops in the cervical third of the ligament did not show any coils and were basically hairpin

shaped and directed towards the root surface. Ryan (1973b) suggests that the epithelium has an influence on vessel formation and maturation. It is possible that the loops may be associated with epithelial cell rests of Malassez which have invoked a vascular response. The rests of Malassez show different patterns of distribution with increasing age (Schroeder, 1986). However, no difference was noted between the young and old animals in the distribution of capillary loops. This association needs to be further investigated.

Hairpin loops are also found in the rat molar periodontal ligament in the coronal third and apical regions (Weekes and Sims, 1986a) and in the mouse molar periodontal ligament in the mid-third region (Wong and Sims, 1987). However, Wong and Sims (1987) did not illustrate the loop pattern or mention their height. They did not explain the significance of these loops.

The annular constriction found in the periodontal loop (5.49/fig. 39) may be artifactual or due to the action of sphincters, as suggested by Duvernoy *et al.* (1981), *vide supra*: 6.7. Nuclei imprints were not observed near the constriction. The location of the constriction in a venular segment suggests that it was an artifact.

In the marmoset interradicular region, a loose venous network could be seen. This network continued with the periodontal ligament network down the root, and extended laterally to join the cervical part of the periodontal ligament network.

Large capacitance venous vessels called *venous ampullae* have not been found in the monkey. The interradicular ampulla was first described by Sims (1987a) in the mouse mandibular

molar and demonstrated in corrosion cast studies in the mouse (Wong and Sims, 1987).

The periodontal ligament vasculature examined thus far was only from the premolar and molar sockets. There was no major difference between the periodontal ligament of the upper and lower premolars and molars. It will be interesting to see if the incisor and canine periodontal ligament vasculature show the same arrangement. As these sockets have not been sectioned yet, a comparable study cannot be presented.

Relationship of papillary loops to the connective tissue papillae:

Previous studies of oral vasculature have failed to relate the vascular architecture to the contour of the epithelial-connective tissue interface (Wong, 1983; Weekes, 1983; Kindlova, 1965; Takahashi *et al.*, 1985). The contour of the oral epithelial-connective tissue interface was recently reviewed by Sloan and Soames (1984). A close association exists between the topography of the epithelial-connective tissue contour, and the subepithelial vasculature architecture. This feature was observed by Folke and Stallard (1967) in monkeys. According to Stablein and Meyer (1984), spacing of capillary loops varies with the spacing of the connective tissue papillae. The height of the loops is also dependent on the height of the papillae, and roughly proportional to the thickness of the overlying epithelium.

The configuration of the marmoset palatal loops corresponds to the connective tissue papillae in the human and rhesus monkey hard palate, which are also sagittally

orientated (Klein-Szanto and Schroeder, 1977; Emslie and Weinmann, 1949). In the hamster hard palate, the connective tissue papillae are arranged in a series of undulating, long, narrow, parallel ridges aligned sagittally (Wysocki *et al.*, 1978). However, no comparative SEM microcorrosion cast studies have been done in the hamster. The significance of a sagittal orientation is not understood.

Klein-Szanto and Schroeder (1977) have demonstrated that the terminal part of the connective tissue papillae in the human hard palate may be bent, or twisted along its long axis. This bending and twisting was also reflected in the marmoset papillary vessel loops. These authors did not find any difference in papillary morphology between the midline and the lateral parts of the palate. However, in the marmoset, the sagittal orientation of papillary vessel loops was less definite near the tooth sockets. This may be due to species differences.

Emslie and Weinmann (1949) found a connective tissue papillary density of 200 per mm^2 for the rhesus monkey hard palate while Klein-Szanto and Schroeder (1977) reported a papillary density of 114 $\pm$ 16 per mm^2 for the human hard palate. In comparison, the capillary loop density was about 200-270 per mm^2 on the rugal crest, 75-160 per mm^2 on the rugal slopes, and 70-140 per mm^2 in the trough area of the marmoset. A higher density of loops on the rugal crest may be related to nutritive and functional factors (*vide supra*: 6.12).

Stablein and Meyer (1984) found the capillary length within 50*um* of the overlying epithelium in the rat palate to range from 44*um* per 100*um* length of epithelial surface in the

inter-rugal area, to 95um per 100um in the rugal area. Loops in the marmoset hard palate were longer at the rugal crest than in the inter-rugal area. This finding agrees with that of Cutright and Hunsuck (1970) for the macaque monkey.

In the marmoset palate, the papillary vessel loops ranged from 70-250um. By comparison, the connective tissue papillary height in the human hard palate is about 190um (Klein-Szanto and Schroeder, 1977).

According to Klein-Szanto and Schroeder (1977), the connective tissue papillary density is 119 $\pm$ 27 per mm^2 in the human buccal attached gingiva and 46 $\pm$ 18 per mm^2 in the alveolar mucosa. The connective tissue papillae were about 170um in height in the buccal attached gingiva, and about 165um in height in the alveolar mucosa. The alveolar mucosa papillae were described as being aligned in parallel rows, sometimes situated on longitudinally running ridges. The orientation of the alveolar mucosa papillae was not specifically mentioned, but was assumed to be antero-posterior.

In comparison, capillary loops ranged from 40-120um in the buccal gingiva, with increased height towards the gingival margin in the marmoset. No well-defined loops were found in the alveolar mucosa, but vessels were aligned antero-posteriorly.

In the marmoset, the most apical vessels beneath the crevicular epithelium in the gingiva formed a circular plexus around the tooth, in close association with the epithelial attachment. Emslie and Weinmann (1949), in tissue separation studies of the rhesus monkey, described the junction of the epithelial attachment with its connective tissue as a smooth

narrow strip. Further coronally, the epithelial surface was pitted, due to the papillae arranged parallel to the long axis of the tooth. This smooth epithelial-connective tissue contour at the epithelial attachment corresponds to the contour of the circular plexus found in the marmoset.

Ooya and Tooya (1981) studied the human gingival epithelium-connective tissue interface after separation, using the SEM. They demonstrated long conical papillae under the crevicular epithelium, orientated almost parallel to the long axis of the tooth. This configuration corresponds to the orientation of the crevicular loops found in this study, and supports the finding by Karring and Loe (1970) of connective tissue papillae orientated parallel to the crevicular epithelial surface.

Nobuto *et al.* (1987) and Kishi *et al.* (1986a) did not mention the orientation of the capillary network in the buccal gingiva in dogs. Examination of the illustrations of Kishi *et al.* (1986a) did not show any particular orientation.

The connective tissue ridges in the hamster gingiva are narrow and undulating, with a pronounced orientation, the direction of which Wysocki *et al.* (1978) did not specify. Neither did they mention the height of the ridges. Ooya and Tooya (1981) showed a distinct antero-posterior orientation in the human free gingival epithelial ridges whereas a honeycomb pattern was present in the attached gingiva, without any particular orientation.

In the marmoset, the buccal gingival vasculature exhibited a horizontal orientation below the gingival margin, but showed an occluso-apical orientation of capillary loops found further from the gingival margin. Emslie and Weinmann

(1949) have shown that the connective tissue ridges run parallel to the gingival margin in the free gingiva, and run vertically/occluso-apically in the attached gingiva. In the human, the connective tissue ridges in the free gingiva also run parallel to the gingival margin (Ooya and Tooya, 1981). Comparative tissue separation studies in the marmoset gingiva will help to substantiate the findings in this study.

Age changes

Ryan (1973a) notes that in old age, the connective tissue papillae shorten, papillary vessel loops are reduced or may even be absent, and a dilated subpapillary plexus may be the only vessel supply. The skin of some old people may have areas in which no vessels can be detected in the upper dermis. Several authors have described arteriosclerotic changes in the blood vessels as a result of ageing (Grant and Bernick, 1970; Levy *et al.*, 1972b). It is possible that the marmoset palatal subepithelial network failed to cast completely in the older animals because of these changes.

No other age differences could be observed in the oral microvasculature from the limited number of animals used.

Suggestions for future research

The advantages of the SEM microcorrosion cast technique have not been fully exploited in vascular studies of the oral structures.

There have been no adequate studies of the normal temporomandibular joint vasculature and soft palate vasculature using this technique. The microcorrosion cast technique would also be useful in embryological studies in

investigating vascular formation during craniofacial development, and the role of the vasculature in the pathogenesis of experimentally induced clefts of the palate.

The changes in the vascular architecture associated with root resorption have not been evaluated three-dimensionally. Also, there is a lack of knowledge of the changes in the microvasculature following experimental trauma (incisions, excisions, burns, fractures), periodontal disease, ageing, induced neoplasia and following tooth extraction or replantation.

Revascularization of healing gingival wounds is found to arise from subepithelial capillaries of adjacent tissues, and is faster from the gingival margin than from the alveolar mucosa or bone (Nobuto *et al.*, 1987). However, no three-dimensional studies have been conducted investigating the revascularization of the periodontal ligament and gingiva following pericision. These areas provide ample opportunity for future research.

An understanding of the epithelial-connective tissue interface topography will help in the interpretation of the subepithelial vascular network. The development of a technique for quantification of microcorrosion cast dimensions, areas, and volumes, will be a major contribution to microvascular research.

CONCLUSIONS

1. The palatal vasculature consisted of a series of papillary loops orientated sagittally. Papillary loops projected from a flat subpapillary network into the connective tissue papillae. On the crests of the rugae, the loops were aligned to form a well-delineated spine, but did not interconnect at their peaks. The subpapillary network formed a canopy over an underlying venous network, which lacked a definite orientation. Arterioles were less commonly found, and tended to lie deeper than venules of corresponding size.

2. Ring vessels were found in the soft palate associated with the ducts of minor salivary glands. These ring vessels may have a role in the secretory function of the salivary gland.

3. In the gingiva, a plexus of circularly arranged vessels, 10-25um in diameter, encircled each tooth beneath the crevicular epithelium, at the level of the epithelial attachment. The circumferential arrangement of the circular plexus, and its anastomoses with the periodontal ligament and gingival vessels, may be important in the re-distribution of blood when the tooth is under functional load.

4. Crevicular loops arose from this circular plexus, extending occlusally. They were found on the mesial, distal, buccal and lingual aspects. There was some variation in the crevicular loop pattern.

5. A gap was found between the vasculature on the crevicular side, and that on the oral/proximal side of the gingiva.

However, anastomoses occurred across the gap at a deeper level.

6. Vessels in the gingiva anastomosed with those of the periodontal ligament and the palate. Anastomoses were also found between the gingival, periodontal ligament and medullary vasculature. These anastomoses were important sources of collateral blood supply, for example, in the revascularization of gingival wounds from periodontal ligament vessels.

7. The vestibular gingival vasculature was composed of occluso-apically orientated papillary loops. These loops drained into similarly orientated venules lying at a deeper level. Arterioles ran apico-occlusally towards the gingival margin. Surgical incisions in the vestibular gingiva should therefore be orientated occluso-apically to minimize disruption of the blood supply.

8. The capillaries in the buccal alveolar mucosa had an antero-posterior orientation. No distinct loops were found in the alveolar mucosa.

9. The interdental col consisted of loops orientated bucco-lingually, draining into a similarly orientated venous network.

10. The periodontal ligament vasculature was an occluso-apically orientated network. In the cervical and middle thirds, the microvascular bed was composed mainly of postcapillary-sized venules, 20-35 um in diameter. Capillaries and arterioles were less common.

Arterioles ran a straighter course, had few branches, and showed a constant diameter. Venules ran a more sinuous course, had more branches, and possessed a varying diameter.

11. Capillary loops were found in the cervical third of the periodontal ligament, but not in the middle and apical thirds. A relationship of periodontal ligament capillary loops with epithelial rests of Malassez was postulated.

12. A close relationship was found between the contour of the epithelial-connective tissue interface and the sub-epithelial vasculature architecture. An understanding of the relationship is important in studies of the micro-vascular bed.

13. An age-related difference was noted in the palatal vasculature. Age changes in other sites were not observed from the limited number of animals used.

14. Species differences with the mouse, rat, dog and macaque monkey were discussed. These differences may be important in understanding vascular function in the oral cavity. Also, the considerable variation in vascular morphology between animals, and within the animal in different sites of the mouth, suggest caution in the interpretation of microvascular studies.

CHAPTER 8 APPENDIX

Appendix 1: Chemical reagents and suppliers

Di-sodium hydrogen phosphate, Na_2HPO_4 (Ajax Chemicals, Sydney, N.S.W., Australia).

Glutaraldehyde (Bio-Rad, P.O. Box 33, Hornsby, N.S.W., Australia).

Heparin (Heparin sodium injection B.P. Mucous, Glaxo Australia Pty. Ltd., Mountain Highway, Boronia, Victoria, Australia).

Hydrochloric Acid (BDH Chemicals Australia Pty. Ltd., Victoria, Australia).

Ilford film and print developer and fixer (Ilford Ltd., Mobberley, Cheshire, England, U.K.).

Mercox (Vilene Hospital Ink and Chemical Co. Ltd., Tokyo, Japan).

Osmium tetroxide (Johnson Metthey Chemicals Ltd., Hertfordshire, England, U.K.).

Pancreatin (Stansens Scientific & Surgical Divisions, 3, Percy Court, Adelaide, S.A., Australia).

Papaverine hydrochloride injection 120 mg/10 ml (David Bull Laboratories Pty. Ltd., Victoria, Australia).

Polyvinylpyrrolidone M.W. 40,000 (Polysciences, Inc., Warrington, PA 18976, U.S.A.).

Potassium hydroxide (Analytical and Research Chemical Co., Adelaide, Australia).

Saffan anaesthetic injection (Glaxovet, Glaxo Australia Pty. Ltd., Mountain Highway, Boronia, Victoria, Australia).

Silver Dag (Acheson Colloids Co., Prince Rock, Plymouth, England, U.K.).

Sodium chloride (Ajax Chemicals, Sydney, N.S.W., Australia).

Sodium dihydrogen orthophosphate, NaH_2PO_4 (Ajax Chemicals, Sydney, Australia).

Sodium hypochlorite (Ajax Chemicals, Sydney, N.S.W., Australia).

Sodium nitrite crystal (J. T. Baker Chemical Co., Phillipsburg, N. J., U.S.A.).

Appendix 2: Equipment and materials

Ilford FP4 B & W film (Ilford Ltd., Mobberley, Cheshire, England, U.K.).

Ilford Ilfospeed photographic paper (Ilford Ltd., Mobberley, Cheshire, England, U.K.).

Membra-Fil membrane filter (Johns-Manville, Canada).

Polyethylene tube, Medical grade (Dural Plastics and Engineering, Dural, N.S.W., Australia).

	Inner diameter (mm)	Outer diameter (mm)
SP 10	0.28	0.61
SP 45	0.58	0.96
SP 61	0.86	1.27
SP 95	1.20	1.70

Silastic, Medical grade tubing (Dow Corning Corporation Medical Products, Midland, Michigan, U.S.A. 48640)

	Inner diameter (in.)	Outer diameter (in.)
602-285	0.062	0.125
601-325	0.104	0.192

Stereoviewer "Geoscope" (Instrument Supply Co., 177, Payneham Road, St. Peters, S.A., Australia).

BIBLIOGRAPHY

Beattie J. (1927) The anatomy of the common marmoset. *Proc. Zool. Soc. Lond.*, pp. 593-718.

Black J.T. (1974) The scanning electron microscope: Operating principles. In: *Principles and Techniques of Scanning Electron Microscopy*. Biological Applications (Ed. M.A. Hayat) Vol. 1, pp. 1-43. Van Nostrand Reinhold Co., New York.

Boyde A. (1973) Quantitative photogrammetric analysis and qualitative stereoscopic analysis of S.E.M. images. *J. Microsc.*, **98**, 452.

Boyde A. (1979) The perception and measurement of depth in the SEM. *Scan. Electron Microsc.*, Part **II**, pp. 67-78.

Boyer C.C. and Neptune C.M. (1962) Patterns of blood supply to teeth and adjacent tissues. *J. Dent. Res.*, **41**, 158-171.

Carranza F.A., Itoiz M.E., Cabrini R.L. and Dotto C.A. (1966) A study of periodontal vascularization in different laboratory animals. *J. Periodont. Res.* **1**, 120-128.

Casley-Smith J.R. and Vincent A.H. (1978) The quantitative morphology of interstitial tissue channels in some tissues of the rat and rabbit. *Tissue and Cell*, **10**, 571-584.

Castelli W. (1963) Vascular architecture of the human adult mandible. *J. Dent. Res.* **42**, 786-792.

Castelli W. and Dempster W.T. (1965) The periodontal vasculature and its responses to experimental pressures. *J. Am. Dent. Assoc.*, **70**, 890-905.

Chatfield E.J. (1978) Introduction to stereo scanning electron microscopy. In: *Principles and Techniques of Scanning Electron Microscopy.* Biological Applications (Ed. M.A. Hayat) Vol. 6, pp. 47-88. Van Nostrand Reinhold Co., New York.

Cimasoni G. (1983) Gingival vasculature and crevicular fluid. In: *Crevicular Fluid Updated,* Monographs in Oral Science, (Ed. H.M. Myers), pp. 14-19, S. Karger, Basel.

Cohen L. (1960) Further studies into the vascular architecture of the mandible. *J. Dent. Res.* **39**, 936-964.

Cutright D.E. (1969) The proliferation of blood vessels in gingival wounds. *J. Periodontol.*, **40**, 137-141.

Cutright D.E. and Bhaskar S.N. (1967) A new method of demonstrating microvasculature. *Oral Surg.*, **24**, 422-430.

Cutright D.E. and Hunsuck E.E. (1970) Microcirculation of the perioral regions in the *Macaca rhesus*. Part I. *Oral Surg.*, **29**, 776-785. Part II. *Oral Surg.*, **29**, 926-934.

De Almeida O.P. and Bohm G.M. (1979) Vascular permeability in the rat gingiva. A model of vessel response in chronic inflammation. *J. Pathol.*, **127**, 27-34.

Douvartzidis I. (1984) A morphometric examination of the periodontal ligament vasculature of the marmoset molar. M.D.S. Thesis, The University of Adelaide.

Duvernoy H.M., Delon S. and Vannson J.L. (1981) Cortical blood vessels of the human brain. *Brain Res. Bull.*, **7**, 519-579.

Edwall L.G.A. (1982) The vasculature of the periodontal ligament. In: *The Periodontal Ligament in Health and Disease*. (Eds. B.K.B. Berkovitz, B.J. Moxham and H.N. Newman) Chapter 7, pp. 151-171, Pergamon Press, London.

Egelberg J. (1966) The blood vessels of the dento-gingival junction. *J. Periodont. Res.* **1**, 163-179.

Emslie R.D. and Weinmann J.P. (1949) The architectural pattern of the boundary between epithelium and connective tissue of the gingiva in the rhesus monkey. *Anat. Rec.*, **105**, 35-57.

Folke L.E.A. and Stallard R.E. (1967) Periodontal microcirculation as revealed by plastic microspheres. *J. Periodont. Res.* **2**, 53-63.

Forsslund G. (1959) The structure and function of the capillary system in the gingiva in man. *Acta. Odont. Scand.* **17**, Suppl. 26 (Thesis).

Freeman E. and Ten Cate A.R. (1971) Development of the periodontium. An electron microscopic study. *J. Periodontol.*, **42**, 387-385.

Freezer S.R. and Sims M.R. (1987) A transmission electron-microscope stereological study of the blood vessels, oxytalan fibres and nerves of mouse-molar periodontal ligament. *Archs. Oral Biol.*, **32**, 407-412.

Gannon B.J. (1978) Vascular Casting. In: *Principles and Techniques of Scanning Electron Microscopy.* Biological Applications (Ed. M.A. Hayat) Vol. 6, pp. 170-193. Van Nostrand Reinhold Co., New York.

Gannon B.J. (1985) Vascular Casting Workshop. 10th Congress of New Zealand Electron Microscope Society.

Garfunkel A. and Sciaky I. (1971) Vascularization of the periodontal tissues in the adult laboratory rat. *J. Dent. Res.*, **50**, 880-887.

Gasparini F. (1949) Sulla presenza di anastomosi artero-venose nel periostio alveolare. *Atti. Soc. med.-chir. Padova*, **27**, 87-91. (Cited by Kindlova, 1965, 1967b).

Gerszberg T., Roa N. and Korte G.E. (1985) Cleaning vascular casts for scanning electron microscopy. *E.M.S.A. Bull.*, **15**, 106.

Goldman H.M. (1956) Gingival vascular supply in induced occlusal traumatism. *Oral Surg.*, **9**, 939-941.

Gotze W. (1976) Quantitative Untersuchungen zur Verteilung der Blutgefasse im Desmodont. *Dtsch. zahnaerztl. Z.*, **31**, 428-430.

Grant D. and Bernick S. (1970) Arteriosclerosis in periodontal vessels of ageing humans. *J. Periodontol.*, **41**, 170-173.

Hansson B.O., Lindhe J. and Branemark P.-I. (1968) Microvascular topography and function in clinically healthy and chronically inflamed dento-gingival tissues - A vital microscopic study in dogs. *Periodontics*, **6**, 264-271.

Hayashi S. (1932) Untersuchungen uber die arterielle Blutversorgung des Periodontiums. *Deutsche Monatsschrift fur Zahnheilkunde.*, **50**, 145-192. (Cited by Saunders and Rockert, 1967).

Hill W.C.O. (1957) Primates: Comparative Anatomy and Taxonomy, pp. 115-116, University Press, Edinburgh.

Hock J. and Nuki K. (1970) Evidence for the absence of vascular loops in non-inflamed gingiva. *J. Dent. Res.*, **49**, Special Issue, p. 200, IADR Abstract No. 607.

Hock J. and Nuki K. (1971) A vital microscopy study of the morphology of normal and inflamed gingiva. *J. Perio. Res.*, **6**, 81-88.

Hock J. and Nuki K. (1975) Microvascular response to chronic inflammation in gingiva. *Bibl. Anat.*, No. **13**, 186-187, Karger, Basel.

Hodde K.C. (1981) Cephalic vascular patterns in the rat. A scanning electron microscopic (SEM) study of casts. Doctoral Thesis, University of Amsterdam.

Hodde K.C. and Nowell J. (1980) SEM of micro-corrosion casts. *Scan. Electron Microsc.*, Part **II**, pp. 88-106.

Hodde K.C., Miodonski A., Bakker C. and Veltman W.A.M. (1977) Scanning electron microscopy of microcorrosion casts with special attention on artero-venous differences and application to the rat cochlea. *Scan. Electron Microsc.*, Part **II**, pp. 477-484.

Howell P.G.T. (1975) Taking, presenting and treating stereo data from the SEM. *Scan. Electron Microsc.*, pp. 697-698.

Huelke D.F. and Castelli W.A. (1965) The blood supply of the rat mandible. *Anat. Rec.*, **153**, 335-342.

Ichikawa T., Watanabe O. and Yamamura T. (1977) Vascular architecture in oral tissues by vascular casts method for scanning electron microscopy. *Bibl. Anat.*, No. **15**, 544-546.

Irino S., Ono T. and Shimohara Y. (1982) Microvascular architecture of the rabbit ventricular walls: a scanning electron microscopic study of corrosion casts. *Scan. Electron Microsc.*, Part **IV**, pp. 1785-1792.

Ishimitsu K. (1960) Beitrag zur Kenntnis der Morphologie und Entwicklungsgeschichte der Glomeruli periodontii. *Yokohama Med. Bull.*, **11**, 415-432. (Cited by Schroeder, 1986).

James W.W. (1960) The jaws and teeth of primates. Pitman Medical Publishing Co. Ltd., London.

Karring T. and Loe H. (1970) The three-dimensional concept of the epithelium-connective tissue boundary of gingiva. *Acta Odontol. Scand.*, **28**, 917-933.

Kennedy J. (1969) Experimental ischemia in monkeys. **II**. Vascular response. *J. Dent. Res.*, **48**, 888.

Kennedy J. (1974) Effects of inflammation in collateral circulation of the gingiva. *J. Periodont. Res.*, **9**, 147-152.

Khouw F.E. and Goldhaber P. (1970) Changes in vasculature of the periodontium associated with tooth movement in the rhesus monkey and dog. *Archs. Oral Biol.*, **15**, 1125-1132,

Kindlova M. (1963) Blood circulation in pulp and periodontium of rat incisors and molars. *Dental Abstracts*, **8**, 106.

Kindlova M. (1965) The blood supply of the marginal periodontium in Macacus Rhesus. *Archs. Oral Biol.* **10**, 869-874.

Kindlova M. (1967a) Vascular supply of the periodontium in periodontitis. *Int. Dent. J.*, **17**, 476-489.

Kindlova M. (1967b) Glomerular vascular structures in the periodontium. In: *The Mechanism of Tooth Support. A Symposium.* (Eds. D.J. Anderson, J.E. Eastoe, A.H. Melcher and D.C.A. Picton), pp. 76-79, Wright, Bristol.

Kindlova M. (1970) The development of the vascular bed of the marginal periodontium. *J. Periodont. Res.*, **5**, 135-150.

Kindlova M. and Matena V. (1959) Blood circulation in the rodent teeth of the rat. *Acta. Anat.* **37**, 163-192.

Kindlova M. and Matena V. (1962) Blood vessels of the rat molar. *J. Dent. Res.* **41**, 650-660.

Kindlova M. and Trnkova H. (1972) The vascular arrangement beneath the sulcular and junctional epithelium in different degrees of cellular infiltration of dog gingiva. *J. Periodont. Res.*, **7**, 323-327.

Kishi Y. and Takahashi K. (1977) A scanning electron microscope study of the vascular architecture of the periodontal membrane. (In Japanese). *Jpn. J. oral Biol.*, **19**, 192-207. (Cited by Weekes, 1983).

Kishi Y., Wang T., So S., Yoshizaki E. and Takahashi K. (1986a) A scanning electron microscope study of the capillary loops of oral epithelial papillae using corrosive resin casts. Part **I**. Gingiva, alveolar mucosa, buccal mucosa. *Jpn. J. oral Biol.*, **28**, 247-252.

Kishi Y., Wang T., So S., Endo K. and Takahashi K. (1986b) A scanning electron microscope study of the capillary loops of oral epithelial papillae using corrosive resin casts. Part **II**. Tongue. *Jpn. J. oral Biol.*, **28**, 239-246.

Klein P.B., Weilemann W.A. and Schroeder H.E. (1979) Structure of the soft palate and composition of the oral mucous membrane in monkeys. *Anat. Embryol.*, **156**, 197-215.

Klein-Szanto A.J.P. and Schroeder H.E. (1977) Architecture and density of the connective tissue papillae of the human oral mucosa. *J. Anat.*, **123**, 93-109.

Lametschwandtner A., Lametschwandtner V. and Weiger T. (1984) Scanning electron microscopy of vascular corrosion casts - technique and applications. *Scan. Electron Microsc.*, Part **II**, pp. 663-695.

Lametschwandtner A., Miodonski A. and Simonsberger P. (1980) On the prevention of specimen charging in scanning electron microscopy of vascular corrosion casts by attaching conductive bridges. *Mikroskopie*, **36**, 270-273.

Lenz P. (1968) Zur Gefasstruktur des Parodontiums. *Dtsch. Zahnaerztl. Z.*, **23**, 357-361. (Cited by Edwall, 1982).

Lenz P. (1974) Zur Gefass-Struktur des marginalen Parodontiums - rasterelektronen-mikroskopische Untersuchungen. *Dtsch. zahnaerztl. Z.*, **29**, 868-870. (Cited by Edwall, 1982).

Levy B.M. (1971) The nonhuman primate as an analogue for the study of periodontal disease. *J. Dent. Res.* Suppl. to No. 2, Vol. **50**, 246-253,

Levy B.M., Dreizen S. and Bernick S. (1972a) The Marmoset Periodontium in Health and Disease. In: *Monographs on Oral Science,* Vol. 1 (Ed. H.M. Myers), S. Karger, Basel.

Levy B.M., Dreizen S. and Bernick S. (1972b) Effect of aging on the marmoset periodontium. *J. oral Pathol.*, **1**, 61-65.

Levy B.M., Dreizen S., Bernick S. and Grant D. (1970) Comparative study of the periodontium of aged marmosets and humans. *J. Dent. Res.*, Vol. **49**, Special Issue, p. 199, IADR Abstract No. 604.

Low F.N., Olson G.E., Persky B. and Van Rybroek J.J. (1981) Technical aspects of stereoprojection for electron microscopy. In: *Three Dimensional Microanatomy of Cells and Tissue Surfaces*. (Eds. D.J. Allen, P.M. Motta and L.J.A. DiDio), pp. 1-20. Proceedings of the Symposium on Three Dimensional Microanatomy held in Mexico City, Mexico, August 17-23, 1980. Elsevier/North-Holland, New York.

Miodonski A., Kus J. and Tyrankiewicz R. (1981) SEM Bloodvessel Cast Analysis. In: *Three Dimensional Microanatomy of Cells and Tissue Surfaces*. (Eds. D.J. Allen, P.M. Motta and L.J.A. DiDio), pp. 71-87. Proceedings of the Symposium on Three Dimensional Microanatomy held in Mexico City, Mexico, August 17-23, 1980. Elsevier/North-Holland, New York.

Mormann W. and Ciancio S.G. (1977) Blood supply of human gingiva following periodontal surgery. *J. Periodontol.*, **48**, 681-692.

Mormann W., Meier C. and Firestone A. (1979) Gingival blood circulation after experimental wounds in man. *J. Clin. Periodontol.*, **6**, 417-424.

Motti E.D.F., Imhof H.-G., Garza J.M. and Yasargil G.M. (1987) Vasospastic phenomena on the luminal replica of rat brain vessels. *Scanning Microsc.*, **1**, 207-222.

Murakami T. (1971) Application of the scanning electron microscope to the study of the fine distribution of the blood vessels. *Arch. Histol. Jpn.*, **32**, 445-454.

Murakami T. (1972) Vascular arrangement of the rat renal glomerulus. A scanning electron microscope study of corrosion casts. *Arch. Histol. Jpn.* **34**, 87-107.

Murakami T. (1975) Pliable methacrylate casts of blood vessels: Use in scanning electron microscope study of the microcirculation in rat hypophysis. *Arch. histol. Jpn.*, **38**, 151-168.

Murakami T., Unehira M., Kawakami H. and Kubotsu A. (1973) Osmium impregnation of methyl methacrylate vascular casts for scanning electron microscopy. *Arch. histol. Jpn.*, **36**, 119-124.

Nakamura M.T., Kiyomura H., Nakamura T.K. and Hanai H. (1983) Scanning electron microscopy of vascular system of rat molar periodontium. *J. Dent. Res.*, Vol. **62**, Special Issue, p. 651, Abstract No. 16.

Nobuto T., Tokioka T., Imai H., Suwa F., Ohta Y. and Yamaoka A. (1987) Microvascularization of gingival wound healing using corrosion casts. *J. Periodontol.*, **58**, 240-246.

Nowell J.A. and Lohse C.L. (1974) Injection replication of the microvasculature for SEM. *Scan. Electron Microsc.*, Part **I**, pp. 267-274.

Nowell J.A. and Tyler W.S. (1974) SEM of LM-oriented injection replicas. *8th Int. Congr. El. Microsc.*, Canberra, 152-153. (Cited by Hodde and Nowell, 1980)

Nowell J.A., Pangborn J. and Tyler W.S. (1970) SEM of the avian lung. *Scan. Electron Microsc.*, pp. 249-256.

Nuki K. and Hock J. (1974) The organization of the gingival vasculature. *J. Periodont. Res.* **9**, 305-313.

Olson K.R. (1980) Application of corrosion casting procedures in identification of perfusion distribution in a complex microvasculature. *Scan. Electron Microsc.*, Part **III**, pp. 357-364, 372.

Ooya K. and Tooya Y. (1981) Scanning electron microscopy of the epithelium-connective tissue interface in human gingiva. *J. Periodont. Res.*, **16**, 135-139.

Pawley J.B. and Nowell J.A. (1973) Microdissection of biological SEM samples for further study in the TEM. *Scan. Electron Microsc.*, Part **III**, pp. 333-340.

Phillips I.R. and Grist S.M. (1975) Clinical use of CT 1341 anaesthetic alphaxalone alphadolone acetate in marmosets (*Callithrix jacchus*). *Lab. Anim.*, **9**, 57-60.

Provenza D.V. (1964) Oral Histology. Inheritance and Development, pp. 338-341. J.B. Lippincott Company, Philadelphia.

Provenza D.V., Biddington W.R. and Cheng T.C. (1959) Studies on the etiology of periodontosis. **I.** The role of vascular changes in the periodontium. *Oral Surg.*, **12**, 676-684.

Provenza D.V., Biddix J.C. and Cheng T.C. (1960) Studies on the etiology of periodontosis. **II.** Glomera as vascular components in the periodontal membrane. *Oral Surg.*, **13**, 157-164.

Rhodin J.A.G. (1967) The ultrastructure of mammalian arterioles and precapillary sphincters. *J. Ultrastruct. Res.*, **18**, 181-223.

Rhodin J.A.G. (1968) Ultrastructure of mammalian venous capillaries, venules and small collecting veins. *J. Ultrastruct. Res.* **25**, 452-500

Rhodin J.A.G. (1973) Dimensions and geometry of the microcirculation: Introductory remarks. *Microvasc. Res.*, **5**, 313-315.

Rohen J.W., Arnold W.H. and Wachter M. (1984) Rasterelektronenmikroskopische Untersuchungen uber die Architektur der Wurzelhautgefasse. *Dtsch. zahnaerztl. Z.*, **39**, 958-964.

Ryan T.J. (1973a) Structure, pattern and shape of the blood vessels of the skin. In: *The Physiology and Pathophysiology of the Skin*. (Ed. A Jarrett). Vol. 2, Chapter 16, pp. 577-651. Academic Press, London.

Ryan T.J. (1973b) Factors influencing growth of vascular endothelium in the skin. In: *The Physiology and Pathophysiology of the Skin*. (Ed. A Jarrett). Vol. 2, Chapter 21, pp. 779-805. Academic Press, London.

Saunders R.L. de C.H. (1967) Microangiographic studies of periodontic and dental pulp vessels in monkey and man. *Can. Dent. Assoc. J.*, **33**, 245-252.

Saunders R.L. de C.H. and Rockert H.O.E. (1967) Vascular supply of dental tissues, including lymphatics. In: *Structural and Chemical Organization of Teeth* (Ed. A.E.W. Miles), Vol. I, Ch. 5, pp. 199-245, Academic Press, N.Y.

Schroeder H.E. (1986) The Periodontium. Handbook of Microscopic Anatomy, Vol. V/5, Springer-Verlag, Berlin.

Schweitzer G. (1909) Uber die Lymphgefasse des Zahnfleisches und der Zahne bei Menschen und bei Saugetieren. IV. Feinerer Bau bei Saugetieren, nebst Beitragen zur Kenntnis der feineren Blutgefassverteilung in der Zahnpulpa und Zahnwurzelhaut. *Arch. mikr. Anat.*, **74**, 927-999. (Cited by Kindlova, 1965).

Scott J.H. and Symons N.B.B. (1982) The mucous membrane of the mouth and related structures. In: *Introduction to Dental Anatomy*, pp. 295-319, Churchill Livingstone, Edinburgh.

Shaw J.H. and Auskaps A.M. (1954) Studies on the dentition of the marmoset. *Oral Surg.*, **7**, 671-677.

Sims M.R. (1983) The microvascular venous pool and its ultrastructural associations in mouse molar periodontal ligament - Periodontal microvasculature & nerves. *Aust. Orthod. J.*, **8**, 21-27.

Sims M.R. (1987a) Ultrastructure of the venous ampulla in the interradicular microvascular bed of the mandibular molars of *Mus musculus*. *J. Morphol.*, **191**, 217-224.

Sims M.R. (1987b) A model of the anisotropic distribution of microvascular volume in the periodontal ligament of the mouse mandibular molar. *Aust. Orthod. J.*, **10**, 21-24.

Sims M.R., Sampson W.J. and Fuss J.M. (1988) Glomeruli in the molar gingival microvascular bed of germ-free rats. *J. Periodont. Res.*, **23**, 248-251.

Sloan P. and Soames J.V. (1984) Microscopic anatomy and regional organization of the lamina propria. In: *The Structure and Function of Oral Mucosa*. (Eds. J. Meyer, C.A. Squier and S.J. Gerson), pp. 141-157, Pergamon Press, Oxford.

Sobin S.S. and Tremer H.M. (1980) Methods for determination of three-dimensional microvascular geometry. In: *Microcirculation*, (Eds. G. Kaley & B.M. Altura), Vol. III, Chap. 15, pp. 303-310. University Park Press, Baltimore.

Stablein M.J. and Meyer J. (1984) The vascular system and blood supply. In: *The Structure and Function of Oral Mucosa*. (Eds. J. Meyer, C.A. Squier and S.J. Gerson), pp. 237-256, Pergamon Press, Oxford.

Stahl S.S. (1965) Healing of gingival tissues following various therapeutic regimens - A review of histologic studies. *J. Oral Therapeutics & Pharm.*, **2**, 145-160.

Steinhardt G. (1935) Die Gefassversorgung des gesunden, kranken und zahnlosen Kiefer. *Dtsch. Zahn-, Mund- u. Kieferheilkd.* **2**, 265-339. (Cited by Schroeder, 1986).

Takahashi T., Sayo Y., Matsuo M., Ono O., Wang T.-C. and Takahashi K. (1985) A scanning electron microscope study of the venous plexus of dog palate mucosa using vascular corrosion casts. *Bull. Kanagawa dent. Coll.*, **13**, 13-20.

Tompsett D.H. (1970) Anatomical techniques (2nd ed.) pp. 93-212, E.S. Livingstone, London.

Watanabe Y. and Suzuki S. (1963) An experimental study on capillary vascularization in the periodontal tissue following gingivectomy or flap operation. *J. Dent. Res.*, Vol. **42**, p. 758, Abstract No. 10.

Wedl C. (1881) Ueber Gefassknauel im Zahnperiost. *Virchows Arch. Pathol. Anat.*, **84**, 175-177. (Cited by Kindlova, 1965).

Weekes W.T. (1983) Vascular morphology of rat molar periodontium. M.D.S. Thesis, The University of Adelaide.

Weekes W.T. and Sims M.R. (1986a) The vasculature of the rat molar periodontal ligament. *J. Periodont. Res.*, **21**, 186-194.

Weekes W.T. and Sims M.R. (1986b) The vasculature of the rat molar gingival crevice. *J. Periodont. Res.*, **21**, 177-185.

Weekes W.T. and Sims M.R. (1986c) Gingival vascular architecture of the common marmoset (*Callithrix jacchus*). *J. Dent. Res.*, **65**, p. 755, Abstract No. 267.

Weiger T. (1981) Die Verwendbarkeit der polymerisierenden Kunststoffe Methylmethacrylat und Mercox CL zur Herstellung von Korrosionspraparaten zur rasterelektronenmikroskopischen Untersuchung der Gefassarchitektur tierischer Gewebe und Organe. Hausarbeit, Zoological Institute of the University, Salzburg. (Cited by Lametschwandtner *et al.*, 1984).

Weiger T., Lametschwandtner A. and Adam H. (1982) Methylmethacrylat und Mercox CL in der Raster-elektronenmikroskopie von Korrosionspraparaten. *Mikroskopie*, **39**, 187-197. (Cited by Lametschwandtner *et al.*, 1984).

Wergin W.P. and Pawley J.B. (1980) Recording and projecting stereo pairs of scanning electron micrographs. *Scan. Electron Microsc.*, Part **I**, pp. 239-250.

Wiedeman M.P. (1984) Architecture. In: *Handbook of Physiology*, (Volume editors: Renkin E. M. and Michel C. C.), Section 2: The Cardiovascular System, Volume IV, Microcirculation, Part I, Chapter 2, pp. 11-40. *Am. Physiol. Soc.*, Bethesda, Maryland.

Wilson N.H.F. and Gardner D.L. (1982) The postnatal development of the temporomandibular joint of the common marmoset (*Callithrix jacchus*). *J. Med. Primatol.*, **11**, 303-311.

Wong R.S.T. (1983) Vascular morphology of the mouse molar periodontium. M.D.S. Thesis, The University of Adelaide.

Wong R.S.T. and Sims M.R. (1987) A scanning electron-microscopic, stereo-pair study of methacrylate corrosion casts of the mouse palatal and molar periodontal microvasculature. *Archs. Oral Biol.*, **32**, 557-566.

Wysocki G.P., Wallitschek J. and Hardie J. (1978) Epithelium-connective tissue interface of oral mucous membranes. *Oral Surg.*, **45**, 416-423.

Zweifach B. (1961) Functional behaviour of the microcirculation. Springfield, Thomas.